Investigating the Impact of c-Cbl Deficiency in Adipose Tissue: Its Role in Insulin Sensitivity and Adipokine Production

Department of Cellular and Molecular Physiology, Institute of Translational Medicine, Faculty of Health and Life Sciences

Thesis submitted in accordance with the requirements of the University of Liverpool for the degree of Doctor of Philosophy by

Gulizar Issa Ameen

23rd July 2018

Table of contents: **Page No.**

Declaration

I declare that his thesis is the result of my own work, unless otherwise stated, and it is based upon the results from experimental work performed as a PhD student in Department of Cellular and Molecular Physiology at University of Liverpool. Neither this thesis nor any part of it has been submitted in support of an application for another degree or qualification at this or any other university or institute of learning.

Acknowledgements

I thank Almighty Allah, for His favor and all blessings.

Special thanks go to KRG Human Capacity Development Program (HCDP) scholars for giving this scholarship and funding my PhD project in the UK.

I would like to express my profound appreciation to my supervisor, Dr. Silvia Mora, for introducing me to the interesting field of adipose tissue biology, and for all her guidance, constant support and encouragement along the way.

I am deeply grateful to my second supervisor, Professor Graham Dockray, for his good advice and support during the practical part of this study and for offering his time to review my thesis.

Many thanks go to Christine Cashman for great support and help with histological analysis of the tissue samples.

My sincere acknowledgements go to the Biomedical Service Unit (BSU) for their help and support and for training.

I am very thankful to Professor Andrea Varo, the Institute Director of post graduate studies for her assistance.

I would like to say thank you to all friends, colleagues, current staff and former members of the Department of Cellular and Molecular Physiology.

I thank my lovely friends who gave me the passion and support to complete this work: Asia, Sirod, Wazeera, Justyna and Majida.

Finally, I would like to express my deepest appreciation to my family, specially my mother for her guidance, sacrifice, endless love and patience, and my brothers and sisters who have always been by my side. I dedicate this PhD thesis to my mother with love.

Publications and Conference Reports

1. Thondam SK, Daousi C, Wilding JP, Holst JJ, **Ameen GI**, Yang C, et al. Glucose-dependent insulinotropic polypeptide promotes lipid deposition in subcutaneous adipocytes in obese type 2 diabetes patients: a maladaptive response. American Journal of Physiology-Endocrinology and Metabolism. 2017;312(3):E224-E33.

2. **Ameen GI**, Mora S. Cbl downregulation increases RBP4 expression in adipocytes of female mice. The Journal of Endocrinology. 2018;236(1):29-41. doi:10.1530/JOE-17-0359.

3. Adipokine profiling in white adipose tissue of c-Cbl null mice: Effects of fasting and high fat diet. Poster presented at 13th Global Diabetes Conference and Medicare Expo. August 08-10, 2016 Birmingham, UK.

LIST OF FIGURES

Figure Number ....Page No.

LIST OF TABLES

Table Number.....Page No.

Abbreviations

AA	Arachidonic acid	CNS	Central nervous system
AC	Adenylate cyclase	COX	Cyclooxygenase
Acrp30	Adipocyte complement-related protein of 30 kDa	CRK	Adaptor protein CRK
AdipoR1	Adiponectin receptor type 1	CRP	C-reactive protein
AdipoR2	Adiponectin receptor type 2	DAB	Diaminobenzidine
AdPLA	Adipose-specific phospholipase A2	DAG	Diacylglycerol
AgRP	Agouti-related peptide	db/db	Genetic model of obesity and T2D
AICAR	Aminoimidazole-4-carboxamide ribonucleotide	DMEM	Dulbeco Modified Eagle's media
AMPK	5'-adenosine monophosphate-activated protein kinase	DPX	Dibutylphthalate polystyrene xylene
apM1	Adipose most abundant gene transcript 1	E1	Ubiquitin-activating enzyme
APS	Adaptor protein with PH and SH2 domains	E2	Ubiquitin-conjugating enzyme
APS	Ammonium persulfate	E2	Estradiol
ARC	Arcuate nucleus	E3	Ubiquitin ligase enzyme
AS160	AKT substrate of 160 kDa	EB	Ethidium bromide
AT	Adipose tissue	ECM	Extracellular matrix
ATGL	Adipose triglyceride lipase	EE	Energy expenditure
ATP	Adenosine trisphosphate	EGF	Epidermal growth factor
AUC	Area under the curve	EGFR	Epidermal growth factor receptor
BMI	Body mass index	ELISA	Enzyme-linked immunosorbent assay
BMMC	Bone marrow-derived mast cells	EP3	Prostaglandin EP3 receptor
BSA	Bovine serum albumin	ER	Estrogen receptors
BW	Body weight	ERE	Estrogen response elements
β-AR	Beta-adrenergic receptors	ERK	Extracellular regulated kinase
C3G	Guanyl nucleotide exchange factor	ER-α	Estrogen receptor-alpha
cAMP	Cyclic adenosine monophosphate	ER-β	Estrogen receptor-beta
CAP	Cbl associated protein	ES	Embryonic stem
CART	Cocaine- and amphetamine-regulated transcript	EV	3T3L1 cells infected with lentiviral particles containing an empty vector shRNA
Cbl	Casitas B-lineage lymphoma	fAd	Full length form of adiponectin
Cbl $^{-/-}$	c-Cbl knockout mice	FAK	Focal adhesion kinase
Cbl $^{+/+}$	Wild type mice	FAs	Fatty acids
Cbl $^{A/-}$	Cbl mice with mutated RING finger domain	FFA	Free fatty acids
Cbl KD	Knockdown 3T3L1, adipocyte cells depleted of c-Cbl gene	FGF	Fibroblast growth factor
CCL	CC-chemokine ligands	G6Pase	Glucose-6-phosphatase
cDNA	complementary DNA	Gab-1	GRB2-associated binding protein 1
CHO	Carbohydrates	gAd	Globular domain adiponectin
CIP4	CDC42 interacting protein 4	GBP28	Gelatin-binding protein

GDP	Guanosine diphosphate	$Lepr^{db}$/$Lepr^{db}$	Leptin receptor deficient
GIP	Glucose-dependent insulinotropic polypeptide	LepRs	Leptin receptors
GLP-1	Glucagon-like peptide-1	LFD	Low-fat diet
GLUT4	Glucose transporter type 4	LPL	Lipoprotein lipase
GLUT4 -/-	GLUT4 knockout mice	LPS	Lipopolysaccharide
gp130	Glycoprotein 130	M1	Pro-inflammatory phenotype of macrophage
Grb2	Growth factor receptor binding protein 2	MAG	Monoacylglycerol
GSK3	Glycogen synthase kinase-3	MAPK	Mitogen-activated protein kinase
GSVs	GLUT4 storage vesicles	MEK	MAPK (also known MEK)
GTP	Guanosine triphosphate	MGL	Monoglyceride lipase
GTT	Glucose tolerance test	MPD	Myeloproliferative disease
Gαi	Inhibitory G-protein	MRC	Mitochondrial respiratory chain
HFD	High-fat diet	mTORC2	Mammalian target of rapamycin complex 2
HMW	High molecular weight	NK	Natural killer
holo-RBP4	RBP4 bound to retinol	NPY	Neuropeptide Y
HSL	Hormone sensitive lipase	NT-shRNA	3T3L1 cells infected with lentiviral particles expressing a non-targeting shRNA
hTCEpi	Immortalized human corneal epithelial cells	ob	obese gene
i.p.	Intraperitoneally	PBS	Phosphate buffered saline
IBMX	Isobutyl-1-methylxanthine	PCR	Polymerase chain reaction
ICAM-1	Intercellular adhesion molecule 1	PDE3B	Phosphodiesterase 3B
IGF-1R	Insulin like growth factor-1 receptor	PDGF	Platelet-derived growth factor
IGFBP	Insulin-like growth factor-binding protein	PDGFR	Platelet-derived growth factor receptor
IGFBP-2	Insulin-like growth factor binding protein-2	PDK	Phosphoinositide dependent kinase
IGFs	Insulin-like growth factors	PEPCK	Phosphoenolpyruvate carboxykinase
IL-2	Interleukin-2	PGE2	Prostaglandin E2
IL-6	interleukin-6	PH	Pleckstrin homology
IL-6R	Interleukin-6 receptor	PI (3,4,5) P3	Phosphatidylinositol (3,4,5) triphosphate
IR	Insulin receptor	PI (4,5) P2	Phosphatidylinositol (4,5) biphosphate
IRR	Insulin receptor-related protein	PI3K	Phosphatidylinositol-3-kinase
IRS	Insulin receptor substrate	PKA	Protein kinase A
ITT	Insulin tolerance test	PKB	Protein kinase B
JAK 2	Janus Kinase 2	PKCζ	An isoform of protein kinase C, PKC zeta
JNK1	c-JUN N-terminal kinase 1	PMSF	Phenylmethylsulfonyl fluoride
Lep^{ob}/Lep^{ob}	Leptin deficient	POMC	Pro-opiomelanocortin
LepRb	Leptin receptor b	PPAR-α	Peroxisome proliferator-activated receptor

PTKs	Protein tyrosine kinase	TACE	TNF-α-converting enzyme
RASMCs	Vascular smooth muscle cells	TAE	Tris-acetate-EDTA
RBP4	Retinol binding protein-4	TAG	Triacylglycerol
RBPR2	RBP4 receptor-2	TBC	Tre-2, BUB2, CDC16
RC	Regular chow	TBC1D4	TBC1 domain family member 4
RF	RING finger domain	TBS	Tris buffer saline
RGC	RAL–GAP complex	TC10	Small GTP binding protein
RING	Really Interesting New Gene	TEMED	N,N,N',N'-tetramethylethy-lenediamine
RNAi	RNA interference-mediated	TGs	Triglycerides
RQ	Respiratory quotient	TKB	Tyrosine-kinase-binding
RTKs	Receptor tyrosine kinase	TLR4	Toll-like receptor 4
SDS	Sodium dodecyl sulfate	TMB	Tetramethylbenzidine
SDS-PAGEs	SDS-polyacrylamide gel electrophoresis	TNFR1	TNF-α receptor 1
SF-1	Steroidogenic factor 1	TNFR2	TNF-α receptor 2
SH2	Src homology 2	TNF-α	Tumor necrosis factor-α
SH3	Src homology-3 domain	TTR	Transthyretin
sIL-6R	soluble forms of IL-6R	Ub	Ubiquitylation
SOCS-3	Suppressor of cytokine signalling-3	UCP-1	Uncoupling protein-1
SoHo	Gut peptide sorbin	v-Cbl	viral Cbl
SOS	Son-of-sevenless	VEGF	Vascular endothelial growth factor
STAT3	Signal transducer and activator of transcription 3	VLDLs	Very low-density lipoproteins
STRA6	Stimulated by retinoic acid-6	VMH	Ventromedial hypothalamic
SVF	Stromal vascular fraction	WAT	White adipose tissue
Syk	Spleen tyrosine kinase	WHO	World health organization
T1D	Type 1 Diabetes	ZAP-70	70 kDa zeta-chain associated protein
T2D	Type 2 diabetes		

Abstract:

The worldwide obesity epidemic is now well recognised; obesity is a major problem not least because of the many serious metabolic complications that are associated with it. Cbl (Casitas B-lineage Lymphoma) is a receptor tyrosine kinase adaptor protein with E3 ubiquitin ligase activity that regulates receptor and non-receptor tyrosine kinases, resulting in their down-regulation. c-Cbl is a key protein in the alternate pathway of insulin signalling to glucose transporter type 4 (GLUT4) translocation in 3T3-L1 adipocytes. However, the role of c-Cbl in adipokine expression is currently unknown. c-Cbl knockout (Cbl $^{-/-}$) mice were previously found to be more insulin sensitive and resistant to the deleterious effects of a high fat diet than control littermates, but the relevant mechanisms remain incompletely explored. In this study, the role of c-Cbl signalling was examined in white adipose tissue (WAT) of a Cbl $^{-/-}$ mouse model, specifically in glucose and lipid metabolism and adipokine production.

c-Cbl knockout mice exhibited no changes in overall food intake or adiposity. However, there was increased ERK activation in WAT of Cbl $^{-/-}$ mice. The adipokine profile was altered in WAT of female Cbl $^{-/-}$ mice: leptin and RBP4 were increased, whereas adiponectin was reduced. These findings were confirmed in the 3T3L1 adipocyte cell line expressing shRNAs for c-Cbl. Furthermore, 17β-estradiol increased RBP4 mRNA which was attributed to activation of oestrogen receptor alpha (ER-α).

Regarding diet interventions, fasting decreased circulating concentrations of adiponectin in both male and female Cbl $^{-/-}$ mice, while leptin concentrations were decreased only in male Cbl $^{-/-}$ mice. However, RBP4 was increased in female Cbl $^{-/-}$ following a fast. On the other hand, Cbl $^{-/-}$ mice fed a HFD were protected from diet-induced insulin resistance. In addition, Cbl $^{-/-}$ mice fed a HFD exhibited an increase in

energy expenditure (EE) together with decreased WAT leptin levels in males and lower circulating leptin in females. However, under a HFD c-Cbl depletion did not protect against increased RBP4 protein content in the liver.

The findings of this thesis, taken together with the results from other studies, highlight the importance of c-Cbl depletion for the prevention and development of insulin resistance and T2D. This work is worthwhile not least because it holds promise for new treatments by increasing whole-body insulin sensitivity and energy expenditure. Further elucidation of the relevant molecular mechanisms will help develop a better understanding of the validity of c-Cbl inhibition as a therapeutic strategy for T2D.

Chapter 1

Introduction

1 Introduction

1.1 Obesity-general overview

Obesity is now recognised to be a global epidemic and it is estimated that by year 2030, over 1 billion individuals will be obese worldwide [1, 2]. Obesity is a significant risk factor for numerous health problems. It is associated with serious metabolic disorders including type 2 diabetes (T2D) and fatty liver disease and is associated with chronic low-grade inflammation, atherosclerosis, hypertension, asthma, cancer, depression, Alzheimer's disease, infertility, birth complications, sleep apnoea, premature aging and impaired physical ability [2]. The basic cause of obesity is an energy imbalance between calories consumed and calories expended. Modern life promotes the intake of energy-dense foods that are high in fat, salt and sugars, while urbanization and new technologies favour a sedentary life and decreased physical activity [3]. According to the World Health Organization (WHO), obesity is defined as the body mass index (BMI) >30 kg/m², calculated as the weight in kilograms divided by the square of the height in meters [4].

Obesity resuls in adipose expansion both by adipose cell hyperplasia and hypertrophy (Fig. 1) [5, 6]. It is associated with adipose tissue (AT) dysfunction [7] which may be mediated by different mechanisms including increased adipocyte cell death, hypoxia, altered adipokine profile, remodeling of the extracellular matrix (ECM), fibrosis, and inflammation by recruitment and subsequent activation of immune cells notably macrophages [7]. Hypertrophy also leads to AT dysfunction, which contributes to the development of metabolic syndrome, characterized by several metabolic abnormalities, including central (intra-abdominal) obesity, dyslipidaemia, hyperglycaemia, hypertension, hyperinsulinemia, insulin resistance and T2D [8-11]. Recently, it has been revealed that in mice on high fat diets [12], visceral AT primarily

grows through hypertrophy, whereas a hyperplastic response is predominant for subcutaneous AT [12, 13].

White adipose tissue (WAT) is the primary site of synthesis and storage of triglycerides (TGs) supplying fatty acids to other organs during periods of energy deprivation. Adipose tissue also secretes adipokines that regulate energy intake and metabolism [14]. The expansion of AT in obesity is correlated with increased macrophage infiltration and macrophage polarization to a pro-inflammatory phenotype (M1) in WAT. This results in an increase in the cytokines secretion such as tumor necrosis factor-α (TNF-α) and interleukin-6 (IL-6), which induce insulin resistance [9, 15, 16].

Identifying potential therapeutic targets to improve insulin sensitivity and ameliorate T2D has become a major goal of academic and industry research [17, 18]. Over the past decade, several genetically modified mouse models that identify promising targets have been described; the latter range from proteins involved in the insulin signalling pathway, alterations of genes affecting energy metabolism, and transcriptional metabolic regulators [17]. Using genetically manipulated animal models, many genes that result in lean phenotypes have been described [19-22]. These genes include those that regulate appetite, food absorption, and increased energy expenditure in either muscle or adipose tissue. A major advantage of manipulations that increase energy expenditure is that they deplete fat stores not only in adipose tissue but possibly in other cells that are susceptible to lipotoxic damage, thus providing a protective mechanism against the development of insulin resistance and diabetes [18].

c-Cbl is a member of Cbl protein family (c-Cbl, Cbl-b and Cbl-c) in mammals. It was identified as a key protein in the alternate pathway of insulin signalling to GLUT4 translocation in 3T3-L1 adipocytes [23, 24], but the role of c-Cbl in adipokine

signalling has not previously been studied. c-Cbl knockout mice were found to be more insulin sensitive than control wild type mice, but the mechanisms remain incompletely understood. The main aim of the present thesis was to determine the contribution of c-Cbl signalling in glucose and lipid metabolism and adipokine production in adipose tissue.

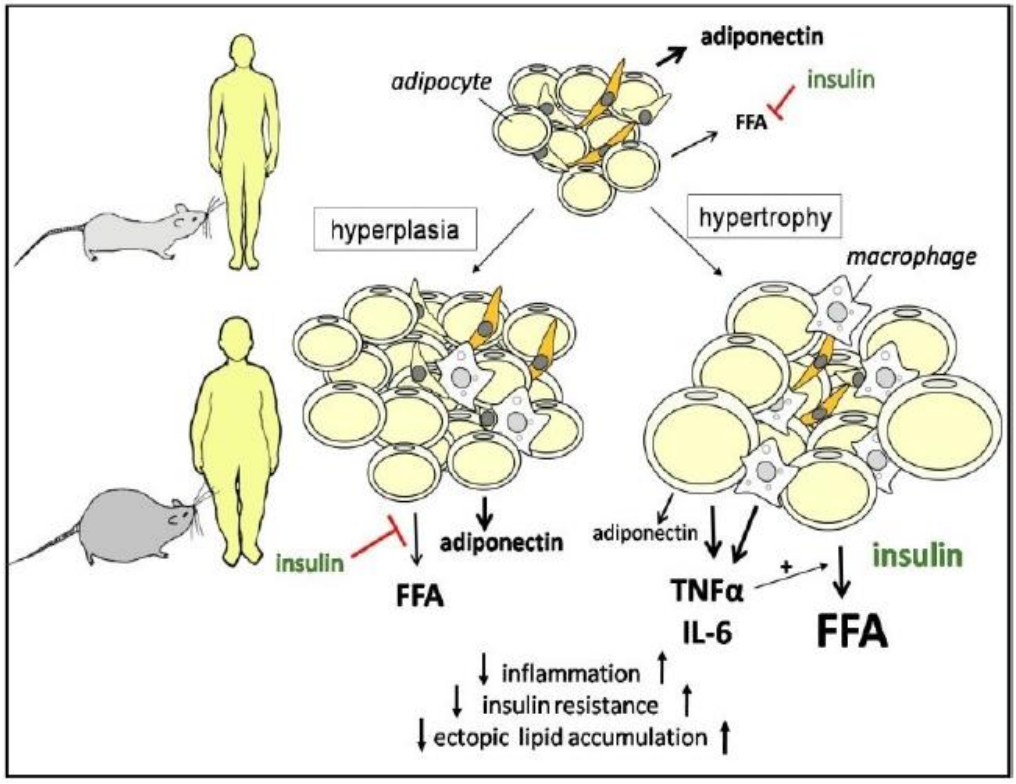

Fig. 1. Adipose tissue expansion via hyperplasia (increased adipocyte cells) and hypertrophy (increased volume of existing adipocytes) and the resulting metabolic consequences; reproduced from [13].

1.2 Diabetes and insulin resistance

Diabetes is a metabolic disorder caused by insufficient insulin secretion and/or insensitivity of tissues to insulin (insulin resistance) [25-28]. There are two main types of diabetes: type 1 (T1D) and T2D. Type 1 diabetes is an autoimmune disorder characterized by the immune mediated destruction of pancreatic β-cells that leads to a deficiency in insulin secretion. It accounts for nearly 10% of all diabetic cases and T2D accounts for the remaining 90% of cases [28, 29]. Type 2 diabetes is strongly associated with the development of obesity although other factors such as, aging, genetic predisposition, and physical inactivity also contribute [28, 30]. The incidence of T2D has reached epidemic rates, affecting around 387 million people worldwide. The prevalence of T2D diabetes is predicted to double in the next 20 years [31].

Insulin resistance is a hallmark of T2D and is defined as the decreased ability of tissue to respond to physiological concentrations of insulin [6, 8]. Insulin resistance occurs when insulin signal transduction is impaired in target tissues (skeletal muscle, liver, adipose tissue and heart) [25, 27]. Defects in insulin action in these tissues, particularly in skeletal muscle, reduce the capacity of insulin to decrease blood glucose after a meal. The pancreatic β-cell produces more insulin to compensate for the impaired insulin sensitivity which progressively leads to β-cell failure and the onset of diabetes [32]. Ectopic lipid accumulation in peripheral tissues contributes to the development of insulin resistance due to lipotoxicity notably in skeletal muscle [33-36], where different lipid entities are accumulated including: ceramides, diacylglycerol (DAG), and long-chain fatty acyl-CoA levels [37-41]. Whereas, hepatic insulin resistance manifests with an increased gluconeogenesis, resulting in high glucose output from the liver [2, 42].

1.3 Adipose tissue

Adipose tissue is considered as one of the most important organs involved in metabolic homeostasis [43]. It consists of adipocytes, nerve fibers, connective tissue, blood vessels and immune cells [3, 4, 44] and traditionally has been divided into two main types [6]: WAT which is energy storing, and brown adipose tissue (BAT) which is energy-expending [3, 43]. Recently, brown-like adipocytes were discovered within WAT and have been called 'beige' or 'brite adipocytes' [45-47].

1.3.1 White adipose tissue: WAT accounts the majority of body's fat [13]. It is composed mainly of mature adipocytes, but it also contains a stromal vascular fraction (SVF) containing preadipocytes, endothelial cells, smooth muscle cells, fibroblasts, leukocytes and macrophages (Fig. 2) [10, 44, 48]. White adipose tissue is distributed either subcutaneously or viscerally (in the mesentery, omentum and around abdominal viscera) [6]. The size of white mature adipocytes is around 25-200 μm [45]. It has long been recognized as the main energy storage site where energy is stored in the form of TG during energy excess (through the processes of lipogenesis) and released as fatty acids (FAs) when the body needs energy (through the processes of lipolysis) [8, 16]. Adipose tissue secretes a large number of proteins collectively grouped under the term "adipokines".

Adipokines act locally as paracrine/autocrine and/or systemically act as endocrine mediators [15, 44]. These adipokines influence physiology through different processes including appetite control, inflammation, glucose metabolism, adipogenesis, cell proliferation and vascularization [15, 44]. Adipokines mediate the crosstalk between adipose tissues and other metabolic organs such as liver, muscle, pancreas, peripheral and central nervous systems. Dysregulation in adipokine production often leads to metabolic dysfunctions such as inflammation, insulin resistance and diabetes [49, 50].

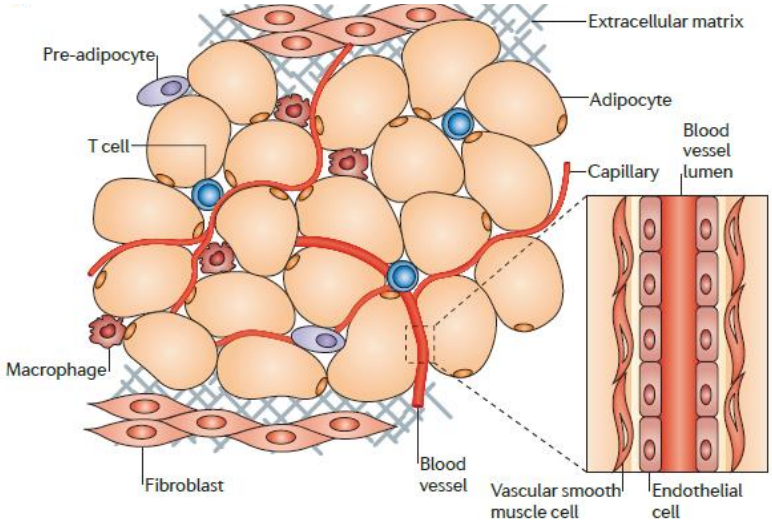

Fig. 2. Adipose tissue composition. Adipocytes are the main cellular component of adipose tissue, and they are crucial for both energy storage and endocrine activity. The other cell types that are present are precursor cells (including pre-adipocytes), fibroblasts, vascular cells and immune cells such as macrophages and lymphocytes, and these cells constitute the stromal vascular fraction of adipose tissue. Reproduced from [51].

1.3.2 Brown adipose tissue: BAT constitutes a small fraction of the overall adipose tissue mass in the body, but is a key site for heat generation via uncoupling protein-1 (UCP-1) [52]. In mice, BAT is abundant in the interscapular, cervical, axillary and perirenal regions. In humans, depots of BAT have been found in the neck and interscapular regions (particularly in newborns) [53], and have been found to gradually decrease with age [45]. Brown adipose tissue is characterized by an increased number of mitochondria, dense vascularization and multilocular lipid droplets compared to WAT which exhibits fewer mitochondria and contains a unilocular arrangement of lipids. BAT dissipates energy to produce heat during adaptive non-shivering thermogenesis such as cold exposure through UCP-1, a protein uniquely expressed in BAT [43, 54-56]. Mitochondria generate adenosine trisphosphate (ATP) through ATP synthase, which allows protons to flow down their concentration gradient across the internal mitochondrial membrane. In contrast, if the gradient is dissipated through UCP1, energy is dissipated as heat (Fig. 3) [56]. Not surprisingly, UCP1 gene expression is increased by several stimuli including: cold exposure, adrenergic stimulation with β3-agonists, retinoid and thyroid hormones, and cyclic adenosine monophosphate (cAMP) [56, 57].

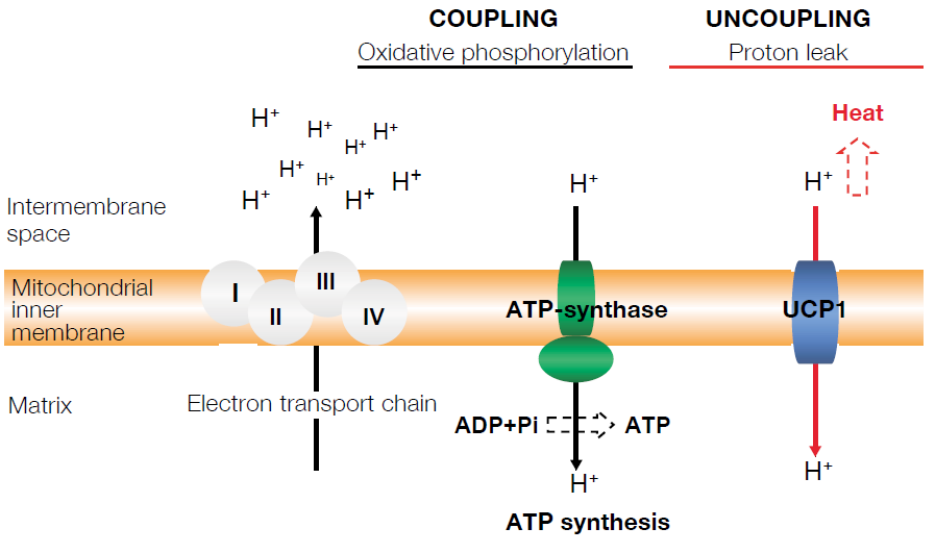

Fig. 3. UCP1 location and function in the mitochondrial respiratory chain (MRC). Numbers I-IV correspond to MRC complexes. ATP-synthase is the fifth complex of the MRC. During respiration, protons are pumped through the MRC complexes, and a proton gradient is generated. The energy of the proton gradient drives the synthesis of ATP by the ATP-synthase complex. UCP1 allows a regulated re-entry of protons into the matrix, uncoupling the MRC and, consequently, reducing ATP synthesis and generating heat. Reproduced from [57].

1.4 Lipogenesis and lipolysis

White adipose tissue plays a pivotal role in the regulation of lipid metabolism [9]. White adipocytes are specialized to store lipids and mobilize fatty acid within the body in times of negative energy balance [9, 58]. The regulation of fat accumulation is maintained by the balance between lipogenesis (TG synthesis) and lipolysis (TG breakdown) [5, 9]. De novo lipogenesis involves the synthesis of FA from acetyl-CoA molecules. However, in WAT the main source of FA for esterification into TG comes from the diet and the activity of the lipoprotein lipase (LPL) which is the primary enzyme responsible for lipolysis of chylomicrons (lipoprotein particles that consist of TGs, phospholipids, cholesterol, and proteins) and very low density lipoproteins (VLDLs) [59].

Lipogenesis is the process by which glycerol is esterified with free fatty acid (FFA) to form TG (Fig. 4). Dietary fat (triglycerides), when ingested with food, are absorbed by the gut and transported in the form of plasma-lipoproteins called chylomicrons. Lipids are released from their carrier lipoproteins through the local activity of LPL and subsequently split into their constituent FA and glycerol [60]. These are taken up by AT where TGs are resynthesized and stored in cytoplasmic lipid droplets. Lipogenesis also includes the anabolic process by which TGs are formed in the liver from excess glucose. Here fatty acids of various lengths are synthesized by the sequential addition of two-carbon units derived from acetyl CoA. Fatty acids generated by lipogenesis in the liver, are subsequently esterified with glycerol to form TGs that are packaged, not in chylomicrons, but with VLDLs and secreted into the circulation. Once in the circulation, VLDLs come in contact with LPL in the capillary beds in the body (adipose, cardiac, and skeletal muscle) where LPL releases TGs for intracellular storage or energy production [60].

Long chain fatty acyl CoA molecules are subsequently attached to glycerol molecule to produce TG. In several sequential steps, firstly through the formation of monoacylglycerol (MAG) and later DAG and triacylglycerol (TAG) [61]. Glucose serves as substrate for the formation of glyceraldehyde 3-phosphate and is a source of acetyl-CoA. Therefore, not surprisingly, a diet rich in carbohydrates stimulates lipogenesis in both adipose tissue and liver, leading to elevated postprandial plasma TG levels [9, 62, 63]. In addition, glucose increases lipogenesis by stimulating the release of insulin and inhibiting the release of glucagon from the pancreas [9, 62]. Insulin stimulates lipogenesis by increasing the uptake of glucose by adipocytes via recruitment of glucose transporters to the plasma membrane, as well as by inhibiting lipolysis. Lipogenesis occurs mainly in adipose tissue, but also in the liver, and to a lesser extend in the muscle, heart and pancreas [61].

The hydrolysis of TGs involves the breakage of 3 ester bonds to release FAs and glycerol (Fig. 4) and occurs during fasting, physical exercise or between meals [8, 10, 62]; the FFA are then released into circulation and used as an energy source by other tissues [62]. This process involves three consecutive steps catalyzed by adipose triglyceride lipase (ATGL; also called desnutrin or PNPLA2) that hydrolyzes TAGs into to DAGs, the hormone sensitive lipase (HSL) that acts on the DAGs and the monoglyceride lipase (MGL) which breaks MAGs to liberate the FA and glycerol (Fig. 4), [13, 64]. Fatty acids are transported in the circulation bound to albumin and conveyed to other tissues for β-oxidation and the generation of ATP [9, 65]. Glycerol is released from adipocytes via an aquaporin type of transport molecule and carried to the liver to be used as a substrate for gluconeogenesis [62, 65]. Lipolysis can be found in all cell and tissue types but it is most active in WAT [65].

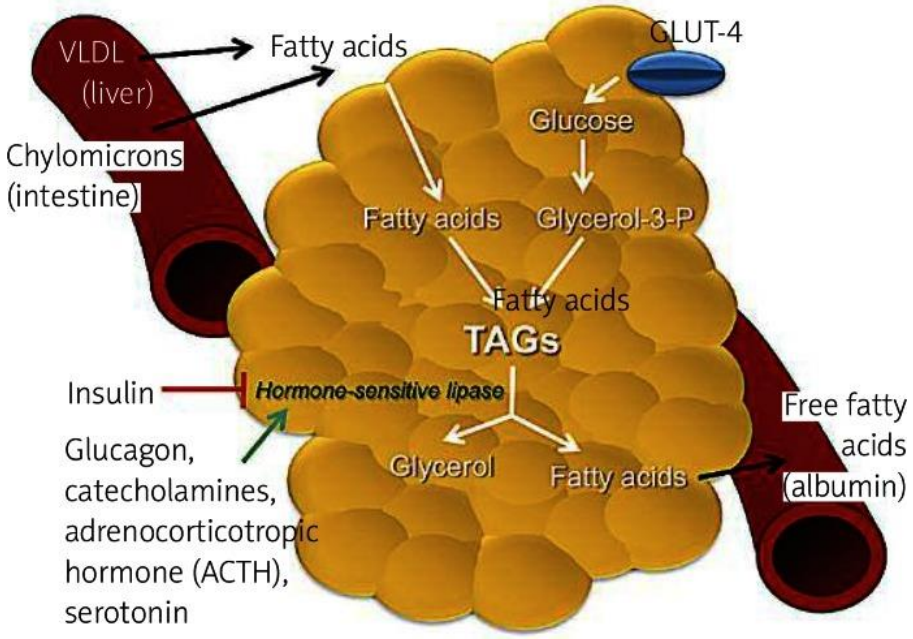

Fig. 4. The primary metabolic roles of adipose tissue. In the postprandial state, insulin-dependent GLUT4 allows the uptake of glucose from the bloodstream into adipocytes. Glycolysis occurs and produces G3P, a substrate required for lipogenesis. FA carried by very low-density lipoproteins (VLDL) form the liver and chylomicrons from the intestine are esterified with G3P to form lipid droplets of triacylglycerols (TAGs). In the fasting state and in stress conditions, hormone-sensitive lipase is activated for lipolysis. Glycerol produced by lipolysis is transported to the liver, while FFA are transported in the circulation to the liver, muscle and other organs to be oxidized. In the circulation, FFA are bound to albumin. Reproduced from [62].

Lipolysis in adipocytes is strongly regulated by hormones (Fig. 5A), which include catecholamines (adrenaline and noradrenaline) [2, 66] and glucocorticoids. During the fasting state, elevated glucocorticoids upregulate desnutrin/ATGL transcription [66, 67]. Furthermore, catecholamines activate lipolysis via interaction with β-adrenergic receptors which are G-protein coupled receptor that activate adenylate cyclase increasing cellular cAMP [68]. The latter binds protein kinase A (PKA) to induce HSL phosphorylation [58, 68]. HSL is phosphorylated at 5 or perhaps more different serine residues [10, 69]. The phosphorylation of HSL on Ser 559/660 is crucial for its activation and translocation to the lipid droplet, where HSL catalyzes the hydrolysis of diglycerides to monoglycerides.

Another lipase, adipose triglyceride lipase, carries out the initial cleavage of triglycerides to diglycerides and most likely is rate limiting for lipolysis, but it does not appear to be regulated directly via PKA phosphorylation [70]. Besides PKA, other protein kinases have also been shown to phosphorylate HSL and regulate enzyme activity. The list includes extracellular signal-regulated kinase (ERK), glycogen synthase kinase-4, $Ca2^{+}$/calmodulin-dependent kinase II, and AMP-activated kinase [60].

The phosphorylated HSL interacts with the lipid droplet protein perilipin, which itself is a target of PKA phosphorylation [60, 71]. The translocation of phosphorylated HSL from the cytosol to the lipid droplet is mediated by the phosphorylated form of perilipin [60, 70] in WAT where it can access the relevant substrates and stimulate lipolysis [58, 60, 68]. Perilipin under basal conditions (non-hormonally stimulated state) is not phosphorylated and prevents the binding of HSL to lipid droplets [60]. It acts as a protective barrier against lipase activity [70]. In response to β-adrenergic stimulation, perilipin is phosphorylated on six consensus serine residues by PKA.

Specifically, the phosphorylation of serines 81, 222, and 276 induces the binding of HSL to perilipin and access to the lipid droplet [60], and possibly the activation of ATGL [70]. Therefore, perilipin, possesses dual functions, both blocking lipolysis in the basal state as well as promoting lipolysis upon its phosphorylation [70].

In contrast, during the fed state insulin suppresses lipolysis (Fig. 5B) [72]. Insulin binds to its receptor in adipocytes and initiates a signalling event that involves the activation of the insulin receptor tyrosine kinase, the phosphorylation of insulin receptor substrates, the activation of phosphatidylinositol 3-kinase (PI3K), and the subsequent production of specific phosphoinositides at the plasma membrane. Phosphoinositides then recruit AKT to the plasma membrane via its pleckstrin homology (PH) domain, where AKT becomes phosphorylated and activated by two upstream kinases. AKT stimulates the translocation of GLUT4 to the plasma membrane, thereby promoting the uptake of glucose into the cell [70]. The mechanism by which insulin inhibits lipolysis has been proposed to involve the reduction of cAMP levels and thus PKA activity (Fig. 5B) [70, 73]. In this model, insulin signalling activates phosphodiesterase 3b (PDE3b) via AKT-mediated phosphorylation of Ser273. Upon activation by AKT, PDE3b catalyzes the hydrolysis of cAMP to 5'AMP, and thus decreases the activation of PKA and lipolysis [70].

Insulin also suppresses expression of desnutrin/ATGL [67]. Recent studies have revealed that lipolysis is dominantly regulated by prostaglandin E2 (PGE2) through adipose-specific phospholipase A2 (AdPLA) [74, 75]. AdPLA hydrolyzes the sn-2 position of phospholipids to generate arachidonic acid (AA), which via cyclooxygenase (COX) produces prostaglandin E2 (PGE2), that acts locally by binding to inhibitory G-protein (Gαi)-coupled prostaglandin receptor (EP3) present in adipocytes, resulting in inhibition of adenylate cyclase (AC) and decreased lipolysis (Fig. 5B) [67].

In obesity, the lipolytic response is often dysregulated due to insulin resistance; basal lipolysis is increased whereas stimulated lipolysis is blunted. Elevated basal lipolysis leads to lipid spill over in other peripheral tissues including the liver, skeletal muscle and the pancreas and results in lipotoxicity [2, 76].

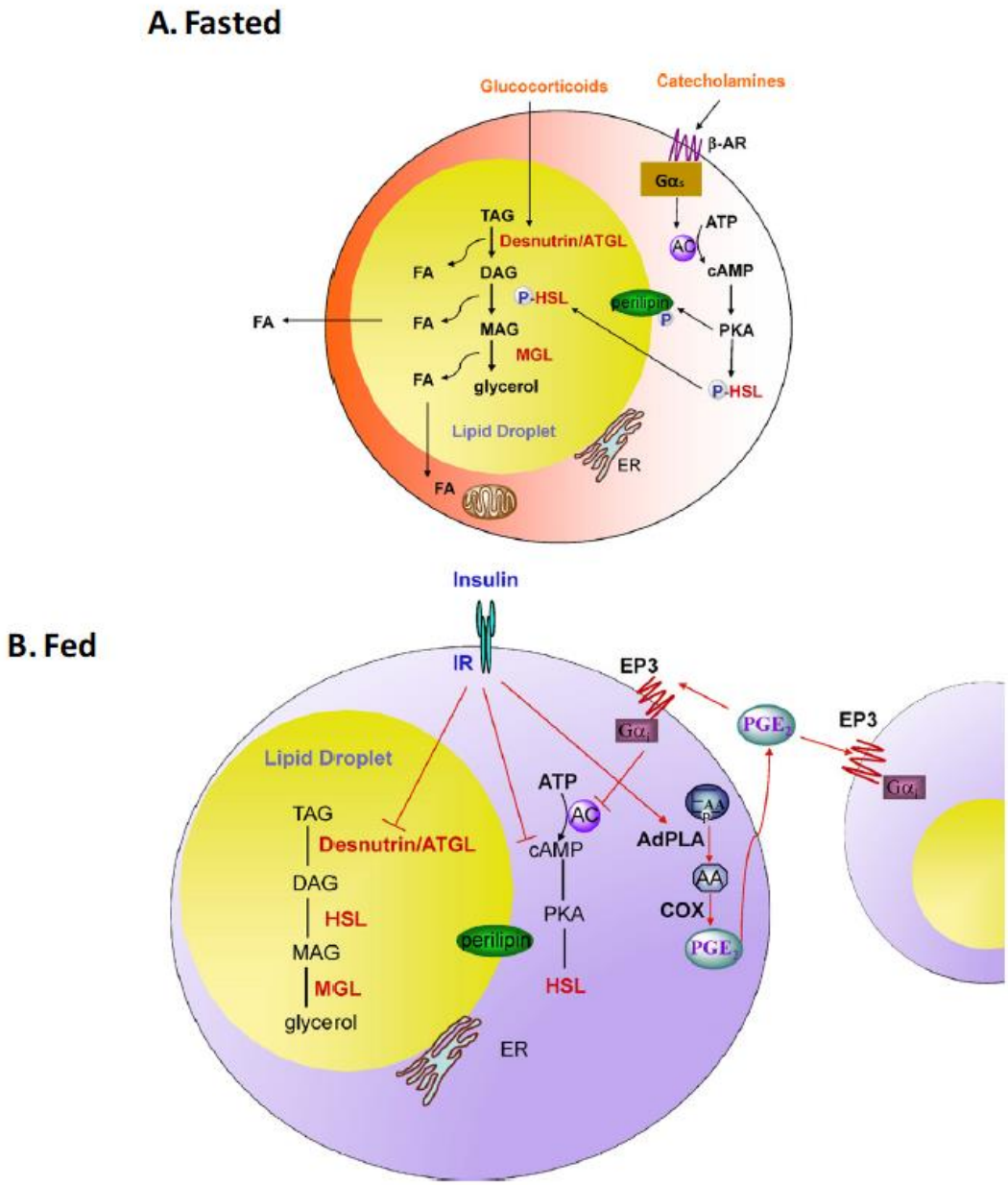

Fig. 5. Regulation of lipolysis in adipocytes. (A) Desnutrin/ATGL initiates lipolysis by hydrolyzing triacylglycerol (TAG) to diacylglycerol (DAG). Hormone-sensitive lipase (HSL) hydrolyzes DAG to monoacylglycerol (MAG) which is subsequently hydrolyzed by MAG lipase to generate glycerol and three fatty acids (FAs). The FAs generated during lipolysis can be released into the circulation for use by other organs or oxidized within adipocytes. During fasting, catecholamines, by binding to Gαs -coupled β-adrenergic receptors (β-AR), activate adenylate cyclase (AC) to increase cAMP and activate protein kinase A (PKA). PKA phosphorylates HSL resulting in translocation of HSL from the cytosol to the lipid droplet. PKA also phosphorylates the lipid droplet associated protein perilipin. Additionally, during fasting, glucocorticoids increase the expression of

desnutrin/ATGL. (B) In the fed state, insulin binding to the insulin receptor (IR) results in decreased cAMP levels and decreased lipolysis. Insulin also suppresses expression of desnutrin/ATGL. Reproduced from [67].

1.5 WAT as an endocrine organ

Adipose tissue releases a wide variety of bioactive peptides or proteins, called adipokines or adipocytokines [11]. Adipokines have multiple functions and contribute to many physiological and pathophysiological processes through autocrine and paracrine mechanism of action [77, 78], including: appetite, inflammation, insulin sensitivity and energy homeostasis [4, 11]. Some adipokines have anti-diabetic effects such as adiponectin and visfatin and improve insulin sensitivity, while others inhibit insulin signalling and induce insulin resistance for example TNF-α, IL-6 and retinol binding protein-4 (RBP4) [4]. Different WAT depots display different adipokine profiles that cause inflammation and insulin resistance in obese rodent and human [11, 16]. Subcutaneous WAT displays a lower proinflammatory profile than visceral WAT [79]. Also, clinical studies have demonstrated that FFA, C-reactive protein (CRP), IL-6 and TNF-α circulate at higher concentrations in patients with greater visceral fat [80]. Adipokine dysregulation has been considered key in the development of obesity and metabolic syndrome [8, 11, 16, 49].

In obesity, adipocytes and AT macrophages exhibit enhanced secretion of pro-inflammatory cytokines that cause a systemic low-grade inflammation and subsequently obesity-related complications [6, 13, 29]. Obese subjects have high plasma levels of leptin, although its action are suppressed due to leptin resistance [6]. Adiponectin secretion is also diminished in obesity [13].

1.5.1 Adiponectin: is a 244 amino acid residue, 30 kDa protein, that is predominantly produced by WAT and, at lower concentrations BAT [81, 82]. It was discovered in the mid-1990 by four independent research groups and according has multiple names: adipocyte complement-related protein of 30 kDa (Acrp30), adipose most abundant gene transcript 1 (apM1), gelatin-binding protein (GBP28) and Adipo Q [77, 81, 83, 84]. Adiponectin monomer is composed of an N-terminal collagen-like domain and a C-terminal globular domain. However, adiponectin circulates as trimers, hexamers, and high molecular weight (HMW) multimers [85]. It acts via two receptors, AdipoR1 and AdipoR2 [77]. AdipoR1 is expressed mainly in skeletal muscle, whereas AdipoR2 is expressed most abundantly in liver in both mice and human [83, 86]. Structurally these two receptors share 67% of identity in their amino acid sequence, and are highly conserved, displaying 95% of identity between human and mice [81]. AdipoR1 has low affinity for full length adiponectin (fAd) and high affinity for the globular domain (gAd), which is a fragment of fAd, generated by proteolytic cleavage at amino acid 110. In contrast, AdipoR2 has intermediate affinity for both forms of adiponectin [81]. Adiponectin activates 5'-adenosine monophosphate-activated protein kinase (AMPK) via AdipoR1 and peroxisome proliferator-activated receptor alpha (PPAR-α) via the AdipoR2 [87], which are essential for glucose uptake, fatty acids oxidation [81, 86, 87] and oxidative stress [87]. In muscle, adiponectin mediated activation of AMPK inhibits acetyl coenzyme A carboxylase and stimulates PPAR-α. This facilitates entrance of FA into the mitochondria for their oxidation [8, 83, 88]. In the liver, adiponectin inhibits hepatic glucose production by suppressing both glycogenolysis and gluconeogenesis. Suppression of glucose-6-phosphatase (G6Pase) and phosphoenolpyruvate carboxykinase (PEPCK) enzymes, inhibits glycogenolysis and gluconeogenesis [89, 90].

In addition, adiponectin has potent anti-inflammatory properties [16] and its expression is reduced by pro-inflammatory cytokines such as TNF-α and IL-6 [16, 89, 91]. Its circulating levels are positively correlated with insulin sensitivity [84, 91], and negatively with BMI [11]. Administration of exogenous adiponectin or overexpression in transgenic mice improves insulin sensitivity. Adiponectin deficient mice (Adiponectin/ACRP30 KO) developed HFD-induced inflammation and insulin resistance in muscle and adipose tissue [16, 92]. Also Adipo R1/R2 double-KO mice develop insulin resistance in the liver [11, 93].

1.5.2 Leptin: is a 16 kDa peptide hormone, which is highly expressed in WAT [6] but is also found in a variety of tissues including placenta, mammary gland, ovary, skeletal muscle, stomach, pituitary gland, and lymphoid tissue [94]. Its structure is similar to that of a family of pro-inflammatory helical cytokines, including interleukin-2 (IL-2) and IL-6 [16]. Leptin was first identified in 1994 [95] as the product encoded by the obese gene (ob), the murine homologue of the human gene LEP [77]. It is one of the most important signals for the regulation of food intake and energy homeostasis. Hypothalamic as well as brain stem nuclei play a critical role in integrating the information on absorbed food, on the amount of energy stored in the form of fat and on blood glucose levels to regulate feeding, energy storage, or expenditure [95].

Leptin exerts its effects by binding to specific leptin receptors (LepRs) located throughout the central nervous system (CNS), as well as elsewhere. Four alternatively spliced isoforms of LepR have been identified in humans. The long isoform of leptin receptor (LepRb) is highly expressed in the hypothalamus and other brain regions, where it regulates energy homeostasis and neuroendocrine function, and considered as the main leptin receptor [96]. The short isoforms of LepR are thought to mediate the transport of leptin across the blood-brain barrier [97].

Leptin inhibits appetite [8] by acting on specific hypothalamic nuclei [77, 78, 82]. In the arcuate nucleus (ARC), leptin interacts with a complex neural circuit to control food intake by activating anorexigenic neurons that produce pro-opiomelanocortin (POMC) and cocaine- and amphetamine-regulated transcript (CART), and inhibiting orexigenic neurons that synthesize agouti-related peptide (AgRP) and neuropeptide Y (NPY) [11, 77, 82, 98, 99].

Leptin deficiency correlates with hyperphagia, insulin resistance, hyperlipidaemia and impaired thermogenesis [83]. During fasting, circulating leptin levels decline rapidly. The fall in leptin stimulates the expression of AgRP and NPY and suppresses POMC and CART, thereby increasing food intake and decreasing energy expenditure [98, 99]. Leptin also acts on ventromedial hypothalamic (VMH) neurons that express the transcription factor steroidogenic factor 1 (SF-1). More recently, brain-derived neurotrophic factor in the VMH has been linked to the effect of leptin on feeding and energy balance. Mice with SF-1 deletion in the VMH are susceptible to diet-induced obesity, associated with impaired thermogenesis [94], whereas leptin deficient Lep^{ob}/Lep^{ob} and leptin receptor deficient $Lepr^{db}/Lepr^{db}$ mice exhibit marked hyperphagia, obesity and insulin resistance [16]. Exogenous administration of leptin to Lep^{ob}/Lep^{ob} mice restores insulin sensitivity and reduces obesity [16]. However, in $Lepr^{db}/Lepr^{db}$ mice the signalling form of the leptin receptor is deleted, and these mice are consequently unresponsive to exogenous or endogenous leptin [100].

Leptin also plays a pivotal role in the regulation of glucose homeostasis, independently of its effects on the central nervous system [8]. It directly increases glucose uptake and fatty acid oxidation in skeletal muscle. It increases insulin-like growth factor binding protein-2 (IGFBP-2) mRNA, a protein that is reduced in obesity and type 2 diabetes, in human skeletal muscle through both signal transducer and

activator of transcription-3 (STAT3) and PI3K, in parallel with enhanced insulin signalling [101]. It also induces an inflammatory response via its full-length isoform receptor (LepRb) and janus kinase 2 (JAK 2) as well as activation of signal transducer and STAT3 pathway [16]. It activates monocytes to produce pro-inflammatory TNF-α and IL-6 and stimulates the production of CC-chemokine ligands (CCL3, CCL4 and CCL5) by macrophages [16].

In obese humans or mice, leptin resistance results in the accumulation of triglycerides despite the high circulating levels of leptin [10, 89]. In fact, the leptin-signalling pathway activates suppressor of cytokine signalling-3 (SOCS-3), which might inhibit insulin signalling [89, 102].

1.5.3 TNF-α (tumor necrosis factor-α): is a cytokine with both proinflammatory and immunoregulatory roles [103]. It was first discovered in 1975 by Carswell *et al.* [104] and named after the discovery of its cytotoxicity to tumor cells in 1984 [105]. TNF-α is produced mainly by monocytes, macrophages [16, 51] and other immune cell types such as T lymphocytes, natural killer (NK) cells and neutrophils [106]. Rodent adipocytes also produce TNF-α but this is much reduced in humans [89]. TNF-α has pleiotropic effects on different cell types and plays an important role in the pathogenesis of many chronic and acute inflammatory conditions, including trauma, sepsis, infection and rheumatoid arthritis [107, 108]. TNF-α also has essential immunoregulatory functions as it increases the levels of C-reactive protein (CRP) and other cytokines and adhesion molecules, thus coordinating acute phase reactions which can lead to fever, anaemia, anorexia and cachexia [109].

TNF-α mediates its actions via two distinct types of receptors TNF-α receptor 1 (TNFR1, also called p55 or p60) and TNF-a receptor 2 (TNFR2, also called p75 or p80). Two bioactive forms of TNF-α exist, a transmembrane form and a secretory

form; transmembrane TNF-α is converted to the secretory active form through proteolytic cleavage by the metalloprotease, TNF-α-converting enzyme (TACE) [106]. TNF-α has an important role in inflammatory and autoimmune diseases [51]. It contributes to the pathophysiology of obesity and insulin resistance [8, 89] and its expression increases in metabolic disorders in both humans [8] and rodents [16].

TNF-α stimulates the phosphorylation of insulin receptor substrate (IRS) at Ser-307 which is associated with insulin resistance in skeletal muscle and adipose tissue [16, 51] and suppression of insulin-induced IRS1 tyrosine phosphorylation and activation of downstream targets [16, 110]. Treatment of AT with TNF-α causes insulin resistance, whereas ablation of TNF-α or its receptors increases insulin sensitivity in obese animals [8]. Nielsen *et al.* [111] found that TNF-α infusion into healthy subjects caused peripheral insulin resistance by interfering with AKT substrate phosphorylation, particularly inhibiting GLUT4 translocation to the cell membrane in both muscle and adipose tissue [111]. However, reduction in body weight in obese subjects and rodents is associated with a reduction in TNF-α expression [51].

1.5.4 IL-6 (interleukin-6): is a multifunctional cytokine with well-known pro- and anti-inflammatory properties [112]. IL-6 was cloned in 1986 by Kishimoto's group [113] as a B-cell stimulatory factor [114]. It is a 184 amino acid residue glycosylated protein [115] that can be secreted by both immune cells (B-cells, T-cells, macrophages, microglia) and non-immune cells (adipocytes, muscle cells, endothelial cells, fibroblast and neurons) [114]. IL-6 induces intracellular signalling pathways through binding to a specific receptor, interleukin-6 receptor (IL-6R), which is a type I transmembrane protein [115] and only expressed on hepatocytes, leukocyte-like neutrophils and T cells [112, 116]. IL-6R lacks the intrinsic capacity for signal transduction [114]. Therefore, signalling is induced though IL-6/IL-6R complex

binding to a second transmembrane receptor B-subunit glycoprotein 130 (gp130), which serves as a signal transducer for IL-6 [115] and can be found ubiquitously in all cell types [112]. In the absence of IL-6R, IL-6 shows no binding affinity for gp130. Therefore, only cells which express IL-6R can respond to IL-6 [115]. In a second pathway, trans-signalling, IL-6 binds to soluble forms of IL-6R (sIL-6R), and IL-6/sIL-6R complexes can activate all cells due to the uniform expression of gp130. Importantly, several soluble forms of gp130 (sgp130) are found in the circulation and act as natural inhibitors of IL-6 trans-signalling. Most pro-inflammatory roles of IL-6 have been attributed to the trans-signalling pathway, whereas anti-inflammatory and regenerative signalling, including the anti-bacterial acute phase response of the liver, is mediated by IL-6 classic signalling [112].

IL-6 abundance correlates positively with adiposity, whereas body weight loss leads to a decline in IL-6 and improved insulin sensitivity [44, 51]. There is also a positive relationship between IL-6 in AT and circulating C-reactive protein, another marker of inflammation [44, 89]. Both IL-6 and C-reactive protein are associated with development of T2D [44]. However, conflicting data exist regarding the correlation between IL-6 and insulin resistance. It was reported that IL-6 decreases insulin-dependent hepatic glycogen synthesis and glucose uptake in adipocytes, whereas it increases glucose uptake and glycogen synthesis in myotubes [95]. The effects of IL-6 on hepatic glucose production is controversial [117, 118]. Kim *et al*. [117] demonstrated that infusion of IL-6 blunted the ability of insulin to suppress hepatic glucose production in mice. In contrast, Inoue *et al*. [118] reported that intraventricular insulin administration resulted in IL-6-mediated inhibition of hepatic gluconeogenesis. In hepatocytes, IL-6 inhibits insulin-stimulated metabolic actions by inducing SOCS-3 expression [51, 119]. Also, it has been shown that administration of IL-6 in mice

suppresses the ability of insulin to inhibit glucose production in the liver [51, 117]. In adipose tissue, however, inhibition of IL-6 signalling via ablation of c-JUN N-terminal kinase (JNK1), protects against the development of insulin resistance by modulating the expression of hepatic SOCS-3 [51, 120].

1.5.5 RBP4 (retinol-binding protein 4): is a 21 kDa protein, that belongs to the lipocalins family that binds small hydrophobic molecules [121]. It is a specific transporter for retinol (Vitamin A) in the circulation. It carries hydrophobic retinol from the liver, where the majority of dietary retinoids are stored as retinyl esters in stellate cells [121]. Adipocytes also store substantial amounts of retinyl esters [122]. The lipid-soluble vitamin retinol is delivered to target cells mainly by two distinct mechanisms: as retinyl esters incorporated in lipoproteins (primarily chylomicrons) or bound to the RBP4 [123]. RBP4 is synthesized mainly by hepatocytes [124], but its mRNA can be expressed in other extra-hepatic tissues including adipose tissue, lung and kidney [121].

RBP4 expression in adipocytes is inversely correlated with that of GLUT4 [16]. The role of RBP4 in obesity and insulin resistance was first discovered in genetically modified mice by Khan's group [125, 126]. They found that adipose-specific GLUT4 knockout mice (adipose GLUT4$^{-/-}$) developed insulin resistance in liver and muscle [125]. In contrast, adipose-specific overexpression GLUT4 mice showed an increased in glucose clearance capacity [126]. Later Yang *et al.* [127] showed that adipose GLUT4$^{-/-}$ mice displayed an increased in RBP4 gene expression, and conversely RBP4 was reduced in mice overexpressing GLUT4 selectively in adipose tissue [126].

RBP4 bound to retinol (named holo-RBP4) is released from hepatocytes and binds transthyretin (TTR) in serum to form a complex that prevent renal filtration and elimination [121, 123]. In target cells, RBP4 binds to its receptor, STRA6 (stimulated

by retinoic acid-6), after dissociation from the TTR complex [123]. STRA6 is expressed in numerous tissues including skeletal muscle, brain, retina, testis and placental endothelial cells, but it is not expressed in liver or intestine [122]. A second receptor for RBP4 was identified in 2013 by Alapatt and his group [122], known as RBPR2 (RBP4 receptor-2). RBPR2 is mainly expressed in liver and small intestine and in adipocytes of obese mice [122], but also it is highly expressed in dendritic cells and lipopolysaccharide (LPS)-treated macrophages [121].

Increased secretion of RBP4 derived from WAT decreases glucose uptake in muscle by inhibiting phosphorylation of PI3K and IRS-1. In contrast in the liver, RBP4 has no effect on PI3K but it increases the expression of the gluconeogenic enzyme PEPCK, thereby increasing glucose output [10, 128, 129]. Many studies [129-132] have found a positive correlation between plasma concentrations of RBP4 and the severity of insulin resistance in obese/T2D and in non-obese subjects with a strong family history with T2D [89, 133], but others have not [126, 134-138]. Injection of recombinant RBP4 into normal mice, or transgenic overexpression of human RBP4, induced insulin resistance. In contrast, insulin sensitivity was improved in mice with reduced RBP4 levels (heterozygous RBP4 KO mice) [139].

1.6 Insulin action on glucose metabolism

Insulin is a peptide hormone which has strong anabolic effects. It is secreted from β- cells of the islets of Langerhans in response to elevated blood glucose [2, 4, 44]. It has a vital role in the regulation of glucose and lipid metabolism, adipogenesis and energy expenditure. It coordinates the processes associated with glucose uptake, lipolysis and gluconeogenesis [140] in multiple target tissues including liver, muscle, adipose tissue and heart [25, 27]. Several factors stimulate the secretion of insulin by the pancreas including a rise in plasma glucose, amino acids and several gastrointestinal hormones named incretins (glucagon-like peptide-1 (GLP-1) and glucose-dependent insulinotropic polypeptide (GIP)) [44].

Adipocyte growth, differentiation and energy homeostasis is regulated by insulin [2]. Energy homeostasis is controlled by insulin through the regulation of lipogenesis, FA uptake, protein synthesis and inhibition of lipolysis (Fig. 6) [2, 4]. Insulin impacts FA metabolism by increasing LPL activity in adipocytes which leads to increase FFA uptake that in turn enhances TGs synthesis [4, 44].

In the liver, insulin stimulates glycogen synthesis through a process called glycogenesis and inhibits hepatic glucose output by inhibiting glycogenolysis [44].

In adipose tissue, heart and skeletal muscle, insulin is known to activate several protein cascades that lead to an increase in glucose uptake. It stimulates the translocation of facilitative GLUT4 from an intracellular store to the cell surface, which facilitates glucose uptake and reduces circulating blood glucose levels [26, 141-143]. GLUT4 has a key role in the regulation of whole-body glucose homeostasis [141, 144, 145]. After a meal about 90% of glucose clearance occurs in skeletal muscle, whereas only 10% in adipose tissue [144].

In the absence of insulin, around 95% of cellular GLUT4 localizes to intracellular compartment(s) [146] and only about 5% of the total GLUT4 pool can be found at the cell surface [144, 147]. Individuals with insulin resistance and T2D exhibit defective insulin-stimulated GLUT4 translocation and consequently much effort has gone into defining the trafficking of GLUT4 in adipocytes and muscle cells [144].

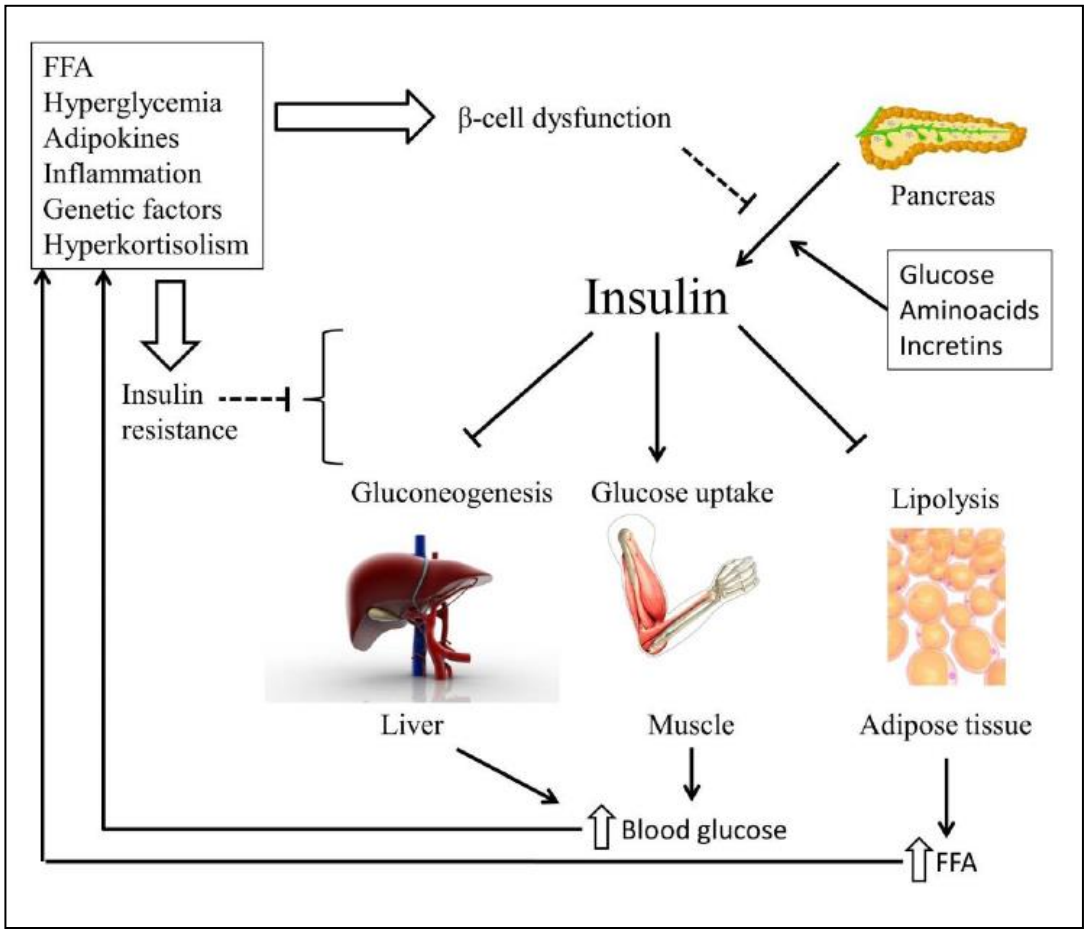

Fig. 6. Function of insulin and pathology underlying insulin resistance and insufficient insulin secretion. FFA = free fatty acids, → = stimulation, ⊥ = inhibition ↑= increase; reproduced from [44].

1.7 Insulin signalling pathways

The insulin receptor (IR) belongs to the receptor tyrosine kinase (RTKs) family of receptors that includes the insulin like growth factor-1 receptor (IGF-1R), the insulin receptor-related protein (IRR), the epidermal growth factor receptor (EGFR) and the platelet-derived growth factor receptor (PDGFR) [149]. The IR has two splice isoforms IR-A and IR-B [150]; IR-A has a higher affinity for insulin-like growth factors (IGFs), especially for IGF-II, whereas IR-B isoform binds predominantly to insulin [150, 151]. IR-A is the predominant IR isoform expressed in cancer cells and fetal tissues [150, 152]. IR-B is expressed in differentiated insulin-responsive tissues [152]. Both receptors contain 2 alpha (α) and 2 beta (β) subunits bound with disulphide bonds. The extracellular α subunit of each hemireceptor contains the ligand binding sites, whereas β subunits span the cellular membrane and the intracellular domain contains the tyrosine kinase activity [140, 150, 153]. IR is ubiquitously expressed in all tissues [140].

Binding of insulin to the **α**-subunit of the receptor leads to a conformational change in the protein which activates the tyrosine kinase domain. The activated IR kinase domain phosphorylates several proximal adaptor proteins including: the IRS1-4 family of proteins, the growth factor receptor binding protein 2 (Grb2)-associated binding protein 1 (Gab-1), adaptor protein APS with src homology 2 (SH2) and PH domains, and the proto-oncogene Cbl [4, 6, 29, 149]. Phosphorylation of these proteins activates at least three different pathways: PI3K-AKT/protein kinase B (PKB) pathway, the Cbl/ Cbl associated protein (CAP) pathway and the Ras-mitogen-activated protein kinase (MAPK) pathway (Fig. 7) [6, 29].

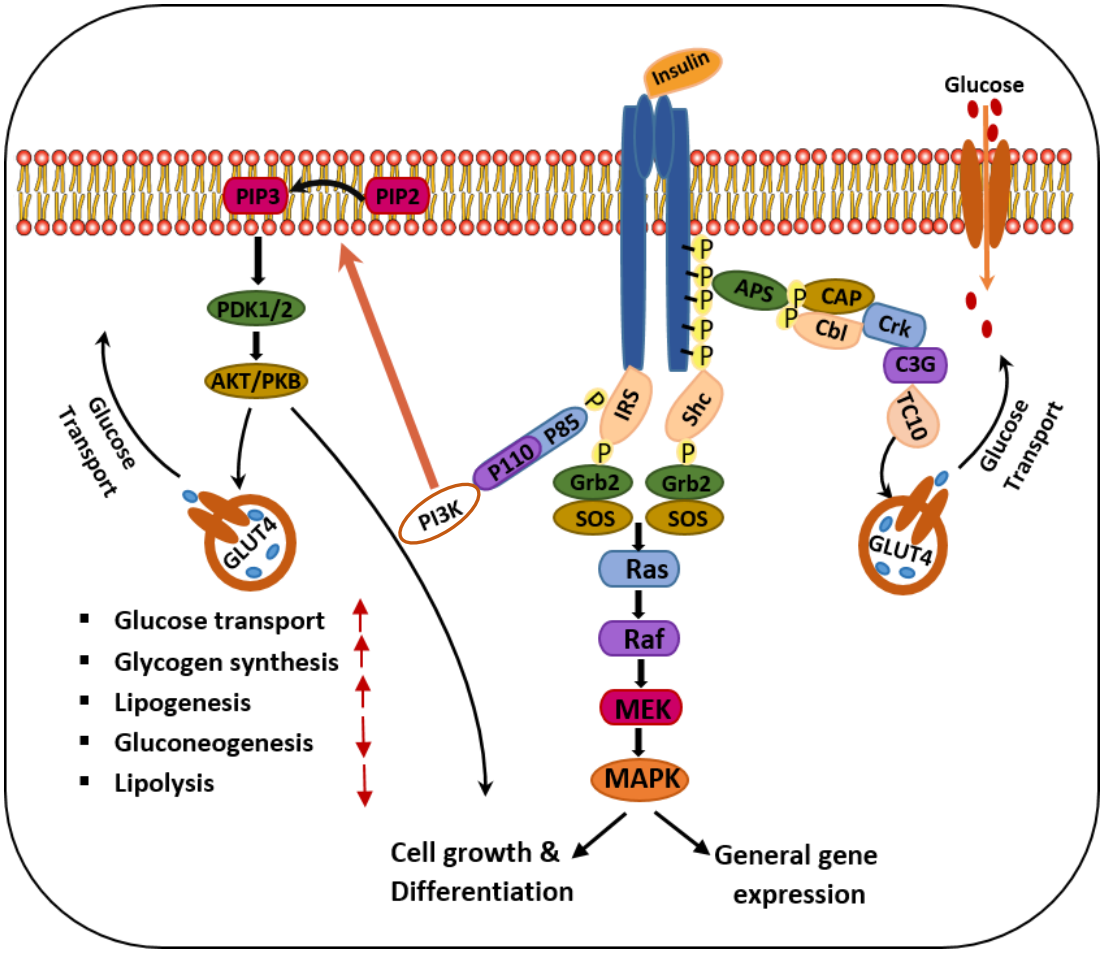

Fig. 7. Insulin signalling pathways in adipose tissue. The red arrows indicate up-regulation (↑) or down-regulation (↓) in response to PI3K-AKT/PKB signalling pathway, adapted from [6, 8, 140].

1.7.1 MAPK- signalling pathway: The Rat sarcoma (Ras) – mitogen-activated protein kinase (MAPK) also termed ERK signalling pathway, comprises a sequence of intracellular cytosolic serine threonine kinases (Fig. 8). Activation of this pathway starts with the phosphorylation of IRS1-4 proteins by the insulin and IGF receptor which leads to the recruitment of the adaptor protein Grb2 to Tyr-phosphorylated IRS [29, 149]. In turn this allows the recruitment of the protein son-of-sevenless (SOS), which is a guanine nucleotide exchange factor. The complex Grb2–SOS causes the conversion of guanosine diphosphate Ras-GDP to Ras-GTP (guanosine triphosphate). The activated Ras-GTP recruits and activates the protein kinase Raf-1, which induces phosphorylation of two protein serine threonine kinases named (MEK)-encoding genes, MEK1 and MEK2 on residues Ser218 and Ser222. Then MEK1 and MEK2 coordinate the phosphorylation and activation of ERK1/2 through threonine and tyrosine residue phosphorylation. ERK1 is phosphorylated by MEK1 and MEK2 on Thr202 and Tyr204 whereas ERK2 on Thr185 and Tyr187 [149].

ERK phosphorylates and regulates the activity of cytosolic proteins and of various nuclear transcription factors that are involved in cell growth, cell survival and differentiation [4, 6, 29, 142, 149, 154-156]. In mammalian cells, there are three well-known MAPK cascades: the ERK1/2, JNK1/2/3 and the p38 MAPK α, β, δ, and γ pathways. ERK, JNK and p38 proteins are grouped according to their activation motif, structure and function. In addition to insulin, ERK1/2 are activated in response to other growth factors including epidermal growth factor (EGF), platelet-derived growth factor (PDGF) and fibroblast growth factor (FGF), and also pro-inflammatory stimuli for example TNF-α, while JNK1/2/3 and p38 MAPK α, β, δ, and γ are activated by cellular and environmental stresses (oxidative or heat stress) in addition to pro-inflammatory stimuli [157, 158].

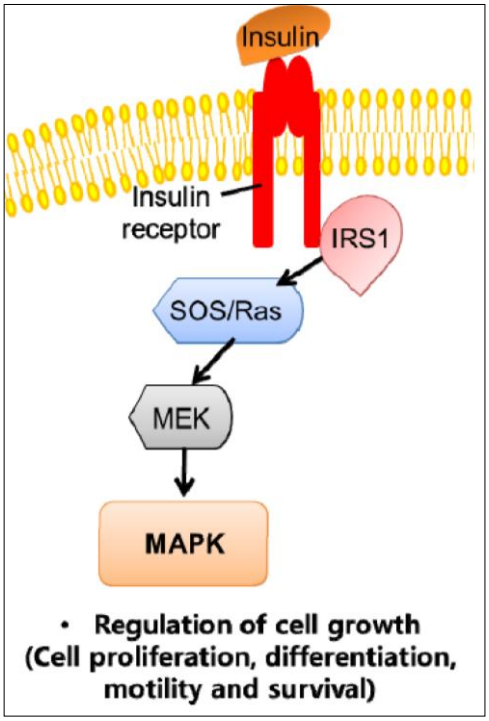

Fig. 8. MAPK signalling pathway. The Ras-mitogen-activated protein kinase pathway leads to the activation of genes which are involved in cell growth, thereby promoting inflammation and atherogenesis. Reproduced from [8].

1.7.2 The PI3K–AKT/PKB pathway: The phosphatidylinositol 3-kinase (PI3K) is a ubiquitous enzyme first discovered in 1984 [159]. Activation of the PI3K-AKT/PKB pathway is a key mechanism regulating cell metabolism and cell survival. When this pathway is activated by insulin in adipocytes it regulates glucose transport and metabolism and stimulates protein and lipid synthesis [149].

PI3K signalling is initiated following insulin receptor-mediated phosphorylation of IRS1-4 proteins (Fig. 9) [4, 149, 159]. The main isoforms of IRS are IRS-1 in skeletal muscle and adipocytes, and IRS-2 in liver [154]. Upon phosphorylation of IRS on tyrosine residues in the cytosol, IRS-1 acts as a docking site for SH2 proteins including the regulatory domain of PI3K named p85. Binding of p85 to IRS-1 results in its recruitment to close proximity of the IR and to its subsequent phosphorylation at tyrosine residues by the insulin receptor. This phosphorylation helps recruit the catalytic subunit p110 and activates the enzyme. Activated PI3K catalyses the synthesis of phosphoinositol second messengers including: phosphatidylinositol (3,4,5) triphosphate (PI (3,4,5) P3) from biphosphate (PI (4,5) P2) in the plasma membrane [4, 144, 149, 159-161]. PIP3 activates the serine/threonine of phosphoinositide dependent kinase 1 (PDK1) which contains a PH domain [149, 159]. Binding of PIP3 to the PH domain alters the conformation of the protein and activates the enzyme. PDK1 then phosphorylates and activates two main downstream kinases, PKB also named AKT and an isoform of protein kinase C, PKC zeta (PKCζ). Binding of PIP3 to the PH domain of AKT facilitates its recruitment to the plasma membrane and causes a conformational change in the protein that exposes and facilitates its phosphorylation at Thr308 by PDK1. Phosphorylation of Thr308 is sufficient and required for the activation of AKT. However, for maximal activation, further phosphorylation is required at Ser473, which is catalysed by the enzyme

phosphoinositide dependent kinase 2 (PDK2), also known as mTORC2 (for mammalian target of rapamacyin complex 2) [149, 159].

AKT is a serine threonine kinase that phosphorylates several intracellular targets. Among them the AKT substrate of 160 kDa (AS160) also known as TBC1 domain family member 4 (TBC1D4), TBC (Tre-2, BUB2, CDC16) domain-containing protein, which is a protein with GAP activity that targets several Rab GTPases [16, 162]. These Rabs are small G-proteins that in their GTP-bound form participate in vesicle movement and fusion [163], notably Rab8 and Rab14 in skeletal muscle and Rab10 in adipocytes, which are components in the GLUT4 storage vesicles (GSVs) [164]. AKT also phosphorylates and inactivates the enzyme glycogen synthase kinase-3 (GSK3) resulting in activation of glycogen synthase and glycogen synthesis in muscle and liver [16, 162].

While there is compelling evidence demonstrating the importance of the PI3K-dependent pathway for the translocation of GLUT4 and activation of glucose uptake [4, 159], some data indicate that the activation of PI3K is not sufficient [165]. A non-PI3K-dependant pathway was reported to contribute to GLUT4 translocation in adipocytes [159].

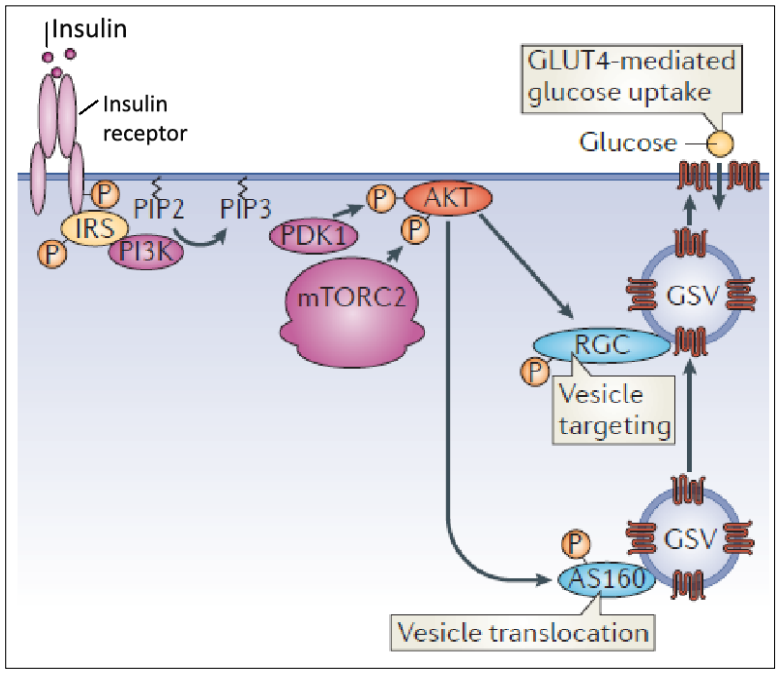

Fig. 9. The PI3K/AKT signalling pathway. The insulin receptor simultaneously initiates the PI3K-dependent signalling cascade by phosphorylating IRS proteins, thus producing docking sites for the recruitment and activation of PI3K. This kinase converts PIP2 to PIP3, which serves as a platform for the recruitment of PDK1 and AKT. When at the plasma membrane, AKT is phosphorylated by PDK1 and mammalian target of rapamycin complex 2 (mTORC2), which results in AKT activation. AKT promotes GSV exocytosis by phosphorylating and inactivating two GTPase-activating proteins (GAPs), AS160 and the RAL–GAP complex (RGC, consisting of a regulatory subunit (RGC1) and a catalytic subunit (RGC2)), which regulate small GTPases that are involved in GLUT4 storage vesicle GSV retention and targeting, respectively. Reproduced from [144].

1.7.3 Cbl-CAP signalling pathway: Casitas b-lineage lymphoma (Cbl) is an adaptor protein with an intrinsic E3 ubiquitin ligase activity that plays a role in regulating receptor tyrosine kinase signalling [22, 166, 167] and was identified as necessary for insulin-mediated activation of glucose transport in 3T3L1 adipocytes independent of the PI3K/AKT pathway [23, 24, 168, 169]. Cbl is recognized as a 120-kDa cytoplasmic protein rapidly phosphorylated following the stimulation with insulin and other growth factors [23].

The discovery of Cbl began with studies of haematopoietic tumors in mice infected with the Cas-Br-M retrovirus [166] in 1989 by Langdon *et al.* [170-172]. The causative retrovirus was called Cas NS-1 and its oncogene named viral Cbl (v-Cbl), for Casitas B lineage lymphoma [166]. Following the cloning of c-Cbl genes in mice it was revealed that v-Cbl encoded only the first 355 amino acids of 913 amino acids of the complete c-Cbl protein [166].

Mammalian Cbl proteins are encoded by three genes known as c-Cbl, Cbl-b and Cbl-c/Cbl-3 (Fig. 10) [172-175]. c-Cbl and Cbl-b are highly related in their primary structure and their domain architecture. In contrast, Cbl-c/Cbl-3 represents a shorter isoform that lacks some of the key domains and motifs in its C-terminal [176, 177]. Cbl-3/Cbl-c isoform is expressed only in the skin, while c-Cbl and Cbl-b are ubiquitously expressed in mammalian cells with c-Cbl being the predominant isoform in mature adipocytes [23, 166, 172]. All three members of Cbl family share a highly conserved region in their N-terminal domain which includes a TKB (tyrosine-kinase-binding) domain and a small linker region and RING (Really Interesting New Gene) finger domain [172-174, 178].

The TKB domain is composed of a four-helical bundle (4H), a calcium binding EF hand and variant SH2 domain [172, 178]. The TKB domain binds phosphotyrosine

residues in multiple protein tyrosine kinases (PTKs) such as ZAP-70 (70 kDa zeta-chain associated protein), Syk (spleen tyrosine kinase) and Src (SH2) [179]. The RING finger domain and the linker region together facilitate binding to E2 ubiquitin-conjugating enzymes and both of these domains are necessary for the E3 ubiquitin ligase activity [174, 178].

The C-terminal part is much less conserved among Cbl proteins. Cbl-c possesses a relatively short region carboxyl to the RING finger (RF) domain. c-Cbl and Cbl-b contain multiple protein-protein interactions motifs including a proline-rich domain that binds with a number of SH2- and SH3-domain. These domains contain proteins such as Src kinase and the Grb2 adaptor protein; a ubiquitin associated-leucine zipper motif at the C-terminus and several tyrosine residues that are phosphorylated by PTK upon cytokine and/or growth factor stimulation [175, 178].

The process of ubiquitylation involves multiple steps and requires three enzymes at least for successful action (Fig. 11). The three enzymes are known as E1, E2 and E3 [173]. The first, E1, is the ubiquitin-activating enzyme that recruits ubiquitin. The second, E2, is the ubiquitin-conjugating enzyme that transfers ubiquitin to the targeted protein. The third, E3, is the ubiquitin ligase that acts as a scaffold protein and interacts with E2 to transfers ubiquitin to the target protein [174]. Cbl specifically transfers ubiquitin to proteins in the RTK family which is important in cell signalling [167].

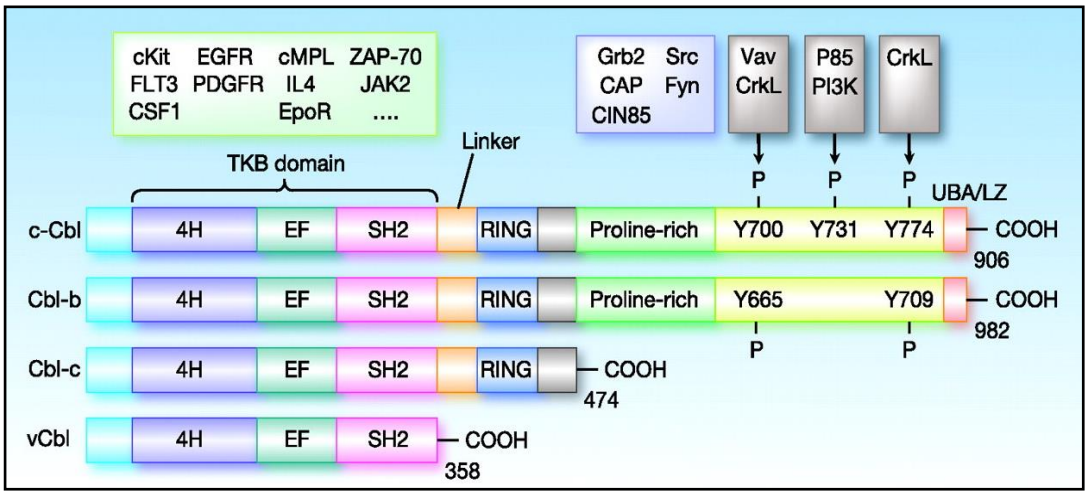

Fig. 10. Structure of Cbl family proteins. Domain structures of Cbl family proteins are illustrated. Major tyrosine phosphorylation sites in c-Cbl are indicated. Molecular interactions of c-Cbl with cytokine receptors and other signalling molecules are also displayed on top. Reproduced from [175].

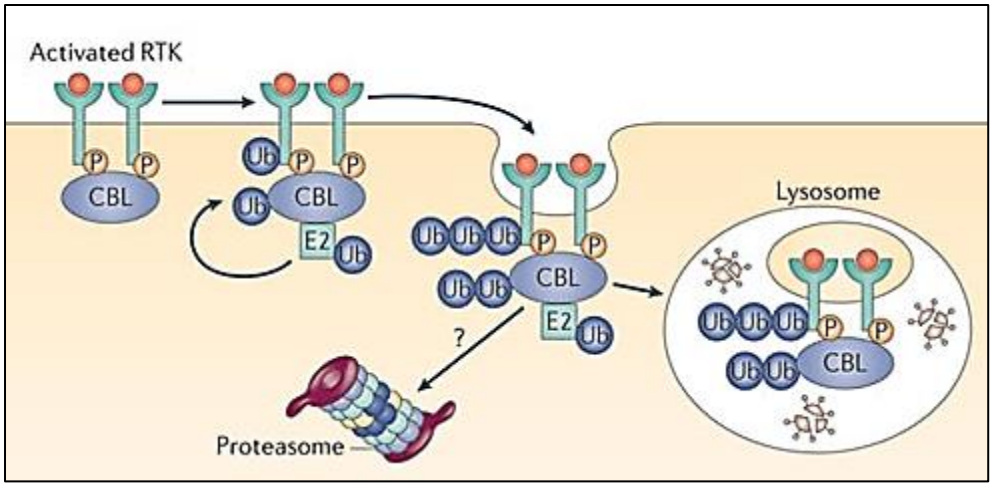

Fig. 11. A schematic of ubiquitylation process in Cbl protein. Cbl proteins mediate ubiquitylation (Ub) and the downregulation of receptor tyrosine kinases (RTKs). Whether Cbl proteins associated with activated complexes are degraded in lysosomes or proteasomes is unresolved. P (phosphorylation) source. Reproduced from [180] .

The Cbl signalling pathway (Fig. 12) is initiated by the recruitment of Cbl to the proximity of the insulin receptor and its phosphorylation at tyrosine residues. Recruitment is facilitated by the adaptor protein APS. This protein is phosphorylated by the insulin receptor at tyrosine 618. Upon phosphorylation APS recruits c-Cbl into proximity with the insulin receptor where Cbl is then phosphorylated at tyrosines 700 and 774 [23]. c-Cbl is bound to Sorbs1 also known as Cbl associated protein (hereafter named CAP). CAP contains three src homology-3 (SH3) domains in its C-terminus and a region of homology to the gut peptide sorbin (SoHo domain) in its N-terminus [23]. CAP is recruited with Cbl via its SH3 domain at the C-terminus and another direct interaction with APS through its N- and C-terminal SH3 domains [149] that allows the association of complex with the caveolae resident protein flotillin. This interaction facilitates the subsequent recruitment of additional downstream proteins. Among them the complex recruits the adaptor protein CrK2 and guanyl nucleotide exchange factor (C3G). C3G is a guanosine triphosphate exchange factor (GTP) protein that regulates the activity of the small GTP binding protein TC10 (also called Rho family GTPase). TC10- is located in caveolae microdomain [23, 140, 149, 181] of the plasma membrane of adipocytes. C3G activates TC10 [149, 181] which in turn interacts with multiple downstream proteins that regulate GLUT4 vesicle exocytosis. In this context, the best understood molecules at the moment include CDC42 interacting protein 4 (CIP4) which forms a stable complex with RAB GEF GAPEX5, and the RAB5 family GTPases that are involved in endosomal traffic of membranes and facilitate translocation and fusion of internal vesicles containing GLUT4 with the plasma membrane [149].

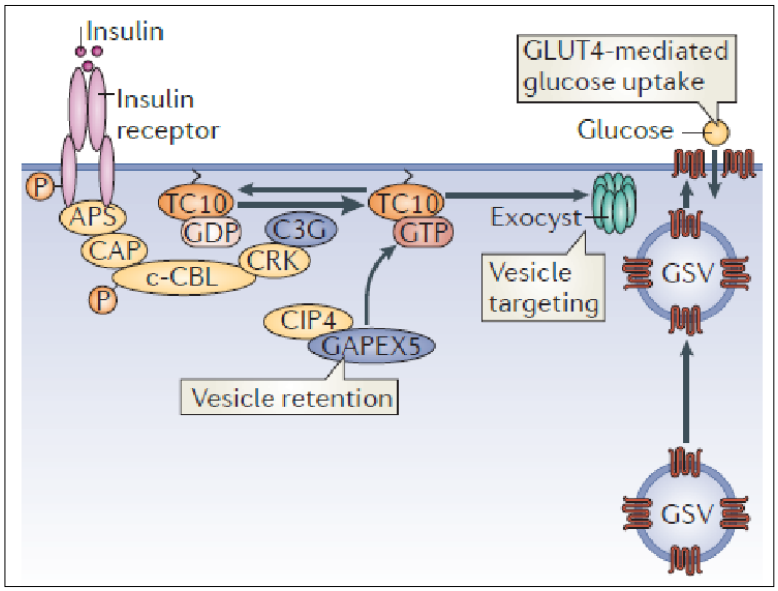

Fig. 12. The Cbl-CAP signalling pathway. The APS (adaptor protein with pleckstrin homology (PH) and Src homology 2 (SH2) domains)–insulin signalling cascade is initiated when the activated insulin receptor recruits the adaptor proteins APS, c-CBL and c-CBL-associated protein (CAP). Insulin receptor-catalysed Tyr phosphorylation of c-CBL in turn facilitates the recruitment of the adaptor protein CRKII and the guanine nucleotide exchange factor (GEF) C3G to the plasma membrane, where C3G activates the small GTPase TC10. GTP-bound TC10 interacts with the exocyst complex, thereby creating targeting sites for the glucose transporter type 4 (GLUT4) storage vesicle (GSV) at the plasma membrane. TC10 also interacts with CDC42-interacting protein 4 (CIP4), which is associated with the RAB5 and RAB31 GEF GAPEX5. Translocation of GAPEX5 to the cell surface modulates the activation state of its target small GTPases, which are involved in GSV retention and translocation. Reproduced from [144].

Hypothesis and aims of the thesis

The overall hypothesis for this thesis is that c-Cbl deficiency impacts on white adipose tissue biology, affecting insulin sensitivity, glucose and lipid metabolism and adipokine production.

The following specific objectives address the hypothesis:

1. To determine the changes in adiposity, adipose tissue morphology and lipid content in c-Cbl knockout (Cbl $^{-/-}$) compared with wild type (Cbl $^{+/+}$) mice.
2. To determine insulin sensitivity *in vivo* in these mice and *in vitro* in 3T3L1 adipocytes.
3. To determine the adipokine expression profile in WAT of Cbl $^{-/-}$ and Cbl $^{+/+}$ animals and in 3T3L1 c-Cbl knockdown and control adipocytes.
4. To investigate how a high fat diet affects WAT in Cbl $^{-/-}$ and Cbl $^{+/+}$ mice.
5. To investigate the possible molecular mechanisms of c-Cbl action.

Chapter 2

Material and methods

2 Materials and methods

2.1 Animals

2.1.1 Generation of c-Cbl deficient mice: Cbl $^{-/-}$ mice were obtained from the laboratory of Dr. Richard Hodes at the National Institute of Health (USA). Originally, the Cbl $^{-/-}$ mice were generated by Naramura [182] on a C57BL/6 background, using a gene-targeting strategy as shown in Fig. 13A. One exon (second exon) of the c-Cbl gene was deleted from the targeting vector (embryonic stem (ES) cell clone), followed by electroporation of the targeting construct into E14.1 ES cells. ES cells were selected with G418 and ganciclovir. Double-resistant clones were detected for homologous recombination by southern hybridization. The targeted clones were transiently transfected with a Cre recombinase expression vector to remove the neomycin-resistance gene and the second exon of the c-Cbl gene as indicated in Fig. 13A. Finally, resultant ES clones were injected into blastocysts to obtain chimaeric mice. In c-Cbl mutant mice, the absence of aberrant transcripts of the c-Cbl gene was confirmed by reverse transcription-PCR, and the Cbl protein was not detected by an antibody against the C terminus of the protein (Fig. 13B, C) [182].

2.1.2 Animals and breeding: C57BL6/J wild type control mice (Cbl $^{+/+}$) were purchased from the Jackson laboratories (Bar Harbour ME, USA). Cbl $^{-/-}$ and Cbl $^{+/+}$ mice were bred to obtain heterozygous animals (Cbl $^{+/-}$) and expanded to obtain an experimental cohort of animals. After five generations of het x het breeding additional pairs of Cbl $^{-/-}$ x Cbl $^{-/-}$ and Cbl $^{+/+}$ x Cbl $^{+/+}$ were crossed within our colony to establish an adequate supply of animals for our experiments. In all experiments, Cbl $^{+/+}$ littermate controls or age and gender matched control animals from our colony were used. Animals were housed in a pathogen-free animal facility, at the Biomedical Service Unit on a 12-hr light/dark cycle and constant temperature 22–24°C.

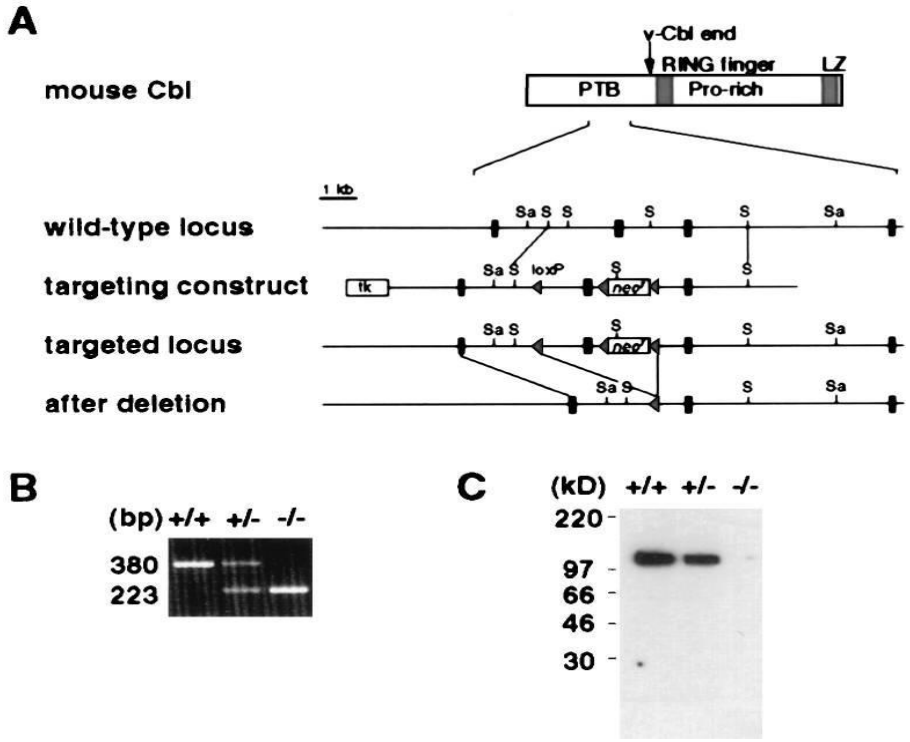

Fig. 13. **Generation of Cbl-deficient mice by gene targeting [182]**. (**A**) Partial restriction map of the c-*cbl* locus, the targeting construct, and the mutated c-*cbl* locus. The second exon in the figure, which was subsequently deleted by Cre/loxP-mediated DNA recombination, corresponds to nucleotides 681–837 of the published mouse c-*cbl* cDNA sequence (GenBank accession no. X57111). Black rectangles represent exons and triangles represent loxP sequence. Sa, *Sac*I; S, *Sph*I. (**B**) Reverse transcription–PCR analysis of c-*cbl* transcripts from wild-type (+/+), heterozygous (+/-), and homozygous (-/-) c-*cbl* mutant thymocytes. The sequences of the primers used in PCR correspond to nucleotides 640–663 (sense orientation) and to nucleotides 996-1019 (antisense orientation) of mouse c-*cbl* cDNA. (**C**) Western blot analysis of the Cbl protein.

2.2 Diet interventions

The mice had free access to water and diet (standard chow: CRM (P), Rat and Mouse Breeder and Grower, standard AIN93G-based pelleted diet, product code 801722, Special Diet Services, Witham, Essex, UK). This diet provided 3.59 kcal/g of energy with 9.08% calories as fat, 68.9% as carbohydrate (CHO) and 22.0% as protein, and contained fat, carbohydrate and protein at 3.4, 4.2 and 18.4% w/w respectively [183]. Two interventions were tested in this work. First, a group of animals were fed either the standard chow (as above) or a high fat diet (HFD) obtained from Special Diet Services (UK) containing 45, 20 and 35% of total energy intake deriving from fat, protein and carbohydrates respectively (diet code: 824053). The HFD experiment was started when animals were aged 4-5 weeks and maintained for 8 weeks. Body weight (BW) was recorded twice per week (Friday and Tuesday) from 4 to 12 weeks old. Second, the effects of fasting were studied. Animals at age 12-14 weeks of both genders were allowed free access to the standard chow diet every day; before the experimental day they were fasted overnight (5:00 PM to 8:00 AM) prior to sacrifice. Mice were sacrificed by decapitation for tissue dissections and blood was withdrawn via cardiac puncture. Blood was collected in tubes containing 8µl of EDTA (500 mM) and plasma was obtained by centrifugation at 2,000 x g for 10 min at 4 °C. Tissues were either snap frozen in liquid nitrogen then stored at -80 °C or cultured in Dulbeco Modified Eagle's media (DMEM) high glucose until further biochemical and molecular analyses or fixed and preserved for histological analysis (as described in section 2.14). All animal procedures were performed according to the Animals (Scientific Procedures) Act, 1986, UK regulations for animal welfare [184] and with appropriate licenses from the Home Office UK.

2.3 DNA preparation and genotype polymerase chain reaction (PCR)

Genomic DNA was prepared from an ear notch sample at 3 weeks of age using the proteinase K (Roche, REF 03115887001) protocol modified from [185]. Tissues were digested in lysis buffer pH 8.5 (100 mM Tris, 5 mM EDTA, 200 mM NaCl, 0.2 % SDS and 100 µg/ml proteinase K) at 50°C, overnight. Then samples were vortexed for 10 seconds and centrifuged at 12,000 x g for 2 minutes. 5 µl were taken as an aliquot from the supernatant and diluted 1:20 in 95 µl RNase free water, followed by heat inactivation at 95 °C in a dry bath for 15 minutes, then placed on ice. 3-5 µl of that dilution was taken for a PCR reaction later. For the detection of the mice genotype a PCR was used to amplify specific sequences of the mouse genome. A specific DNA fragment was amplified from complex genomic samples by this technique. The genotype PCR was performed with Bio-Rad C1000™ PCR/Thermal cycler. PCR GoTaq polymerase from PROMEGA was performed (25µl per reaction). The reaction mixture contained: 4.0 µl DNA sample, 11.88 µl H_2O, 5 µl of 5 x Flexi GoTaq buffer, 1.5 µl of 25 mM $MgCl_2$, 0.5 µl of 10 mM dNTP-mix, 1µl of 20 µM stock forward primers, 1µl reverse primers and 0.12 µl of 1U GoTaq HotStart-Pol. The reaction conditions were: 95°C for 2 min, 94°C for 45 sec, 55°C for 30 sec, 72°C for 1 min plus 35 cycles, then 72°C for 10 min and 4°C forever. Genotypes were determined by PCR of genomic DNA using the following primer sets: LOXP: 5’ TGG CTG GAC GTA AAC TCC TCT TCA GAC CTA ATA AC 3’; CBL-10: 5’ GAC GAT AGT CCC GTG GAA GAG CTT TCG ACA 3’; CBL-11: 5’ CCT AAG TGG TAG GAT TAT AAT TGC AAG CCA CCA C 3’ and CBL-13: 5’ TCC CCT CCC CTT CCC ATG TTT TTA ATA GAC TC 3’ which amplify the targeted and non-targeted genes, respectively. PCR products were visualised by agarose gel electrophoresis. A 2% agarose gel was made. DNA samples (8-10 µl per well) were loaded and separated by

electrophoresis at 100 v for 45 minutes. The expected product size are: ~200 bp for Cbl $^{+/+}$ and ~250 bp for Cbl $^{-/-}$. For reference a DNA ladder (100 bp, # 10488-058) was used. Results were visualized in a Syngene Gene Flash Bio Imaging Gel Documentation System.

2.4 Food intake

Mouse food intake was assessed for 8 weeks from week 4 to week 12 of age. At the beginning of the experiment, the cages and mice were weighed separately, and the mice were put in their cages for a designated experimental time. Body weight (n = 2-4 mice per cage) and food intake was measured weekly (2-day per week, (every Tuesday and Friday) and averaged. Mice and cages with food were weighted separately. After that it was divided by the number of days and the number of animals per cage, to determine food intake per individual mouse. Results are presented as an average ± SEM.

2.5 Blood glucose analysis

Glucose tolerance tests (GTT) and insulin tolerance tests (ITT) were done to assess how quickly the glucose cleared from the blood; and to examine the body response to insulin independently of pancreatic function. The mice were fasted overnight (5:00 PM to 8:00 AM). The next morning, BW was taken. The relative amount of glucose or insulin administration intraperitoneally (i.p.) was adjusted according to body weight of individual mice. Insulin solutionhuman recombinant (10mg/ml) from Sigma (#I9278), used in this study, is an intermediate-acting insulin with a slower onset of action and a longer duration of activity (up to 24 hours) than that of regular human insulin. Blood glucose concentrations were measured with a one-touch blood glucose

monitor (Freestyle Lite glucose monitor) at week 9-10 of age. GTT and ITT were analyzed as described [186, 187].

2.5.1 GTT: GTT was performed on mice fasted overnight (16 hours). Glucose saline solution was prepared at a concentration of 30g/100 ml. Glucose at 2 g/kg of body weight was administered intraperitoneally (i.p.) and subsequently blood samples were obtained from the tail vein at the indicated times, 0 min before glucose administration, and 30 min, 60 min, 90 min, and 120 minutes post-injection. Glucose concentrations were measured using a glucometer (Freestyle freedom lite glucose monitor).

2.5.2 ITT: ITT was performed on mice fasted overnight (16 hours). Animals were injected intraperitoneally with insulin (0.75 U/kg of body weight, 12 µl/20 ml of saline). Blood glucose concentrations were determined using the Freestyle Lite glucometer at 0 min, 30 min, 60 min and 90 minutes after injection.

2.6 Indirect calorimetry

In indirect calorimetry, energy expenditure (EE) is determined by measuring the the amount of oxygen consumed and carbon dioxide produced. The respiratory quotient (RQ), which provides information about metabolic substrate utilization (lipid or carbohydrate), is calculated by dividing the volume of CO_2 produced by the volume of O_2 consumed ($RQ = VCO_2 / VO_2$) [188-190]. In metabolism software (Metabolism (V3000), user manual) the following equation is used to calculate EE:

$$\mathbf{EE = (3.815 + (1.232 \times RQ)) \times VO_2 \times 1.44}$$

Where 1.44 is the conversion factor to convert the cal/min unit into Kcal/day unit (1440 min/1000).

Energy expenditure, respiratory quotient, activity, food intake and water consumptions were measured using a four-chamber indirect calorimetry system

(OxyletPro system from Panlab, Harvard apparatus, UK) and using metabolism software 3.0. The system detects air, and measures the gas concentration of the incoming and outgoing air for both O_2 and CO_2 in the sealed chambers [191]. Measurements were taken for one minute at every 15-minute intervals for 48hr. The experiment lasted for 48 hours, during which mice were free to consume food and water. Animals were housed individually in metabolic chambers and allowed to acclimatize for 4 hours (from 2:00 – 6:00 PM). Data from this first time of period were not used in the results analysis. The data including VO_2, VCO_2, energy expenditure, respiratory quotient (RQ) and spontaneous physical movement (activity) were simultaneously recorded for each mouse, over a 48-hr period under a constant environmental temperature (22°C), then used in analysis of the metabolic phenotype. EE, RQ and the activity of mice were then calculated from groups of 5-6 mice per experimental condition (per genotype and diet intervention). Graphs are made showing means and standard error.

2.7 3T3L1 adipocytes culturing and differentiation

Culture and differentiation of 3T3L1 adipocytes was carried out as described previously [192]. 3T3L1 cells were obtained from the American Type Tissue Culture repository. Cells were cultured in DMEM supplemented with 25 mM glucose, 10% calf serum at 37 °C with 8% CO_2. Cells were differentiated into adipocytes with 1µg/ml insulin, 1µM dexamethasone, and 0.5mM isobutyl-1-methylxanthine (IBMX), as described previously [192]. 3T3L1 cell lines stably expressing shRNAs specific for c-Cbl or empty PKLO puro vector or a non-targeting (NT)-shRNA were generated as previously described [193]. 3T3L1 fibroblasts were grown in DMEM media

supplemented with 10% calf serum, and 3 μg/ml of puromycin. Once confluent, cells were differentiated in regular differentiation media as above.

2.8 3T3L1 adipocytes lysate

Adipocyte cells were lysed in ice-cold lysis buffer (Hepes 50 mM pH=7.5, NaCl 150 mM, EDTA 10 mM, sodium pyrophosphate 10 mM, 10% Glycerol, sodium vanadate 2 mM, NaF 100 mM, phenylmethylsulfonyl fluoride (PMSF) 2 mM, 1% Triton x-100, pepstatin A 2 μg/ml, leupeptin 2 μg/ml and aprotinin 2 μg/ml). Cells were serum starved for 24-hours and stimulated with insulin (at a final concentration of 100 nM) for 30 minutes as indicated in the figure legends. Cells were washed with ice cold PBS and then 0.2 – 0.5 ml of lysis buffer per well was added. Cells were then incubated on ice for 10-15 minutes in a rocking platform and centrifuged at 14,000 x g for 10 minutes at 4°C. The supernatant was taken for protein quantitation using the Bio-Rad (Bradford assay, 2.11).

2.9 Culture of adipose tissue explants

WAT adipose tissue explants were obtained according to the protocol of Fried [194]. Epididymal WAT was dissected from Cbl $^{+/+}$ and Cbl $^{-/-}$ mice from both males and females aged 10-14 weeks and after dissection was directly placed into 5-10 ml of DMEM with high glucose. Tissue was transferred into a sterile Petri dish, minced into small pieces (1-2 mm diameter) under sterile conditions, and subsequently incubated for 2 hours in DMEM. After 2 hours of incubation, the media was changed to fresh DMEM and cultured further for up to 24 hours. Tissue was incubated in the presence of increasing concentrations of insulin (0 nM, 1 nM, 10 nM and 100 nM insulin) for

30 minutes (or as indicated in figure legends). Tissues were snap frozen in liquid nitrogen and stored at -80°C until analysis.

2.10 Adipose tissue lysates

Tissue samples were homogenised in a DOUNCE glass homogenizer, in ice-cold lysis buffer (NaCl 100 mM, EDTA 1 mM, 1% Triton x-100, NaF 50 mM, sodium pyrophosphate 2 mM, sodium vanadate 1 mM, PMSF 1 mM, pepstatin A 2 µg/ml, leupeptin 2 µg/ml and aprotinin 2 µg/ml). Samples were rotated at 4°C for 30 minutes, centrifuged at 14,000 x g for 15 min at 4°C and protein concentration of the supernatant was determined using the Bio-Rad (Bradford assay).

2.11 Protein quantification (Bradford assay)

Total protein concentrations were measured in the tissue and cell lysates. The Bradford protein assay was performed (Bio-Rad # 500-0006). The reagent was diluted 1:5 with distilled water. The standard curve was prepared using IgG (1mg/ml) from Bio-Rad. 200 µl/well of diluted reagent was placed into 96-well sterilin plates (Thermo-Fisher Scientific, Cat # 611F96). The IgG standard was added at concentration of 0, 1, 2, 4, 6, and 8 ug/µl into the assigned wells and 1-2 µl/well of the samples into the other wells. The absorbance reading for the samples and the standard was measured in duplicate at 595 nm using the plate reader (ELX 800). A standard curve was made and if the R square value for the standard was between 0.95-0.99 that standard was considered acceptable and was used for protein calculation.

2.12 Sodium dodecyl sulfate-polyacrylamide gel electrophoresis (SDS-PAGE) and western blot analysis

2.12.1 Samples preparation for SDS-PAGE: Samples prepared for western blot contained equal amounts of protein (40-80 µg) and were placed into 1.5 ml Eppendorf tube. Then one third of the total volume of 3x concentrated Laemmli sample buffer (LSB), and distilled water were added to the samples, heated for 10 minutes at 95˚C to denature the proteins, and placed in ice for 1 minute; samples were then centrifuged for few seconds at 12,000xg.

2.12.2 Gel preparation: SDS-PAGE gel was prepared to separate the proteins according to their molecular weight: 10 or 12% running gel pH 8.8 and stacking gel pH 6.8 was made. The glass electrophoresis plates were wiped and cleaned with 70% ethanol and the two plates then assembled together into a sitting rig. Sterile water was added to check for absence of leak and ensure that the plates were tightly sealed. Then resolving gel and stacking gels were made as described in the appendix. The chemical components of the stacking gel were mixed and then poured to the top of resolving gel between the plates and wells created by inserting a comb (1.5 mm thickness, 10 or 16 wells). After 20-30 minutes, once the stacking gel was set the comb was removed vertically. Encased gels within the glass plates were transferred to a tank containing 1L of 1X running buffer pH 8.6 (25 mM tris base, 192 mM glycine and 0.1% SDS). Samples were loaded using specific loading tips (Fisher, UK). Samples were resolved by electrophoresis, running voltage 110-120 v for 2-3 hours. To identify the molecular weight of the proteins in the samples a prestained protein ladder (10-250 kDa) ladder was run on the first lane of the gel.

2.12.3 Protein transfer to the membrane (blotting) and its detection: After separation by SDS-PAGE, proteins were transferred into nitrocellulose membranes using the following steps. Transfer cassettes contained the following layers: the cathode ((-), black cassette face), sponge, Whatman filter paper, SDS-PAGE gel, nitrocellulose membrane, Whatman filter paper, sponge, and the anode ((+), white cassette face). All equipment was pre-soaked in transfer buffer and it was ensured that no bubbles were trapped between the gel and membrane. The transfer cassette was then placed in a transfer tank filled with transfer buffer pH 8.3 (25 mM tris base, 192 mM glycine, 0.1% SDS and 20% methanol) for 1:30 hour at a constant 0.36 amps. Following the transfer, nitrocellulose membranes were stained with Ponceau stain to visualise protein transfer and distained in distilled water and TBST. Nitrocellulose membranes were treated with 5% skimmed dried milk in TBST (TBS/Tween (0.1%) for 1 hour at room temperature to block non-specific binding protein sites. The membrane was then washed three times in TBST for 10 minutes each and incubated at 4°C overnight with the primary antibody diluted in 3% BSA/PBS with 0.02% sodium azide. After washing three times in TBST for 10 minutes each, the membrane was incubated in secondary antibody conjugated with fluorescent dye, in 5% skimmed dried milk in TBST for 1 hour at room temperature. Nitrocellulose membranes were again washed three times in TBST for 10 minutes each. Proteins were then visualised by the Odyssey LICOR system scanner. The abundance of protein was determined by image analysis using an Image J software (NIH).

2.13 Triglyceride (TG) quantification

Triglyceride was determined with an enzymatic assay kit (free glycerol reagent, # F6428) and lipase (L1754, Sigma). The procedure involved enzymatic hydrolysis by lipase of triglyceride to glycerol and free fatty acids. Glycerol was further converted to glycerolphosphate by glycerol kinase and to dihydroxyacetone phosphate and hydrogen peroxide by glycerolphosphate oxidase. Subsequently, hydrogen peroxide (H2O2) together with 4-aminoantipyrine (4-AAP) and sodium N-ethyl-N-(3-sulfopropyl) m-anisidine (ESPA) were added to produce a coloured quinoneimine dye which was spectrophotometrically detectable with maximum absorbance at 540 nm [195, 196]. Tissue homogenates were obtained as detailed in section 2.10. Lysates were incubated at 70°C for 5 minutes, cooled and 10 µl aliquots incubated with 5 µl of lipase (2 mg/1 ml in PBS) overnight at 37°C. Subsequently, triglyceride concentrations were determined by quantifying spectrophotometrically (540 nm) the released glycerol using a commercial kit, SIGMA-Free Glycerol Reagent F6428. The abundance of TGs was normalized to the protein content of the tissue homogenate (section 2.11) which was determined using the Bio-Rad protein assay kit.

2.14 Immunohistochemistry of adipose tissue

Adipose tissue (WAT and BAT) dissected from Cbl $^{-/-}$ and Cbl $^{+/+}$ mice (male and female) was fixed in 4% PFA (4 gm paraformaldehyde /100 ml PBS) overnight at 4°C, then placed in PBS until processing. Samples were dehydrated through a series of ascending graded ethanol solutions (50, 70, 80, 95, 100%) for 10 minutes in each concentration. Following that, tissues were placed into a mixture of 50% isopropanol and 50% paraffin, which was pre-warmed in an incubator for 1 hour at 55-60℃. Samples were then changed into paraffin for further 1 hour in the same conditions. The

paraffin was replaced with fresh paraffin and tissue was incubated overnight in the incubator. The next day, samples were embedded in a fresh paraffin peel-away and left to harden overnight before sectioning.

2.14.1 Haematoxylin and eosin staining: Tissue was sectioned in a microtome (5-7 µm thick sections), dewaxed in Histoclear (5 minutes, twice), rehydrated through a series of descending ethanol concentrations (100, 95, 80, 70, 50%) for 2 minutes in each, stained with Mayer's haematoxylin (2 gm haematoxylin, 100 ml ethanol (100%), 100 ml glycerol, 100 ml distilled water, 10 ml glacial acetic acid and 30 gm of potassium aluminium sulphate) for 8 minutes, rinsed in water and acidified water for 10 seconds in each. Sections were counterstained with eosin for 2-3 minutes, washed in tap water dehydrated in ascending graded ethanol concentrations (50, 70, 80, 95, 100%) for 1 minutes in each, cleared in Histoclear and mounted using dibutylphthalate polystyrene xylene (DPX) mounting medium. Sections were visualized in a Leica inverted microscope (Leica microsystems, equipment No.11227510) at 40x magnification and images taken with a colour camera (Leica DFC. 450C, Germany, 541007) using a software program (LAS v4.2). Image analysis of histological tissue preparations (cell size and diameter) were carried out using Adiposoft-ImageJ software (is an automated open source software for the analysis of adipose tissue cellularity in histological sections)[197].

2.14.2 Immunohistochemistry for UCP-1: Immunolocalization was performed using ImmPRESS REAGENT Anti-Goat IgG reagent according to the manufacturer's guidelines. The ImmPRESS™ staining system is based on a novel method of polymerizing enzymes and attaching these micropolymers to antibodies. It is characterized by very high sensitivity, increased signal intensity and considerably less background staining in immunohistochemical applications. Immunostains for UCP-1

(antibody: C-17, sc-6528 from Santa Cruz) were done simultaneously on serial sections on separate slides. In brief, 7 μm thick sections were deparaffinized in Histoclear and rehydrated in progressively reducing concentrations of ethanol (100, 95, 75, 50, 25%) for 5 minutes in each. Antigen retrieval was performed heating the samples in Tris-EDTA buffer (pH 9.0) in a microwave oven in 2 cycles for 20 minutes in total in boiling buffer, followed by cooling at room temperature for 30 minutes. Primary antibody diluted in normal horse blocking serum (ImmPRESS REAGENT, # MP-7405) was applied to the sections which were then incubated overnight at 4°C. Endogenous peroxidase activity was blocked with 1% (v/v) H_2O_2 in PBS. Slides were placed in a humidified chamber during the incubation periods to prevent drying out. The slides were washed twice in PBS (5 min/wash), and the excess buffer was wiped away. Sections were encircled with wax using a PAP pen to minimize the volume of antibody solution needed for the immunohistochemical reaction. After washing in PBS, sections were blocked for 1 hour with provided ready-to-use (2.5% v/v) normal horse blocking serum to reduce the nonspecific signal. Sections were then incubated with monoclonal antibodies against UCP-1 (1:200), in blocking solution (normal horse serum) overnight at 4°C. To ascertain the specificity of the staining, negative control slides were included for each of the antibodies tested (is incubated without primary antibody, only with blocking serum). In these slides the primary antibody solution was substituted with blocking buffer. After washing in PBS 2 times for 5 minutes each, sections were incubated with the ImmPRESS™ reagent for 30 minutes at room temperature. After PBS washes (2 times/5min) peroxidase activity was developed with diaminobenzidine (DAB) as substrate. Sections were counterstained with Mayer's haematoxylin for 1-2 minutes, dehydrated in ascending graded ethanol concentrations

(50, 75, 95, 100%) for 1 minute, cleared in Histoclear for 5 minutes, then mounted with coverslips using DPX mounting medium.

2.15 ELISA determination of adipokine content, concentration

Quantification of adipokine concentrations was determined by ELISA using commercially available kits (RBP4, adiponectin, leptin, R&D, Minnesota, USA; TNF-α, IL-6, BD biosciences). Sandwich ELISA (enzyme-linked immunosorbent assay) is a technique designed to quantify proteins using specific antibodies. Sandwich ELISA measures the antigen between the two layers antibodies (capture and detection antibody). The capture antibody (primary antibody) was a monoclonal or polyclonal antibody specific for the protein (antigen) of interest and was diluted according to the manufacturers recommendations with 1x PBS and coated on a Falcon microplate (Ref.353279, Bioscience), then incubated overnight at 4°C. The plate was washed 3 times with PBS/Tween (0.05%) and blocked with 3% BSA (Bovine serum albumin) in PBS for 2 hours at room temperature followed by washing 3 times with PBS/Tween (0.05%). Each assay used a standard made by recombinant adipokine supplied by the manufacturer. Both standard and samples were added and incubated overnight at 4°C. Standards and samples bind to this antibody, whereas unbound antigens are washed away. Next, an enzyme-labelled detection antibody (secondary antibody) specific for the antigen, was added for 1 hour at room temperature. The plate was washed 3-4 times with BPS/Tween (0.05%) and Streptavidin-HRP 1:5000 dilution was added for 1 hour, followed by washing 3 times with BPS/Tween (0.05%). Using a substrate, TMB (Tetramethylbenzidine), which is converted by the enzyme, a colour signal is generated; the protein amount is detectable as intensity of the colour. The reaction was stopped by adding 1N of H_2SO_4 and the plate reader (ELX 800) was set to detection

at 450 nm for measurement of samples and standard intensity. Finally, the results were normalized to total protein content determined by Bradford method.

2.16 Total RNA

Total RNA was isolated from WAT and liver, frozen WAT and liver (50- 100 mg) were placed into a 2 ml Eppendorf tube and 600 µl of TRI reagent (T9424, Sigma-Aldrich UK) was added. The Trizol-tissue mixture was homogenized with a Polytron homogenizer (PT 1600E), the RNA from cell culture samples was extracted by scraping the cells in 600 µl of Tri reagent and centrifuged for 15 min at 14,000 x g at 4°C. The clear supernatant was transferred to a fresh 1.5 ml Eppendorf tube and 200 µl of chloroform (C2432, Sigma) was added per ml of Tri-reagent used, for 5 min. The solution was vortexed and centrifuged for 15 min at 14,000 x g at 4°C for phase separation. The aqueous layer was taken out in a fresh tube and supplemented with 300 µl of 2-propanol (I9516, Sigma). After mixing, the solution was allowed to stand for 5-10 min at room temperature, followed by centrifugation at 14,000 x g for 30 min at 4°C. The RNA precipitate formed a pellet on the side and bottom of the tube. The supernatant was discarded, and the pellet washed twice with 500 µl of 75% ethanol solution, vortexed and centrifuged for 15 min at 14,000 x g at 4°C. The supernatant was then removed, and the pellet air dried for 5-10 minutes and then re-suspended in 20-25 µ RNAse free water. Finally, the purity and concentration of isolated RNA were further measured on a NanoDrop™ Lite spectrophotometer (Thermo Scientific, 840281500). The ratio of absorbances between 1.7-2.0 at both 260/280 and 260/230 was taken as an indication of acceptance of RNA purity. 1-1.5 µg were used for reverse transcription.

2.17 Analysis of mRNA expression by real-time quantitative PCR

cDNA synthesis and quantitative PCR

Total RNA was reverse transcribed to complementary DNA (cDNA) with an iScript cDNA synthesis kit (Bio-Rad, #170-8891). cDNA synthesis from 1.0 - 1.5 µg of total RNA was performed using the high-capacity cDNA reverse transcription Kit. The reaction mixture contained: 4 µl of 5x iScript reaction mix, 1 µl of iScript reverse transcriptase, x µl of nuclease-free water and x µl of RNA template to give a total volume of 20 µl. The tubes were briefly vortexed before being placed into a Bio-Rad C1000™ PCR/Thermal cycler. The reaction conditions were:5 min at 25 °C; 30 min at 42 °C; 5 min at 85 °C and ∞ at 4 °C. cDNA was then stored at -20°C until qRT-PCR analysis. The cDNA was diluted 1:16 in RNase-free water prior to qRT-PCR in 1.5 ml Eppendorf. Validated Taqman probes for RBP4 and 18S (assay IDs: Mn00803264-31 and Hs 99999901 respectively) were obtained from Life Technologies. The RT-PCR reaction conditions were started with preincubation at 95°C for 3 min, denaturation step of 10 sec, at 95 °C followed by annealing 20 sec, at 60 °C and 20 sec, at 72 °C for a total of 40 cycles.

Estrogen receptor isoforms α and β were amplified using Kapa Sybr green, Fast mix from Roche and the following primers: ERα: F: 5'TGATTGGTCTCGTCTG GCG3'; R: 5'CATGCCCTCTACACATTTACC3'; ERβ: F: 5'CTGGCTAACCTC CTGATGCT3'; R: 5'CCACATTTTTGCACTTCATGTTG3' The primers produce amplicons of 100 bp and 91bp respectively. The conditions of the reaction were: denaturation 95ºC 30 seconds, annealing 60ºC 20 seconds, extension 72ºC 30 seconds, for 40 cycles. A melting curve was run at the end of each run. Relative quantification was carried out using the ΔΔCt method using 18S gene expression (primer sequences:

forward: 5’TCAAGAACGAAAGTCGGAGG3’ and reverse: 5’GGACATCTAAGG GCATCACA3’: for normalization, as we have previously reported [198].

The relative abundance of transcripts was quantified out using the ΔΔCT method. Data were obtained as CT values (CT=cycle number at which logarithmic PCR plots cross a calculated threshold line) and used to determine ΔCT values. ΔCT values of the target gene were normalized to ΔCT of 18S (reference gene) and ΔΔCT analysis was performed as described [199]. The calculation for quantitation first determined the difference (ΔCT) between the CT values of the target and the reference gene:

ΔCT = CT (target gene) - CT (reference gene)

The comparative (ΔΔCT) calculation was then used to determine the difference between each sample's ΔCT and the reference’s ΔCT.

Comparative expression level = ΔCT (CT of the target gene) – (CT of the reference gene or housekeeping gene)

Finally, these values were transformed to absolute values using the formula: **Absolute comparative expression level = 2 -** $^{\Delta\Delta CT}$

Chapter 3

Insulin sensitivity in Cbl $^{-/-}$ mice

3 Introduction

Cbl is an adaptor protein with an intrinsic E3 ubiquitin-protein ligase involved in protein ubiquitination and cell signalling previously found to play an important role in regulating translocation of the glucose transporter GLUT4 in 3T3L1 adipocytes [22-24, 166, 168, 169].

Later, an unexpected role for c-Cbl in energy homeostasis was described [170, 200]. c-Cbl knockout mice on a 129/SvJ x C57BL/6 background exhibited decreased adiposity despite hyperphagia and improved whole body insulin action resulting from increased muscle glucose uptake [22]. Cbl $^{-/-}$ mice also exhibited a profound increase in energy expenditure paralleled with increased mitochondrial density and respiratory capacity [22]. When fed a high-fat diet, Cbl $^{-/-}$ mice were reported to be protected from diet-induced weight gain and insulin resistance [18]. It is noteworthy that in another study, the same authors generated transgenic Cbl mice overexpressing a Cbl protein with mutated RING finger domain (Cbl $^{A/-}$) that also resulted in increased energy expenditure and protected mice from high-fat diet-induced obesity and insulin resistance [201]. These mice also displayed increased muscle AMPK activity [18, 22], elevated glucose uptake [202] and increased fatty acid oxidation [203], indicating that Cbl E3 ubiquitin activity may be important for regulating AMPK fatty oxidation in muscle via AMPK .[201].

However, the contribution of Cbl signalling in regulating glucose and lipid metabolism in WAT and adipokine production has not been studied in Cbl $^{-/-}$ mice before. The aim of this chapter was to determine the contribution of Cbl signalling to insulin sensitivity in mice generated on a C57BL6 background and to analyse the role of Cbl in adipose tissue morphology, adiposity and insulin signalling cascades.

3.1 Genotyping of Cbl $^{-/-}$ mice

In order to expand the colony of mice and obtain animals for experimental use, we needed to confirm the genotypes of Cbl $^{-/-}$ mice. This was done by detecting the wild type (Cbl $^{+/+}$) and the Cbl $^{-/-}$ alleles, in two PCR reactions (as described in Chapter 2). A representative PCR result confirming the genetic identity of the mice is shown in Fig. 14 A. To further confirm the genotypes of the founder mice, a tissue lysate was obtained from WAT separated by SDS-PAGE and immunoblotted with specific antibodies for c-Cbl and tubulin (used as a loading control). The absence of c-Cbl protein in Cbl $^{-/-}$ mice confirmed the genotype of the mice tissue (Fig. 14 B).

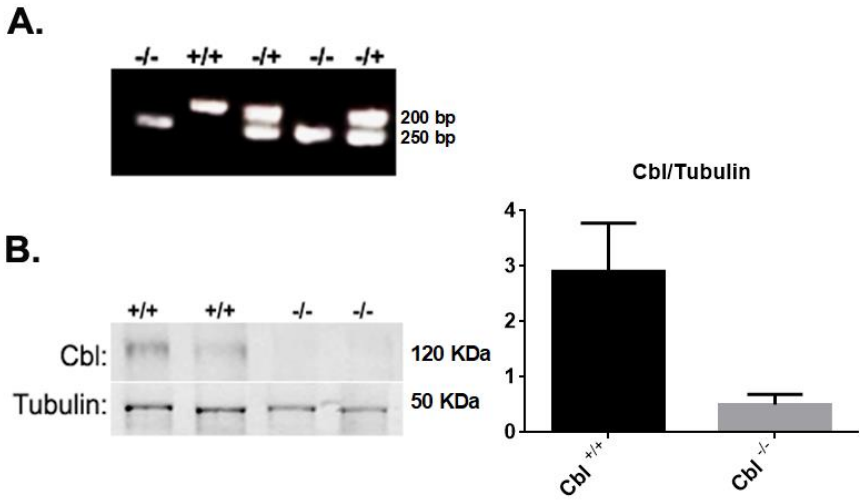

Fig. 14. Genotyping PCR for Cbl $^{-/-}$ and Cbl $^{+/+}$ mice. **A)** The genotype of Cbl mice indicated by PCR ("-/-" Cbl $^{-/-}$, "+/+" Cbl $^{+/+}$, "-/+", Cbl $^{-/+}$ mice). **B)** Left, western blot analysis obtained from Cbl $^{+/+}$ and Cbl $^{-/-}$ mice using Cbl and tubulin antibodies; right, quantification of Cbl/tubulin ratios (n=6).

3.2 Body weight and food intake in Cbl $^{-/-}$ mice

To assess whether c-Cbl depletion in mice results in changes in adiposity, body weight (BW) was recorded twice per week for 8 weeks following weaning at week four (Fig. 15A). In parallel, food intake was evaluated (see 2.4). Male Cbl $^{-/-}$ exhibited no significant difference in BW compared with male Cbl $^{+/+}$ mice, while female Cbl $^{-/-}$ mice had slightly lower BW compared to wild type females at week four. Even so, there was little difference in body weight gain. Male Cbl $^{-/-}$ mice showed a higher food intake compared to wild type male mice (Fig. 15B), whereas in female Cbl $^{-/-}$ mice there was no significant difference in food intake.

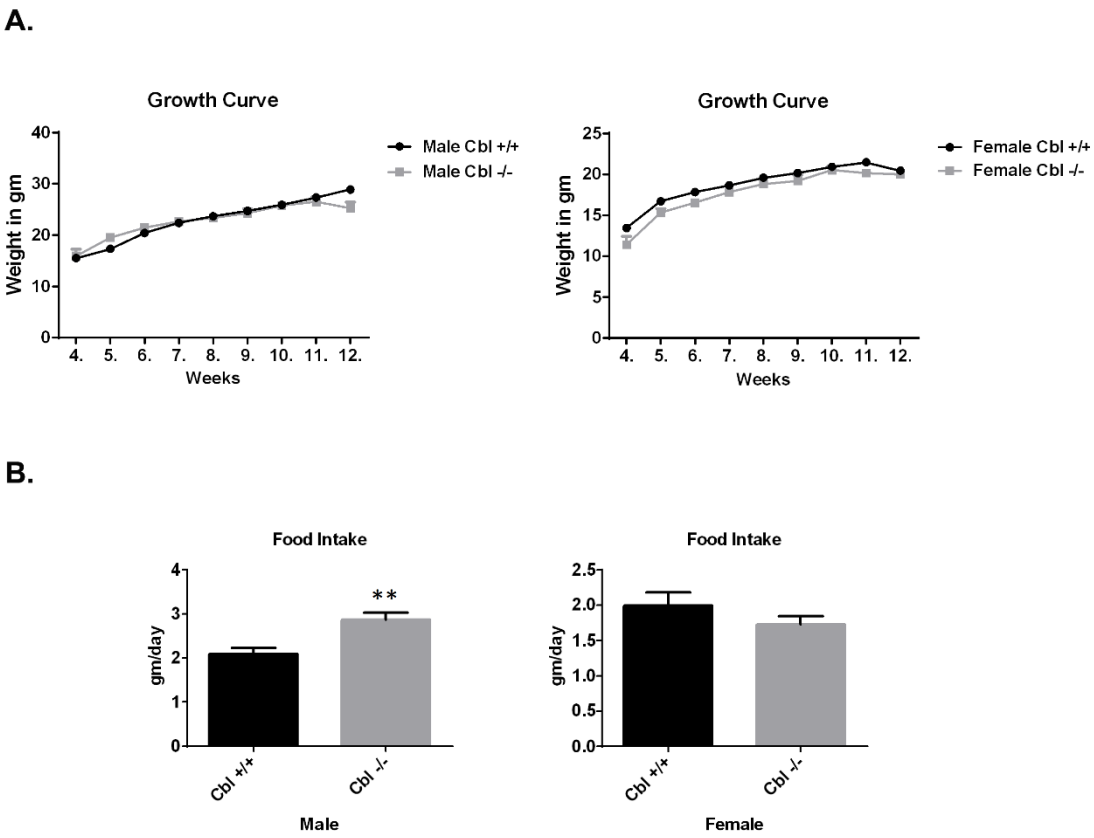

Fig. 15. Growth curves and food intake for Cbl $^{-/-}$ and Cbl $^{+/+}$ mice. A) Growth curves for Cbl $^{-/-}$ and Cbl $^{+/+}$ mice. BW was slightly decreased in female Cbl $^{-/-}$ mice. Data shows mean ± SEM of weekly weight (Cbl $^{+/+}$: male n=18, female n=12; Cbl $^{-/-}$: male n=14, female n=17. **B)** Food intake for Cbl $^{-/-}$ and Cbl $^{+/+}$ mice (n=7-10 males per groups and n=3 females per groups). Food intake was significantly increased in male but not in female Cbl $^{-/-}$ mice. Graphs show mean ± SEM. Statistical analysis: multiple and unpaired t-test were used respectively, ** indicates $p<0.01$.

3.3 White adipose tissue morphology and triglyceride content

Previous findings by Molero *et al.*[18, 22] had reported that the Cbl $^{-/-}$ mice on the 129/SvJ x C57BL/6 background had reduced adipose tissue mass. To determine whether Cbl $^{-/-}$ mice on a C57BL6 background displayed differences in AT morphology, we examined histological sections of perigonadal WAT by haematoxylin and eosin staining (Fig. 16A, B, C, D). We found no differences in adipocyte morphology or cell size in the samples obtained from young (12 weeks) or old (30 weeks old) mice (Fig. 16A, B, C, D). These data were then extended to include biochemical determination of triglyceride content. We found that the triglyceride content of adipose tissue from male Cbl $^{-/-}$ mice was significantly lower compared to Cbl $^{+/+}$ littermates with no significant changes detected in female mice (Fig. 16E).

3.4 Brown adipose tissue morphology, UCP-1 expression and triglyceride content

We next examined BAT morphology in histological sections of interscapular adipose depots. We found that adipose cell size of BAT from male Cbl $^{-/-}$ mice was not different from that of male Cbl $^{+/+}$ in young (12 weeks) or old (30 weeks old) mice (Fig. 17A, B). No differences were observed in triglyceride content of BAT between Cbl $^{-/-}$ and Cbl $^{+/+}$ mice (Fig. 17C). We did not detect any difference in UCP1 expression by western blot analysis (Fig. 18A, B) or by immunohistochemistry (Fig. 19).

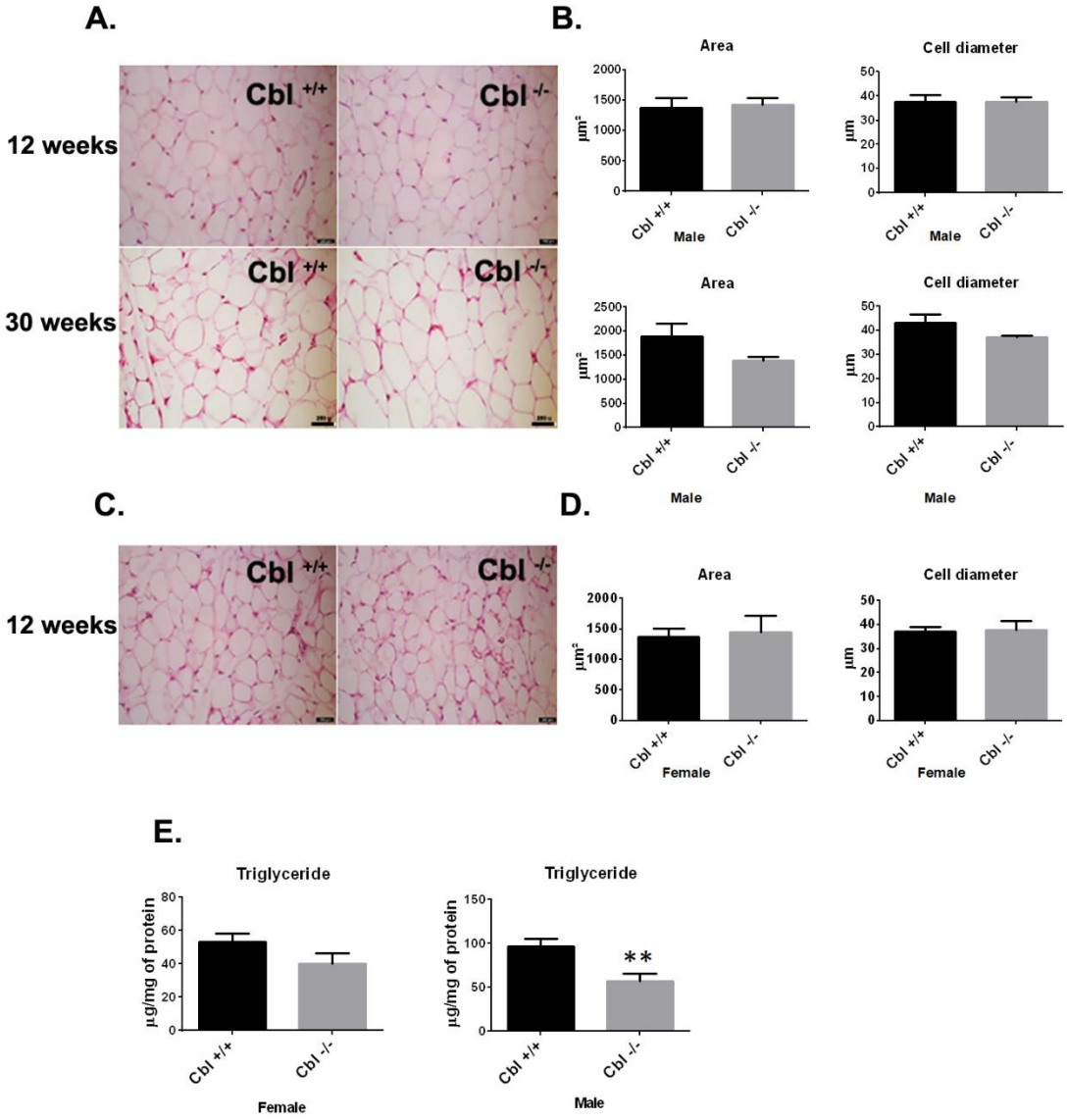

Fig. 16. White adipose tissue (WAT) morphology and triglyceride content. No changes in adiposity in Cbl $^{-/-}$ mice. **A)** Haematoxylin-eosin staining of epididymal WAT of Cbl $^{-/-}$ and Cbl $^{+/+}$ male mice at 12 weeks of age (top panel) and at 30 weeks (bottom panel). Representative images are shown of histochemical pictures obtained at 40X magnification. **B)** Quantification: Adiposoft-ImageJ was used to quantify cell diameter of n=100 cells and cell area n=50 cells per sample. Top graphs correspond to 12 weeks old mice Cbl $^{+/+}$ n=9 and Cbl $^{-/-}$n=12, and bottom to 30 weeks old mice, n= 3 Cbl $^{+/+}$ and 4 Cbl $^{-/-}$. There was a slight decrease in adipocytes area and cell diameter in old age Cbl $^{-/-}$ compared to Cbl $^{+/+}$. **C)** WAT obtained from female mice (12 weeks old) Cbl $^{+/+}$ n=9 and Cbl $^{-/-}$n=12. **D)** Shows quantification of female adipocyte cell area and cell diameter of n=100 cells and cell area n=50 cells per sample. **E)** Triglyceride content in WAT obtained from age matched (12-14 weeks old) Cbl $^{+/+}$ and Cbl $^{-/-}$ mice, n=10-15 mice per genotype

of both gender. Graphs show the mean ± SEM. Statistical analysis: unpaired t-test, ** indicates $p<0.01$.

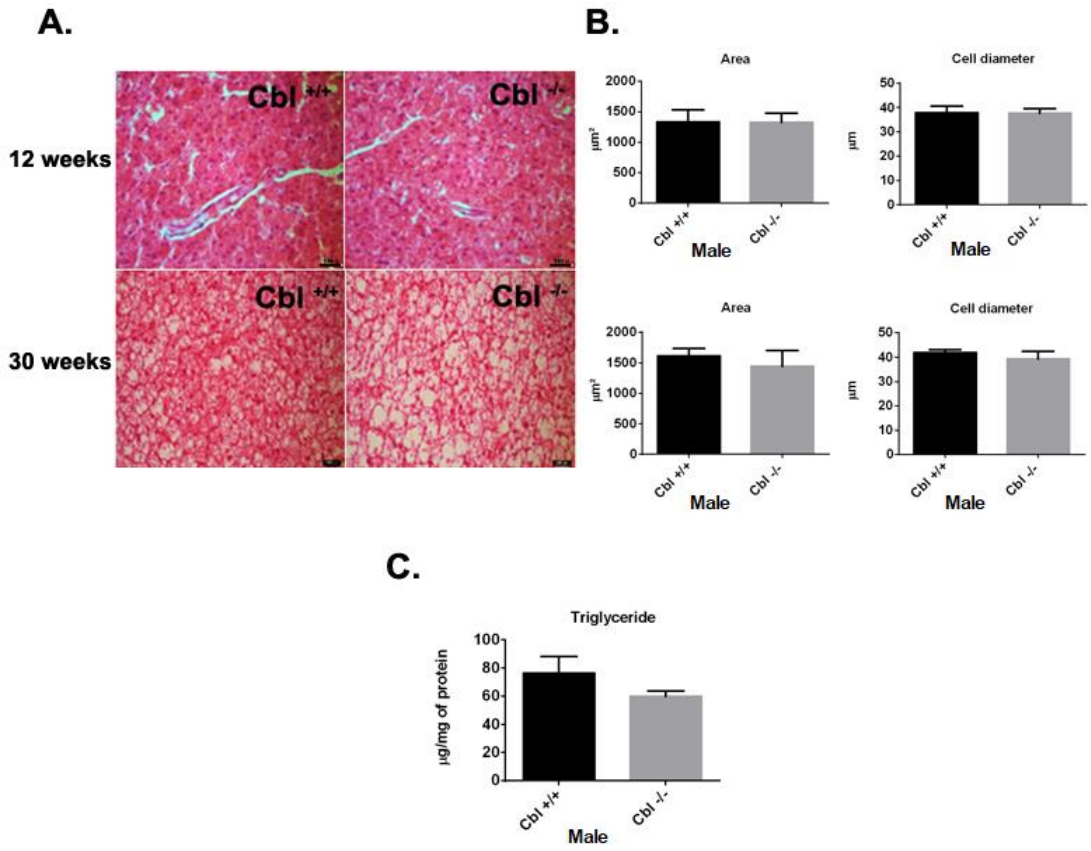

Fig. 17. Brown adipose tissue morphology and triglyceride content. A) Haematoxylin-eosin staining of brown adipose tissue of male Cbl $^{+/+}$ and Cbl $^{-/-}$mice. Representative images are shown of pictures obtained at 40X magnification. Top panels are mice at 12 weeks old and the bottom panels are at 30 weeks of age. **B)** Quantification: Adiposoft-ImageJ was used to quantify cell diameter n=100 cells and cell area n=50 cells per genotype. Top graphs correspond to data obtained from 12 weeks old male and the bottom graphs to 30 weeks old male mice. 12 weeks Cbl $^{+/+}$ and Cbl $^{-/-}$mice n= 4-6 mice per group and 30 weeks old male mice n=4. **C)** Triglyceride content of BAT in age matched (12-14 weeks) Cbl $^{+/+}$ and Cbl $^{-/-}$ mice. Data represent the means ± SEM of 12 weeks old male mice n=4 mice per group.

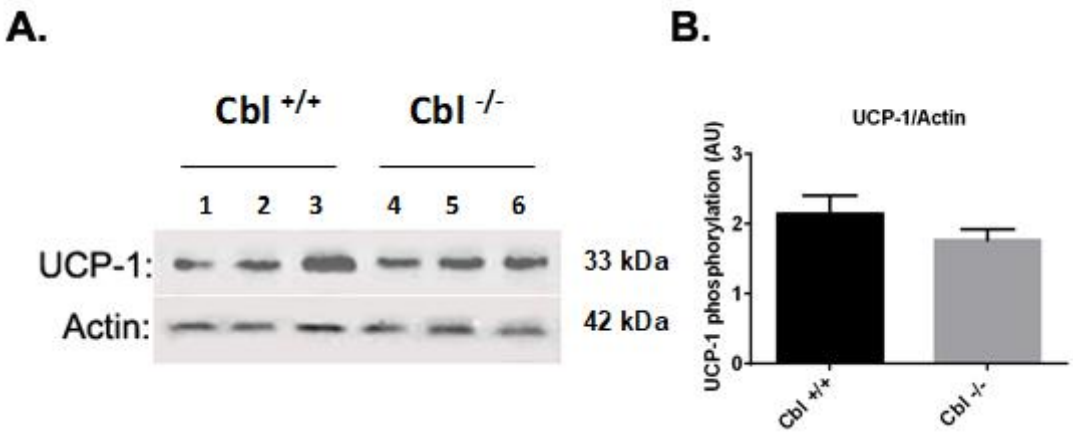

Fig. 18. UCP-1 expression in BAT obtained from Cbl $^{-/-}$ and Cbl $^{+/+}$ mice. **A)** Left panel shows a representative western blot of UCP-1 in BAT lysates obtained from Cbl $^{-/-}$ and Cbl $^{+/+}$ mice. **B)** Right panel shows the blot quantification. Graphs are mean ± SEM of 10 animals per genotypes (male and female). Statistical analysis: unpaired t-test.

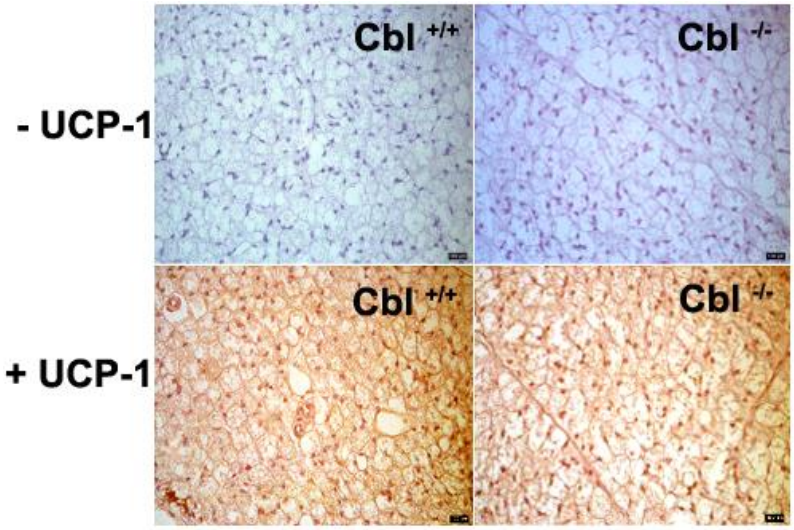

Fig. 19. Immunohistochemical analysis of UCP-1 in Cbl $^{-/-}$ and Cbl $^{+/+}$ mice. Immunohistochemistry was performed on BAT sections using UCP-1 antibody, the goat anti-mouse antibody (1:200) and ImmPRESS REAGENT Anti-Goat Ig, peroxidase Kit (Vector Laboratories) as specified in the methods section. Top panels show a negative control without the primary antibody. Bottom panels show reactivity in the presence of UCP-1 antibody.

3.5 The effects of c-Cbl depletion on insulin sensitivity

Cbl $^{-/-}$ mice from the 129/SvJ x C57BL/6 background had been shown to be more insulin sensitive than wild type mice [22]. We examined insulin sensitivity *in vivo* in Cbl $^{-/-}$ mice on a C57BL6 background (Fig. 20). We performed *in vivo* whole-body glucose tolerance tests and insulin tolerance tests in overnight fasted mice at week 9-10 of age.

Similarly to what was observed in the previous study [22], we found that Cbl $^{-/-}$ mice showed a tendency towards an increase in glucose tolerance although it did not reach statistical significance for either gender (Fig. 20A). However, ITT in male Cbl $^{-/-}$ mice showed improved insulin sensitivity (Fig. 20B) but this was not observed in female mice.

We next examined whether insulin signalling cascades were altered *in vitro* in white adipose tissue obtained from perigonadal depots (Fig. 21). To do this, we cultured adipose tissue explants that were then either untreated or stimulated with insulin for 30 minutes at final concentrations of 0 nM, 1 nM, 10 nM and 100 nM.

Whole tissue lysates were obtained, and we determined the activation or phosphorylation of AKT (PI3 Kinase) and MAPK signalling pathways by western blot analysis. We observed that insulin effectively activated PI3-kinase to a similar extent in both genotypes as determined by the level of phosphorylation of AKT at Ser473 seen in both male and female Cbl $^{-/-}$ and Cbl $^{+/+}$ (Fig. 21A, B, D, E). However, while the maximal activation of ERK proteins was achieved to a similar extent with submaximal insulin concentrations in the two genotypes, both male and female Cbl $^{-/-}$ mice showed a greater ERK phosphorylation in the basal (untreated) state with approximately 40% more phosphorylation of p44/p42 compared to Cbl $^{+/+}$ mice (Fig. 21A, C, D, F) even though the abundance of total ERK protein in the lysates was

similar. One possible contributor to the increased insulin sensitivity is enhanced abundance of insulin signalling molecules in Cbl $^{-/-}$. Thus, we next examined the expression of insulin receptors substrate-1 (IRS-1) and insulin-responsive glucose transporter GLUT4 in WAT (Fig. 22A). We found that the protein content of IRS-1 and GLUT4 in WAT of Cbl $^{-/-}$ compared to Cbl $^{+/+}$ control were not different (Fig. 22B, C).

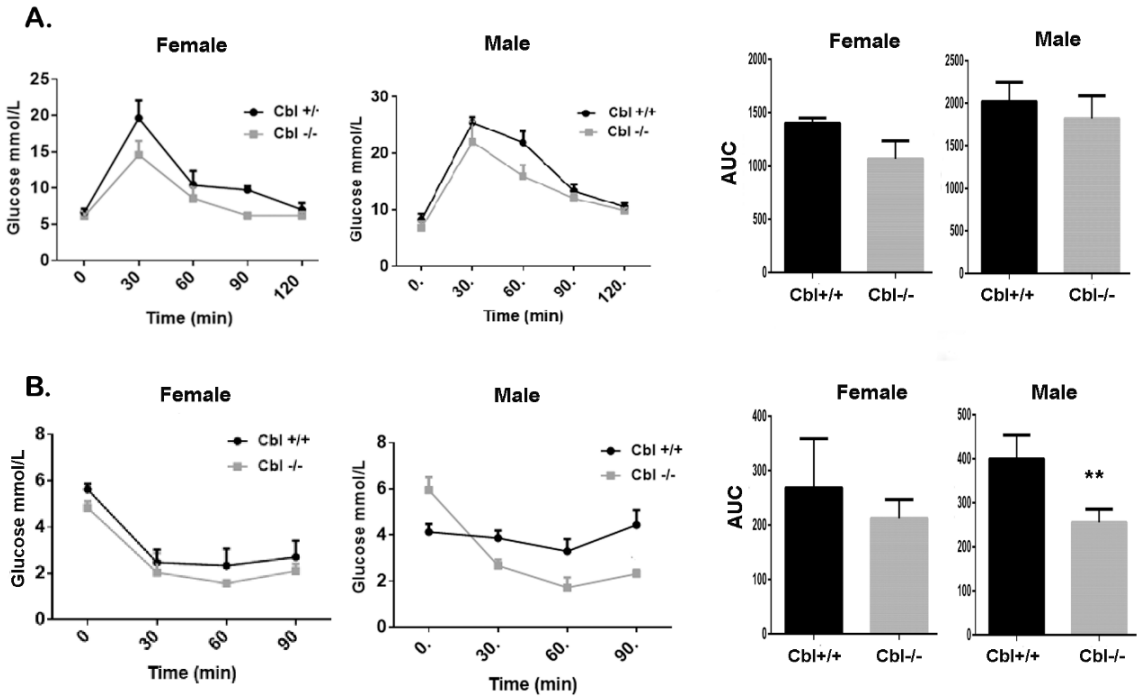

Fig. 20. Glucose tolerance tests (GTT) and insulin tolerance tests (ITT) in Cbl $^{-/-}$ and Cbl $^{+/+}$mice. A) Top left panels represent GTT curves and the right panels are area under the curve (AUC) in female and male mice. GTT was slightly decreased in female and male Cbl $^{-/-}$ mice compared to the control. **B)** Bottom left panels show ITT curves and right panels represent AUC in female and male mice. ITT was significantly decreased in male Cbl $^{-/-}$ mice and slightly so in female Cbl $^{-/-}$ mice compared to their respective wild types. Tests were carried out at weeks 9-10 of age. Mice were injected with glucose 2 g/Kg of body weight or insulin 0.75 U/Kg of body weight and at the times indicated, blood tail samples were obtained, and glucose measured using a glucose meter. Graphs show mean ± SEM of values, male Cbl $^{+/+}$ n = 5, Cbl $^{-/-}$ n = 4; female Cbl $^{+/+}$ n = 3, Cbl $^{-/-}$ n = 3. Statistical analysis, unpaired t-test, ** indicates $p<0.01$.

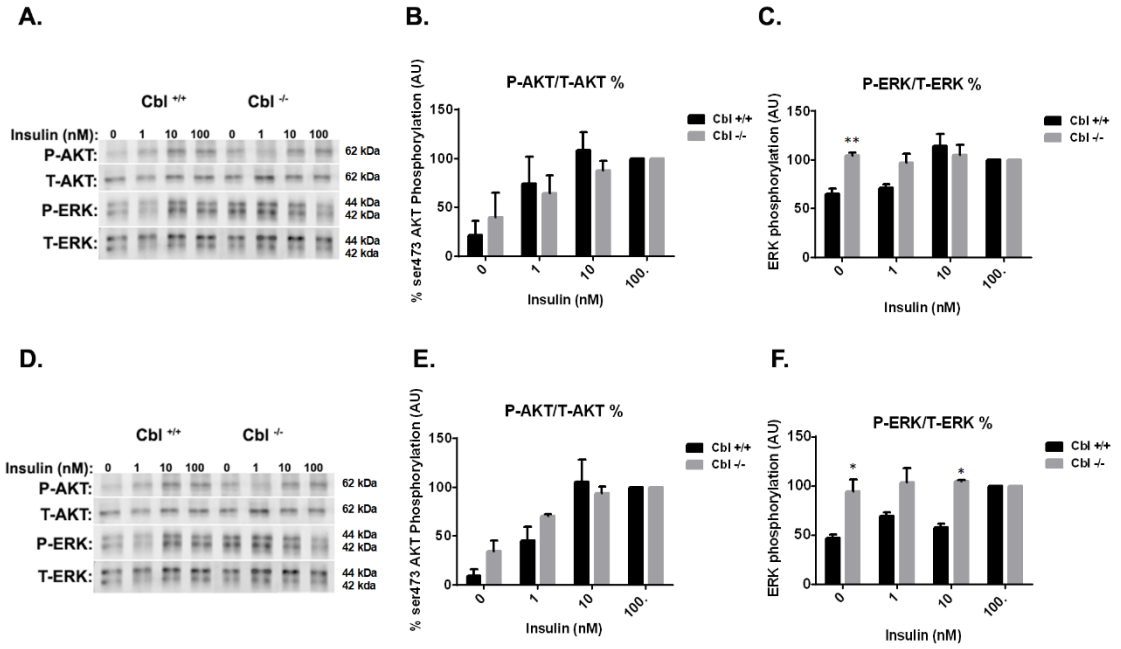

Fig. 21. Insulin activation of PI3K and MAPK pathways in white adipose tissue of Cbl $^{-/-}$ and Cbl $^{+/+}$mice. Increased activation of ERK in adipose tissue of Cbl $^{-/-}$ mice. White adipose tissue explants of Cbl $^{-/-}$ and Cbl $^{+/+}$male **A)** and female mice **D)** were obtained and either untreated or treated with insulin at the indicated concentrations (0-100nM), separated onto SDS-PAGE and immunoblotted with antibodies as indicated. Panels **B) C) E) and F)** show the quantification of AKT and ERK phosphorylation relative to the total AKT or ERK protein respectively from 5 experiments**.** Graph shows mean ± SEM of phosphorylation over basal as % of Ser473 (AKT) or T202/204 and Thr185/Tyr187, respectively. Statistical analysis, multiple t-test, * indicates $p<0.05$ and ** $p<0.01$.

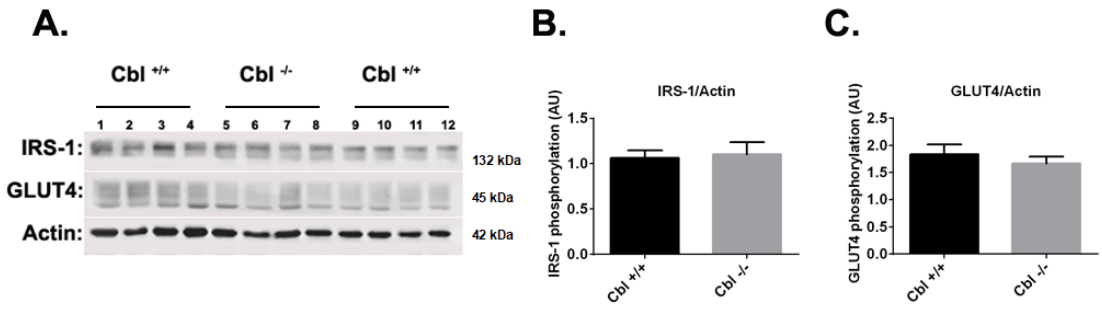

Fig. 22. Expression of insulin signalling proteins and glucose transporter GLUT4 in WAT obtained from Cbl $^{-/-}$ and Cbl $^{+/+}$ mice. **A)** Expression of IRS-1 and GLUT4. **B)** and **C)** Quantification of expression relative to actin. Graphs show mean ± SEM of n=4 Cbl $^{-/-}$ and n=8 Cbl $^{+/+}$ mice. Statistical analysis: unpaired t-test.

3.6 Effects of c-Cbl knockdown in 3T3L1 adipocytes

The data described above suggested that c-Cbl depletion enhances MAPK signalling in Cbl $^{-/-}$ mice. To confirm that c-Cbl gene depletion was directly responsible for the changes in signalling in adipose tissue in the Cbl $^{-/-}$ mice and was not due to alterations in other organs, we reasoned that depletion of c-Cbl expression in the adipocyte 3T3L1 mouse cell line would replicate the findings seen *in vivo*. To this end, undifferentiated 3T3L1 cells were either untreated or infected with lentiviral particles expressing validated shRNAs for the c-Cbl gene (Cbl KD) or infected with lentiviral particles expressing a non-targeting shRNA (NT-shRNA) or infected with lentiviral particles containing an empty vector (EV) as an additional control. Stable cell lines were selected in the presence of puromycin as our group has previously reported [192] and following amplification the selected cells were differentiated to obtain fully differentiated adipocytes [193]. No changes were observed in the differentiation of 3T3L1 cells between Cbl KD and control (NT-shRNA and WT) cells as observed by phase contrast light microscopy (Fig. 23).

Expression of c-Cbl in differentiated 3T3L1 cells was significantly reduced in Cbl KD cells compared to cells expressing NT-shRNA or EV (Fig. 24A). Insulin treatment resulted in the activation of the PI3-kinase cascade and phosphorylation of AKT in Ser473 to a similar extend in Cbl knockdown cells compared to control cells (Fig. 24A, B). Interestingly as found *in vivo,* we detected enhanced phosphorylation of ERK in c-Cbl knockdown cells compared to control cells (Fig. 24A, B). No change was observed in the expression of insulin receptor IR between NT-shRNA and Cbl KD 3T3L1 cells (Fig. 24C, D).

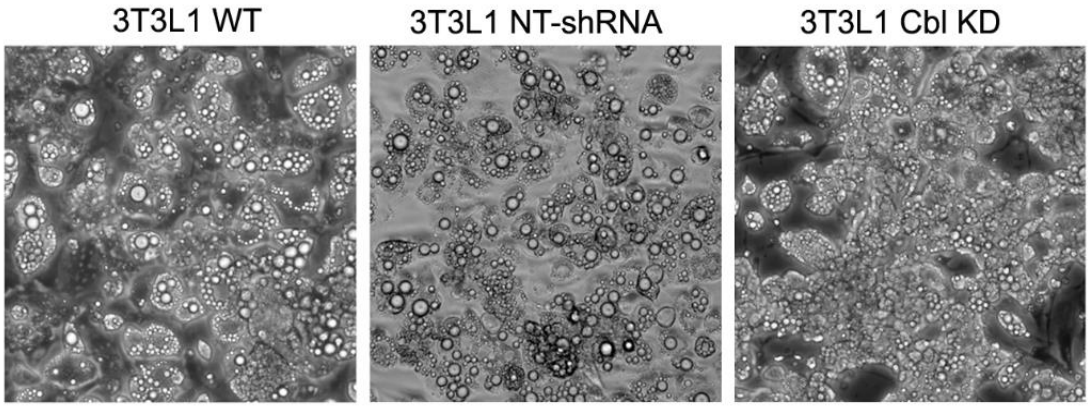

Fig. 23. Differentiation of 3T3L1 adipocytes. Control cells or c-Cbl deficient 3T3L1 adipocytes were differentiated as described in Chapter 2. Images were taken for each group in a Leica DMI 600 inverted microscope at 20x magnification. Representative experiment**.**

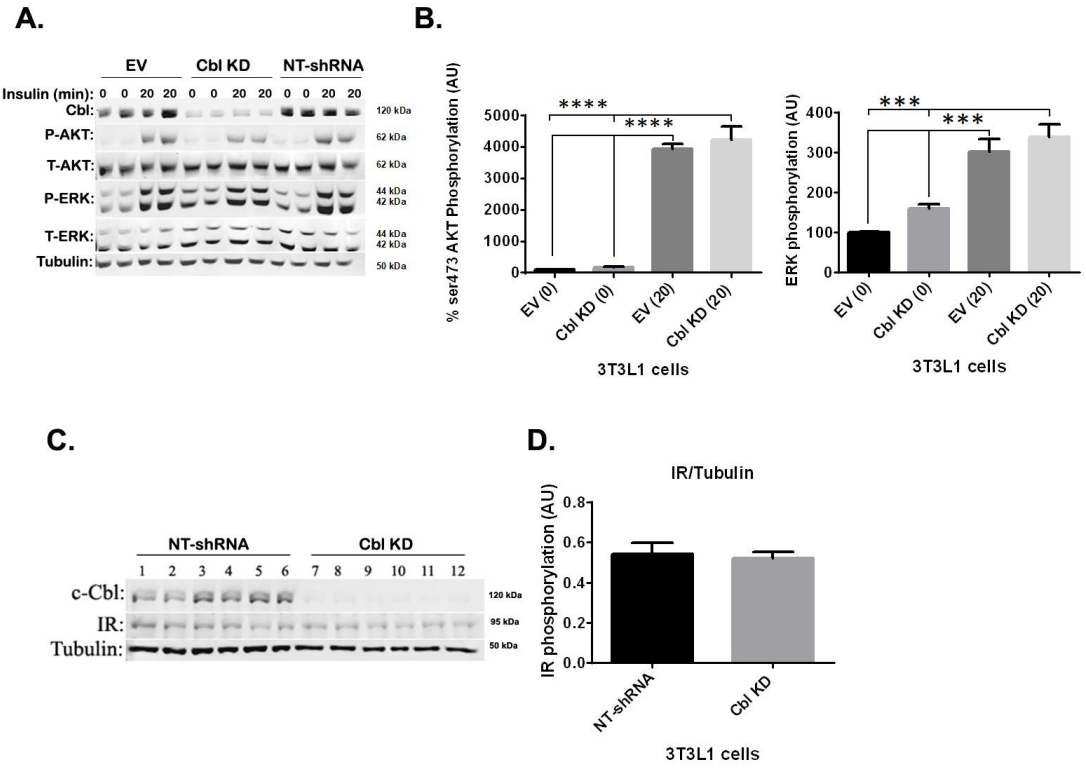

Fig. 24. The PI3K and the MAPK pathways and AMPK in 3T3L1 cells. **A)** Increased activation of ERK in c-Cbl Knockdown 3T3L1 adipocytes. Fully differentiated 3T3L1 adipocyte cells expressing control plasmids (empty vector EV or NT-shRNA) or expressing shRNAs for c-Cbl (Cbl KD) were left untreated (0) or stimulated with insulin (100 nM) for 20 minutes (20). Cellular lysates were obtained, loaded onto SDS-PAGE and immunoblotted with the indicated antibodies. Representative blot of 5 experiments. **B)** Shows the quantification as mean ± SEM of intensities in arbitrary units of AKT (Ser473) and ERK (T202/204 and Thr185/Tyr187) respectively, obtained in 5 independent experiments. Statistical analysis: ANOVA-one way, Tukey's multiple comparisons test, ***indicates $p<0.001$; **** $p < 0.0001$. **C)** IR expression in 3T3L1 cells. Left panel western blot of 3T3L1 cells shows NT-shRAN and Cbl KD. **D)** Right panel shows quantification of the blot. Graphs are mean ± SEM of n=3 experiments. Statistical analysis: unpaired t-test.

3.7 AMPK signalling in WAT of Cbl $^{-/-}$ mice and in 3T3L1 Cbl KD cells

Previously, Molero *et al.*[22] found an increase in AMPK activity in skeletal muscle from c-Cbl $^{-/-}$ mice. Activation of AMPK in adipocytes inhibits lipolysis [204, 205]. We sought to determine whether AMPK was more readily activated in adipocytes depleted of c-Cbl. We examined the relative abundance of AMPK phosphorylation at the Thr172 site in WAT lysates obtained from Cbl $^{-/-}$ or Cbl $^{+/+}$ mice. As a positive control for our western, we included cellular lysates obtained from adipose cells that had been treated with 5-Aminoimidazole-4-carboxamide ribonucleotide (AICAR) a pharmacological activator of AMPK. We observed no significant differences in AMPK phosphorylation in Cbl $^{-/-}$ and Cbl $^{+/+}$ mice (Fig. 25A, B). On the other hand, we found that AMPK phosphorylation was significantly reduced in Cbl KD 3T3L1 cells compared to NT-shRNA, with no significant change in comparison to EV expressing 3T3L1 adipocyte cells (Fig. 26A, B).

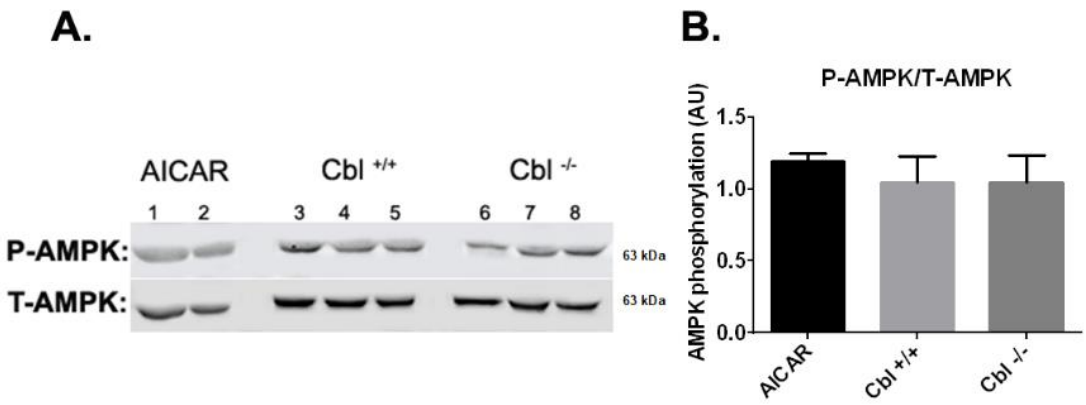

Fig. 25. AMPK phosphorylation in WAT obtained from Cbl $^{-/-}$ and Cbl $^{+/+}$ mice. **A)** Left panel western blot analysis of phospho-AMPK*thr) in WAT from Cbl $^{-/-}$ and Cbl $^{+/+}$mice and AICAR treated 3T3L1 cells. **B)** Right panel shows the quantification. Graphs show mean ± SEM n=3 independent experiments. Statistical analysis: unpaired t-test.

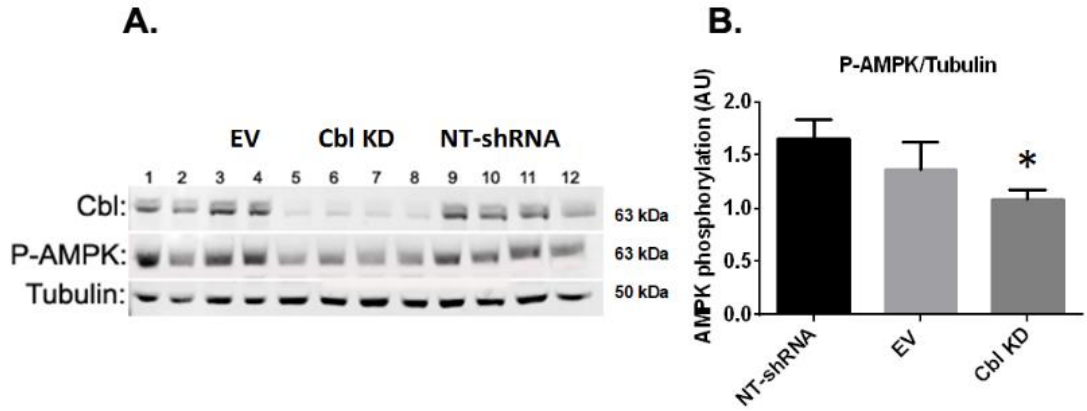

Fig. 26. AMPK phosphorylation in 3T3L1 cells. **A)** Left panel, western blot for phospho-AMPK of cellular lysates obtained from 3T3L1 cells expressing either vector (EV), NT-shRNAs or shRNAs for Cbl KD. **B)** Right panel, quantification of data obtained in 4 independent experiments (n=10 biological replicates). Graphs are mean ± SEM. Statistical analysis: unpaired t-test * indicates $p<0.05$

3.8 Discussion

In the present study, we tested the hypothesis that c-Cbl deficiency impacts on adiposity and insulin responsiveness in C57BL6 mice. It had been previously shown by Molero *et al.* [18, 22] that Cbl $^{-/-}$ mice on a different background showed reduced adiposity, triglyceride levels and increased food intake than control mice. We determined that Cbl $^{-/-}$ mice on a C57BL6 background did not display any significant growth differences compared with Cbl $^{+/+}$ mice. However, food intake was significantly higher in male Cbl $^{-/-}$ compared to wild type mice, while triglyceride content in WAT was significantly lower in male Cbl $^{-/-}$ compared to Cbl $^{+/+}$ mice, which might be attributable to increase energy expenditure in Cbl $^{-/-}$ mice. These findings were consistent with the studies of Molero *et al.* [18, 22].

It was reported that c-Cbl depletion increases muscle metabolism, enhanced energy expenditure and reduced adiposity [22]. The Cbl $^{-/-}$ mice used in our studies did not show any adipose tissue morphology abnormalities or differences in adipocyte cell size, which contradicts the findings of Molero *et al.* [22] who reported lower adipocyte diameter in Cbl $^{-/-}$ compared to wild type. These findings suggest small differences in the phenotype that may be attributable to distinct genomic backgrounds.

Earlier studies [23, 169] have reported that c-Cbl protein is a vital component of the insulin signalling pathway in 3T3-L1 adipocytes that regulates insulin-stimulated glucose transport. Another study [206] reported that suppression of c-Cbl in 3T3-L1 adipocytes by RNA interference-mediated (RNAi-mediated) had no effect on insulin-stimulated glucose transport and suggested that Cbl proteins are not a required for insulin signalling and GLUT4 regulation in either cultured 3T3-L1 or primary adipocytes from Cbl $^{-/-}$ mice [206]. Molero *et al.* [18, 22] found that glucose tolerance and insulin sensitivity were improved in Cbl $^{-/-}$ mice on a Jvs129 x C57BL6

background, and they observed a considerable increase in muscle insulin-stimulated glucose uptake both *in vivo* and *ex vivo*. In the current study, we observed the male Cbl $^{-/-}$ mice replicated the insulin sensitivity phenotype described in the previous studies [18, 22], but females were not significantly different to wild type.

The improvement in insulin sensitivity in Cbl $^{-/-}$ mice, suggested there might be an increase in insulin signalling pathway in Cbl $^{-/-}$ mice. To confirm these findings, we examined insulin signalling in WAT through PI3K and MAPK pathways. We found increased basal activation of ERK1/2 in the adipose tissue of Cbl $^{-/-}$ mice. Consistent with our finding, Zhang *et al.* [207] also showed that the absence of c-Cbl increased ERK phosphorylation in c-Cbl $^{-/-}$ bone marrow-derived mast cells (BMMC) compared to the control cells [207].

To confirm the finding that c-Cbl gene depletion was directly responsible for the increased basal ERK phosphorylation levels and not due to some systemic effect, we established 3T3L1 adipocyte cells depleted of c-Cbl (Cbl KD 3T3L1). We observed a significant increase in ERK phosphorylation levels in Cbl KD cells compared to control cells, similar to our finding in Cbl $^{-/-}$ mice. Together the data indicate that deletion of c-Cbl gene is responsible for increasing MAPK activity. It has been published that activation of MAPK had profound effects on the differentiation program of 3T3-L1 preadipocytes [208, 209] by increasing the phosphorylation of PPARγ [209]. Thus, inhibition of ERK1/2 resulted in reduced adipocyte differentiation [210, 211]. However, we did not observed differences in the differentiation of 3T3L1 adipocytes between Cbl KD and control cells (NT-shRNA and WT).

However, it remains possible that the effects of increased ERK1/2 activation might be dependent on Cbl action as an E3-Ubiquitin ligase for example acting on ERK1/2 regulatory proteins, targeting an upstream ERK kinase or through an inhibitory effect

of an ERK phosphatase. In addition, the regulation of MAP kinase activity by Cbl may be mediated by intermediary molecules, because no direct interaction between Cbl and MAP kinases has been established [182]. Cbl might control MAP kinase activation by inhibiting tyrosine kinases (such as ZAP-70) that have been shown to be linked with MAP kinase activation in T cells. Alternatively, SOS, a Ras GDP release factor, and Cbl bind to the same SH3 domain of Grb2, an adaptor protein known to interact with phosphorylated receptors and to link RTKs with activation of the Ras pathway. Therefore, Cbl may compete with SOS for binding sites on Grb2 and consequently reduce the number of Grb2 molecules available for SOS-mediated activation of the Ras-MAP kinase pathway [182, 212]. Further research is necessary to identify the molecular mechanisms for increased basal ERK1/2 phosphorylation in c-Cbl depleted adipose cells.

Indeed, c-Cbl proteins have dual functionalities. They act as adaptor proteins for tyrosine kinase receptors, including the insulin receptor, and recruit signalling proteins in the caveolae of adipose cells [213]. In addition, c-Cbl proteins can function as an E3-ubiquitin ligase enzyme, thus facilitating the degradation of proteins including TKR. Molero *et al.* [22] had found increased insulin receptor expression in the skeletal muscle of Cbl $^{-/-}$ mice. However, we did not detect any changes in the expression levels of the glucose transporter GLUT4 or IRS-1. Furthermore, we found signalling through PI3-kinase in response to insulin was unremarkable in Cbl $^{-/-}$ compared to the wild type mice indicating equal insulin receptor substrate-1 and PI3-kinase activation. This was consistent with Molero *et al.* [18] who found no significant difference in the phosphorylation of AKT in Cbl $^{-/-}$ compared with Cbl $^{+/+}$ mice, in the absence of insulin stimulation, when they examined skeletal muscle.

We next examined the impact of c-Cbl deletion on AMPK activation in WAT of Cbl $^{-/-}$ mice and 3T3L1 Cbl KD cells. Molero *et al.* [22] found an increase in AMPK activity in skeletal muscle from Cbl $^{-/-}$ mice. We found no significant differences in phospho-AMPK in WAT of Cbl $^{-/-}$ compared to Cbl $^{+/+}$ mice. Whereas in 3T3L1 cells, AMPK phosphorylation was significantly lower in Cbl KD 3T3L1 compared to NT-shRNA 3T3L1 cells. Daval *et al.* [204] reported that activation of AMPK in muscle increases fatty acid oxidation. However, in adipocytes several studies report an anti-lipolytic effect of AMPK [205, 214, 215], whereas others suggest AMPK stimulates lipolysis [216, 217]. AMPK is activated in adipose tissue in conditions of increased lipolysis such as exercise and fasting [204, 205, 218, 219]. This activation inhibits fatty acid and triglyceride synthesis and could limit lipolysis [204]. This is might be the reason for detecting no changes in AMPK activation in Cbl $^{-/-}$ mice because we examined these mice in a fed state.

In this chapter, we have shown that c-Cbl depletion in adipocytes is associated with increased basal activation of extracellular regulated kinases (ERK1/2) in both Cbl $^{-/-}$ mice and c-Cbl knocked-down 3T3L1 adipose cells. Further research is necessary to identify the underlying molecular mechanisms. Moreover, it seems possible that one consequence is altered adipokine expression which might contribute to changes in insulin sensitivity.

Chapter 4

Adipokine secretion in c-Cbl deficient white adipocytes

4 Introduction

Adipose tissue was for many years considered to be energy storage organ, but it is now recognized as an active endocrine organ that secretes a variety of bioactive molecules, known as adipocytokines or adipokines [89, 220], that contribute to the regulation of metabolism [13]. Adipokines act as circulating hormones to communicate with other organs including: the brain, liver, muscle and the immune system, but they also act in an autocrine manner to have effects on adipose tissue itself [16]. Adipokines are recognized to have multiple functions including: regulating food intake, insulin sensitivity and modulating inflammatory processes [62]. For example: leptin functions as a satiety factor and suppresses food intake in the hypothalamus [13, 16]; in the periphery, leptin increases fatty acid oxidation notably in skeletal muscle and improves insulin sensitivity through the activation of AMPK [13, 89, 101]. Moreover adiponectin has direct actions on liver, skeletal muscle and the vasculature, where it improves hepatic insulin sensitivity, increases muscle fatty acid oxidation and decreases vascular inflammation [221]. Additionally, RBP4 is involved primarily in the transport of retinol in the circulation [121], however, it has also been shown that increased RBP4 levels impair insulin signalling in muscle and liver [13, 121], and its expression is inversely correlated with that of GLUT4 in adipocytes [127].

Macrophages residing within AT secrete other proinflammatory cytokines including TNF-α and IL-6 that also contribute to the development of insulin resistance [8, 89, 95].

I reported in the previous chapter, that c-Cbl depletion in mice and in 3T3L1 cells increases basal ERK (p44/p42) activation in white adipocytes. In this chapter I tested the hypothesis that c-Cbl, through this signalling pathway, may contribute to the production and secretion of adipokines/cytokines such as adiponectin, leptin, RBP4,

IL-6 and TNF-α that might influence insulin sensitivity and/or insulin resistance related to obesity and T2D.

To determine whether an altered expression of these adipokines could contribute to increased insulin sensitivity. I examined the expression in WAT of Cbl $^{-/-}$ and Cbl $^{+/+}$ mice using a protein array and ELISA. I determined the circulating levels of several adipokines in both fed and fasting conditions. The findings were confirmed in the 3T3L1 c-Cbl knockdown adipocyte cell line and in control 3T3L1 cells.

4.1 The effects of c-Cbl deletion on adipokine expression in WAT of Cbl $^{-/-}$ mice

To determine the molecular mechanisms of increased insulin sensitivity in Cbl $^{-/-}$ mice and to determine whether altered expression of white adipose adipokines could contribute to this effect, we sought to investigate the adipokine profile in visceral WAT, plasma and liver of Cbl $^{-/-}$ mice and their littermate controls using an adipokine protein array. The latter allows for the rapid detection of 24 different adipokines. Cells and tissues (WAT and liver) were homogenized as specified in chapter 2 sections 2.8 and 2.10 respectively.

We found that the expression of several adipokines was altered in Cbl $^{-/-}$ mice (Fig. 27). These include: resistin, intercellular adhesion molecule 1 (ICAM-1) and insulin-like growth factor-binding protein 3 (IGFBP-3). The expression of these proteins was increased significantly in Cbl $^{-/-}$ mice compared to wild type controls (Fig. 27). There was also an increase in RBP4, adiponectin, IL-6, IGFBP-2, lipocalin-2, leukemia inhibitory factor (LIF) and vascular endothelial growth factor (VEGF) abundance in Cbl $^{-/-}$ mice compared to Cbl $^{+/+}$ mice. In contrast, we found a decrease in the expression

of leptin, insulin-like growth factor-binding protein 5 (IGFBP-5) and FGF acidic in Cbl $^{-/-}$ mice compared to the control Cbl $^{+/+}$ mice.

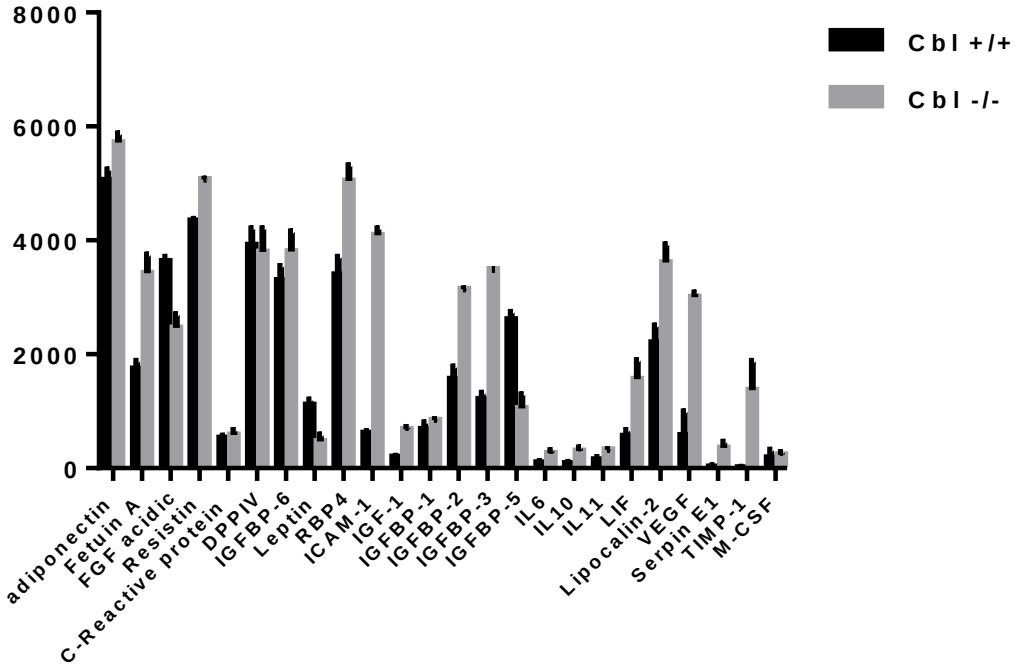

Fig. 27. Protein array for adipokine in WAT of Cbl $^{-/-}$ and Cbl $^{+/+}$. Altered expression of adipokines in WAT of male Cbl $^{-/-}$ mice. Tissue lysates were obtained from perigonadal WAT and adipokines quantified by protein array kit. Graphs show mean ± SD. Cbl $^{+/+}$ and Cbl $^{-/-}$ mice, n=2 male mice per genotype.

These findings were suggestive of a change in adipokines that regulate insulin sensitivity, however this method while informative is not quantitatively accurate. To confirm the results and quantify the relevant adipokines, we validated our data by ELISA or qPCR. All ELISAs were carried out according to the general protocol specified in section 2.15 and section 2.17 for qPCR.

Validation of the results by ELISA revealed a marked gender dimorphism in the white adipose tissue content of some adipokines. In WAT of female Cbl $^{-/-}$ mice (Fig.

28A, B), the abundance of adiponectin was significantly reduced, whereas that of leptin was markedly increased. No significant difference was found in IL-6 in WAT of female Cbl $^{-/-}$ compared to female Cbl $^{+/+}$ mice, whereas IL-6 in male Cbl $^{-/-}$ was significantly reduced compared to male Cbl $^{+/+}$ mice (Fig. 28C). TNFα abundance in WAT was slightly decreased in male Cbl $^{-/-}$, but this was not statistically significant (Fig. 28D), with no change observed in female mice.

The abundance of RBP4 in WAT of female Cbl $^{-/-}$ mice was significantly increased (Fig. 29A). Despite the changes in RBP4 protein levels, no significant changes in the mRNA abundance of RBP4 were detected in WAT (Fig. 29B) of either gender. In contrast, the mRNA abundance of RBP4 in the liver of Cbl $^{-/-}$ mice was markedly elevated compared to that in Cbl $^{+/+}$ mice for both gender (Fig. 29D). However, this did not translate into differences in protein abundance (Fig. 29C).

In the steady state, plasma levels of adiponectin, leptin or RBP4 were unremarkable in Cbl $^{-/-}$ compared to Cbl $^{+/+}$ mice (Fig. 30A, B, C).

We then sought to confirm these data using the 3T3L1 adipocyte cell line depleted of c-Cbl and compared to control cells. Differentiated adipocytes were homogenized and the adipokine content analysed by ELISA. We found that RBP4 abundance was significantly increased in the Cbl KD cells compared to the control cells, leptin abundance was slightly elevated in the c-Cbl depleted cells although this did not reach statistical significance. No changes were observed in adiponectin compared to control cells (Fig. 31A, B, C).

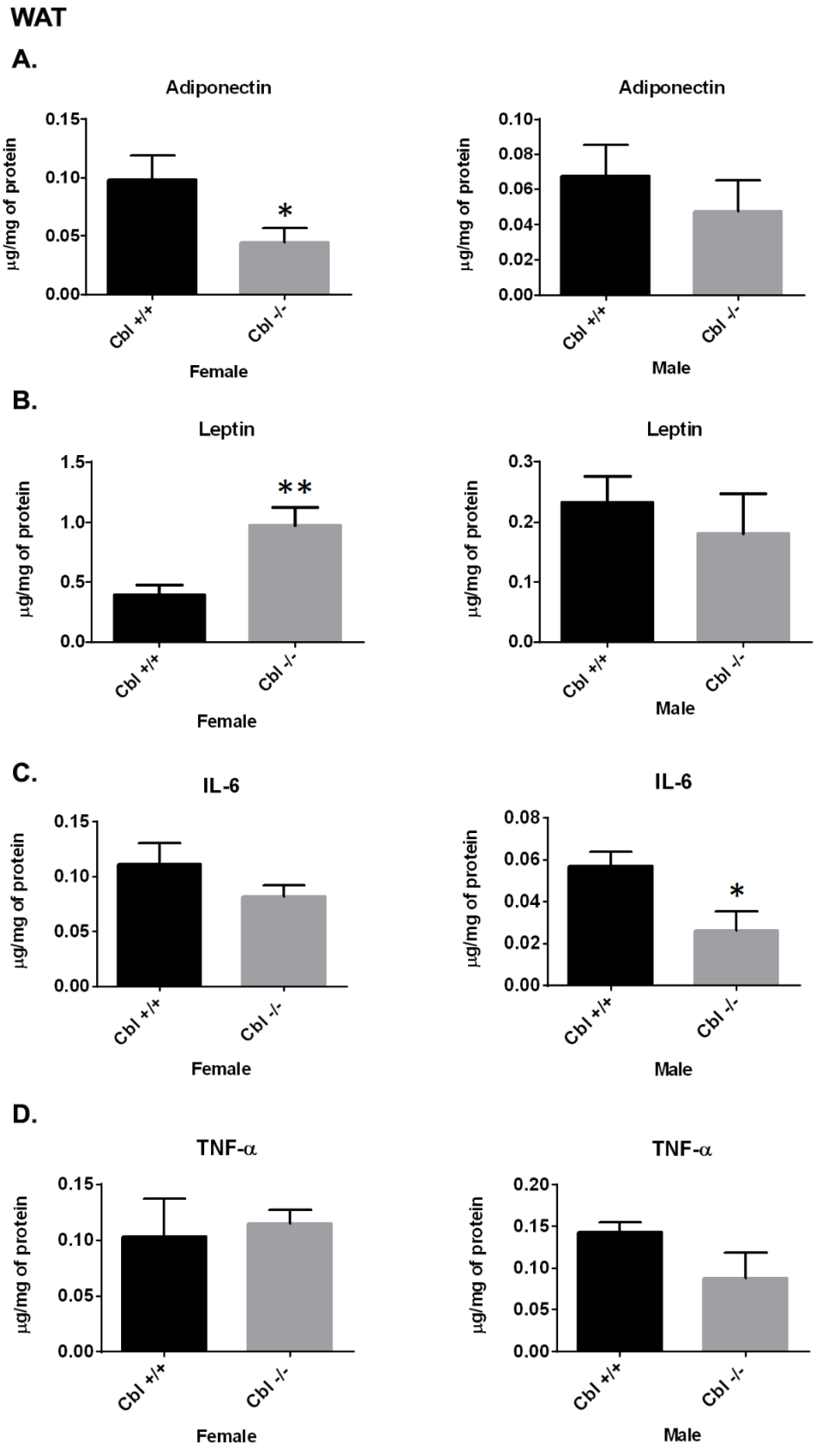
WAT
A.
Adiponectin
µg/mg of protein
0.15
0.10
0.05
0.00
*
Cbl +/+
Cbl -/-
Female
Adiponectin
µg/mg of protein
0.10
0.08
0.06
0.04
0.02
0.00
Cbl +/+
Cbl -/-
Male
B.
Leptin
µg/mg of protein
1.5
1.0
0.5
0.0
**
Cbl +/+
Cbl -/-
Female
Leptin
µg/mg of protein
0.3
0.2
0.1
0.0
Cbl +/+
Cbl -/-
Male
C.
IL-6
µg/mg of protein
0.15
0.10
0.05
0.00
Cbl +/+
Cbl -/-
Female
IL-6
µg/mg of protein
0.08
0.06
0.04
0.02
0.00
*
Cbl +/+
Cbl -/-
Male
D.
TNF-α
µg/mg of protein
0.15
0.10
0.05
0.00
Cbl +/+
Cbl -/-
Female
TNF-α
µg/mg of protein
0.20
0.15
0.10
0.05
0.00
Cbl +/+
Cbl -/-
Male

Fig. 28. Adipokine expression in WAT. Altered expression of adipokines in WAT of female Cbl $^{-/-}$ mice. Tissue lysates were obtained from perigonadal WAT and adipokines quantified by ELISA as specified in the methods section. Adipokine levels were normalized to the total protein content in the lysate. **A)** adiponectin, **B)** leptin and **C)** IL-6 and **D)** TNF-α in WAT (Cbl $^{-/-}$ n= 3 males, 3 females and Cbl $^{+/+}$ n= 7male, 3 females). Graphs show mean ± SEM, statistical analysis: unpaired t-test, * indicates $p<0.05$; ** $p<0.01$.

A. WAT

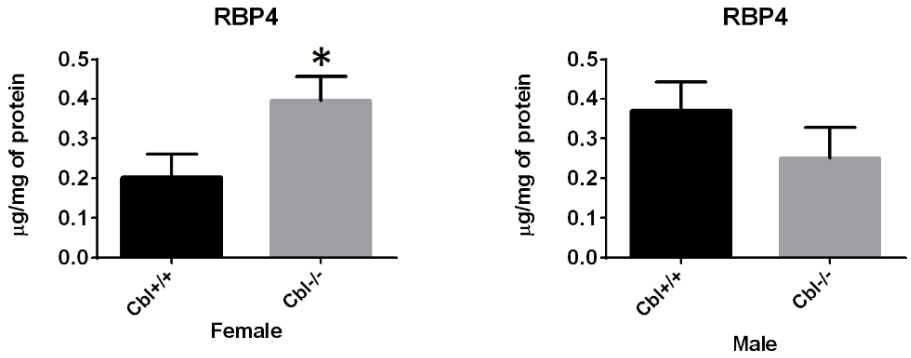

B.

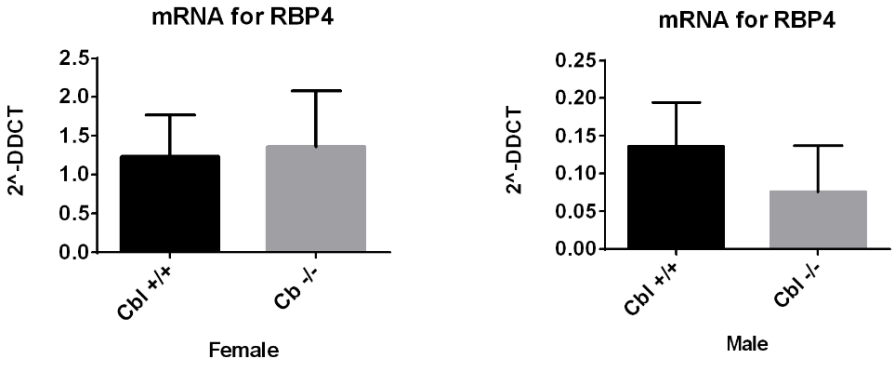

C. Liver

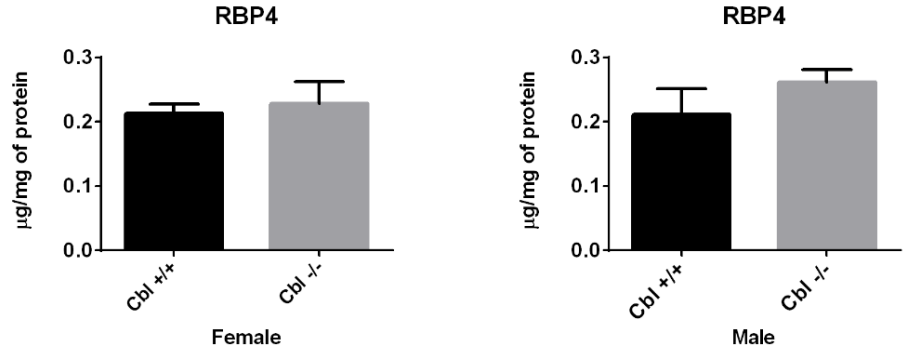

D.

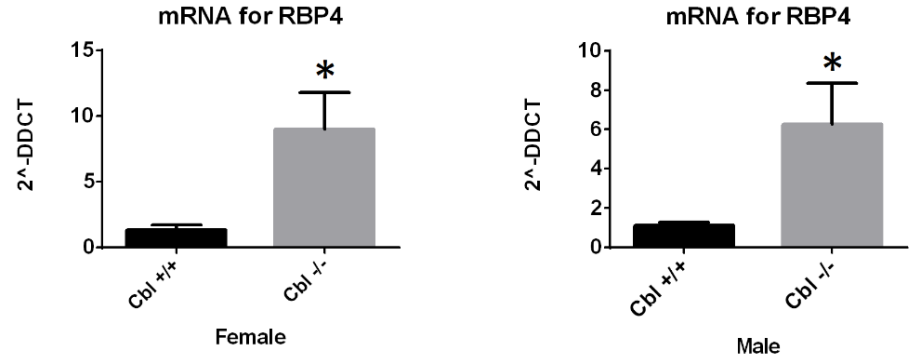

Fig. 29. RBP4 expression in WAT and liver. Increased protein abundance of RBP4 in WAT of female Cbl $^{-/-}$ mice and increased mRBP4 abundance in the liver of Cbl $^{-/-}$ mice for both gender. Tissue lysates were obtained from perigonadal WAT or liver and adipokines quantified by ELISA as specified in the methods section. **A)** RBP4 in WAT (Cbl $^{-/-}$ n= 6 males, 12 females, Cbl $^{+/+}$ n= 15 males, 13 females). **B)** Gene expression of RBP4 abundance relative to 18S determined by qPCR in WAT (Cbl $^{-/-}$ male= 3, female=3 and Cbl $^{+/+}$ male = 3, female= 3). **C)** RBP4 in liver (Cbl $^{+/+}$: male n=4, female n=5; Cbl $^{-/-}$: male n=4, female n=8). **D)** RBP4 mRNA abundance relative to 18S in liver determined by qPCR (Cbl $^{-/-}$ male= 3, female=3 and Cbl $^{+/+}$male = 3, female= 3). Graphs show mean ± SEM of RBP4 normalized to total protein. Statistical analysis: unpaired t-test, * indicates $p<0.05$.

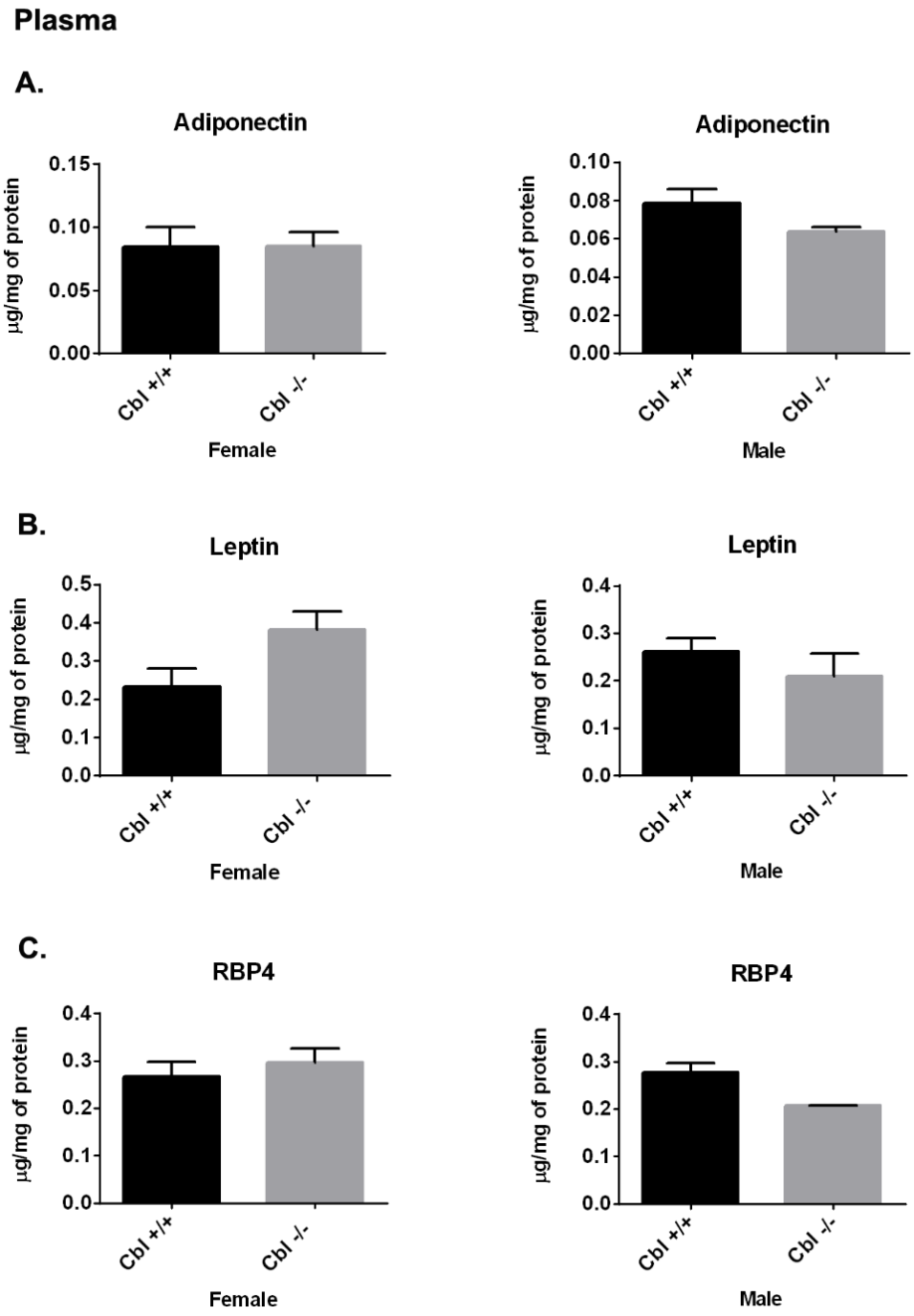

Fig. 30. Adipokine concentrations in plasma. No differences in the plasma abundance of adiponectin, leptin and RBP4. Mice were fasted for 6 hours and euthanized. Plasma was obtained and adipokines were quantitated by ELISA as described in the methods section 2.2 and 2.15 respectively. Graphs show mean ± SEM, statistical analysis: unpaired t-test (Cbl $^{-/-}$ male n= 4, female n= 3, Cbl $^{+/+}$ male n=7, female n=3).

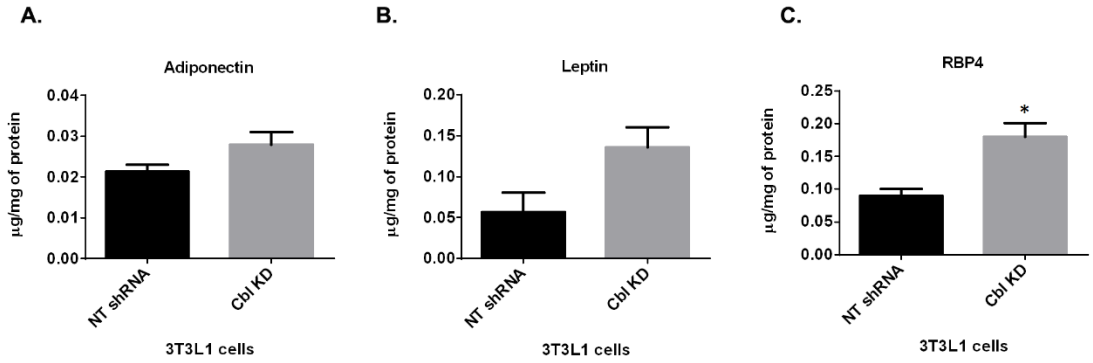

Fig. 31. Adipokine expression in 3T3L1 cells. RBP4, Adiponectin and leptin expression were determined in total cellular lysates by ELISA from control (expressing empty vector (EV) or Non-targeting shRNAs) or Cbl KD cells (expressing shRNAs for c-Cbl). Graphs are mean± SEM of N=5 sample replicates. Statistical analysis: unpaired t-test * indicates $p<0.05$

4.2 Effects of fasting on adipokine expression in the Cbl $^{-/-}$ mice

Calorie restriction and starvation increase the production of anti-inflammatory adipokines such as adiponectin. In contrast, there is a decline in the production of pro-inflammatory adipokines such as leptin and RBP4 and cytokines like IL-6 and TNFα, which informs the host of energy deficits and contributes to the suppression of immune function [222]. To determine whether c-Cbl signalling is involved in the fed/fast transition expression of these adipokines, we determined the adipokine profile in WAT of fed and fasted mice. For this experiment mice were deprived of food for 16 h and then euthanized, blood collected for plasma, and tissues were harvested and frozen for analysis. Tissue lysates were obtained and the adipokine content quantified by ELISA as above. No significant change was observed in the adiponectin and leptin content in WAT of Cbl $^{-/-}$ mice of both genders compared to their respective fed controls (Fig. 32A, B). However, RBP4 abundance was significantly increased in WAT of fasted Cbl $^{-/-}$ female mice (Fig. 32C), while no difference was found in male Cbl $^{-/-}$ mice. On the other hand, a significant reduction in plasma adiponectin concentrations in Cbl $^{-/-}$ for both genders was observed (Fig. 33A), and plasma leptin was significantly decreased in male Cbl $^{-/-}$ (Fig. 33B). No changes were observed in the plasma concentrations of RBP4 in Cbl $^{-/-}$ for either gender (Fig. 33C). In addition, no differences were observed in the RBP4 abundance in the liver following an overnight fast (Fig. 34).

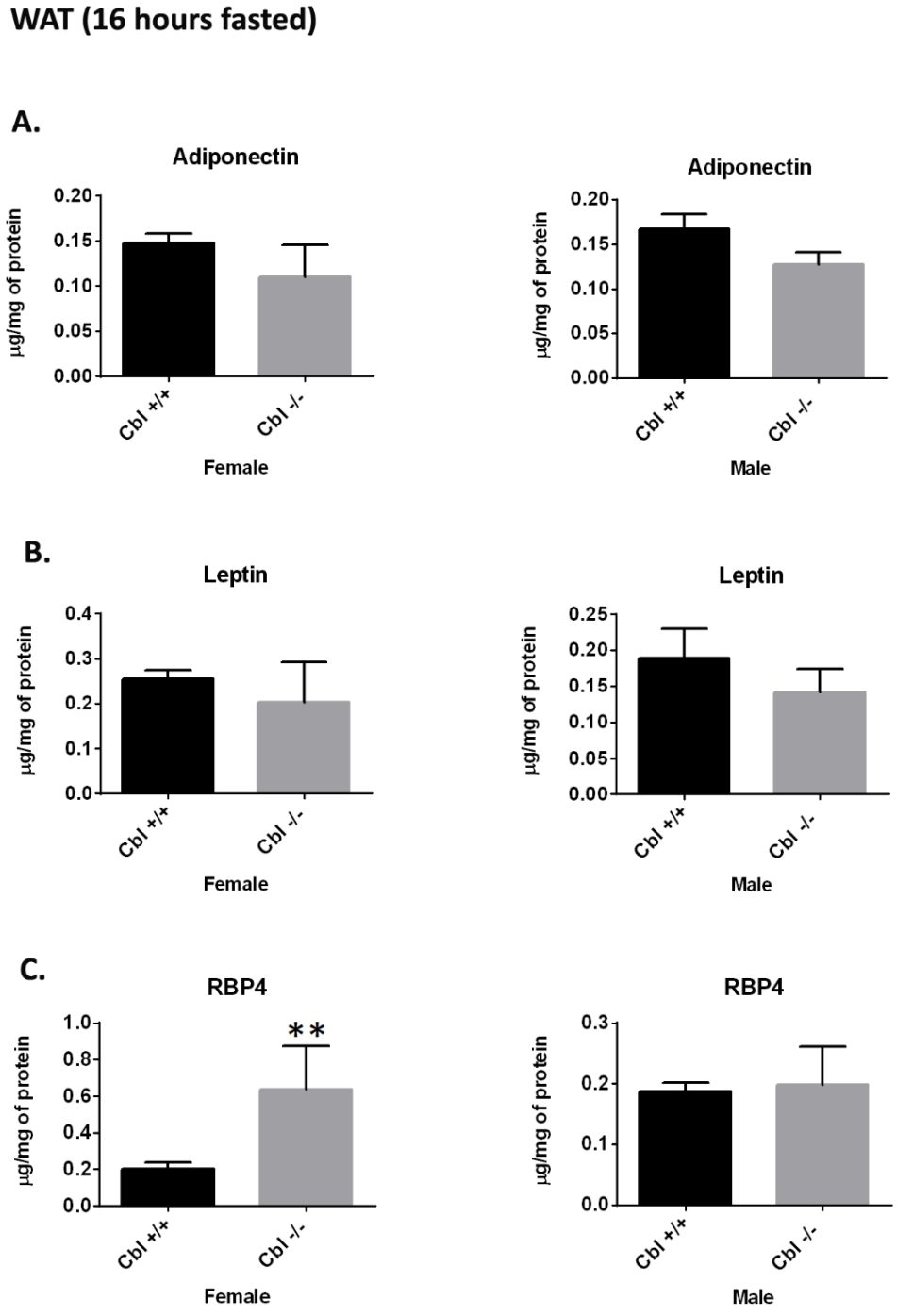

Fig. 32. Adipokine expression in WAT of fast Cbl $^{-/-}$ and Cbl $^{+/+}$ mice. RBP4 protein expression was increased in female Cbl $^{-/-}$ mice. Tissue lysates were obtained from perigonadal WAT and adipokines quantified by ELISA as specified in the methods section. Adipokine abundance was normalized to total protein content in the cellular lysate. **A) a**diponectin and **B)** leptin in white adipose tissue (Cbl $^{-/-}$male n=4 and female n=3; Cbl $^{+/+}$ male n=8 and female n=10). **C)** RBP4 abundance in WAT (Cbl $^{-/-}$ male n=5 and female n=4; Cbl $^{+/+}$ male n=6 and female n=12). Graphs show mean ± SEM, statistical analysis: unpaired t-test, * indicates $p<0.05$; ** $p<0.01$.

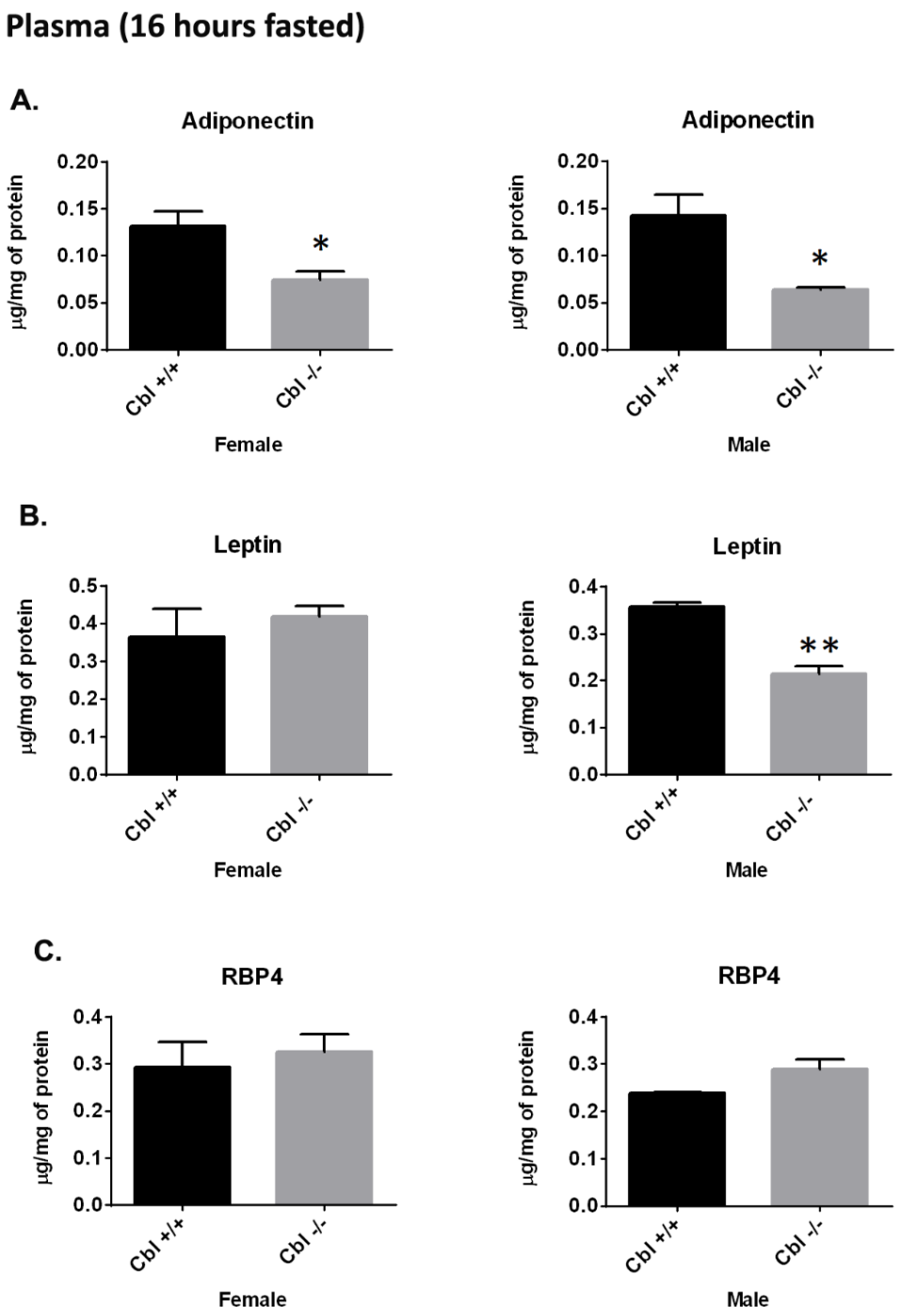

Fig. 33. Adipokine expression in plasma of fast Cbl $^{-/-}$ and Cbl $^{+/+}$ mice. Plasma adiponectin was significantly reduced in both male and female Cbl $^{-/-}$ with a significant decrease in the plasma leptin of male Cbl $^{-/-}$ was detect. **A) a**diponectin, **B)** leptin and **C)** RBP4 concentration in plasma (Cbl $^{-/-}$ male n=3 and female n=3; Cbl $^{+/+}$ male n=3 and female n=3). Data represent means ± SEM. Statistical analysis: unpaired t-test, * indicates $p<0.05$, **

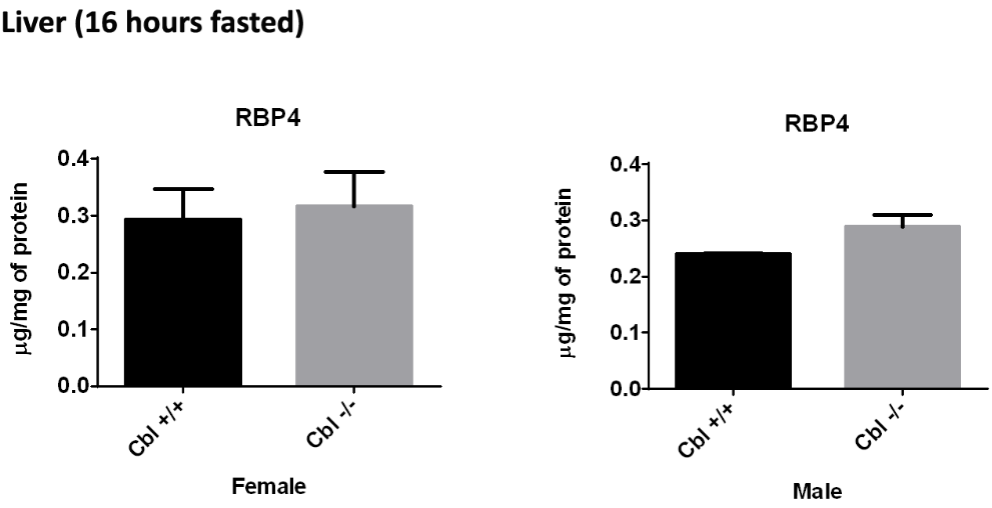

Fig. 34. Expression of RBP4 in the liver of fast Cbl $^{-/-}$ and Cbl $^{+/+}$. No change in liver RBP4 protein expression in fasted Cbl $^{-/-}$ mice (Cbl $^{-/-}$ male n=5 and female n=4; Cbl $^{+/+}$ male n=9 and female n=3). Data represent means ± SEM. Statistical analysis: unpaired t-test.

4.3 Chemical inhibition of ERK 1/2 decreases RBP4 expression in WAT explants of Cbl $^{-/-}$ mice and in Cbl KD 3T3L1 adipocytes

Since in the previous chapter we had observed that c-Cbl deficiency increases basal activation of extracellular regulated kinases p42/p44 in white adipose tissue we decided to investigate whether this signalling pathway is responsible for the elevated expression of RPB4 in Cbl $^{-/-}$ mice. To test this hypothesis, we examined the impact of chemical inhibition of MEK1/2 kinases which regulate ERK in the adipose tissue explants of Cbl $^{-/-}$ mice and in 3T3L1 Cbl KD cells (Fig. 35).

Visceral adipose tissue explants were obtained and cultured *in vitro* in DMEM in the absence or presence of two chemical inhibitors of MEK1/2 (10 µM of PD98059 and 20 µM of U0126) for 3 and 24 h. Subsequently, adipose tissue was collected, and lysates or total RNA were extracted. The efficacy of ERK pathway inhibition was determined by western blot analysis of the lysate proteins (Fig. 35A). Both inhibitors

significantly reduced ERK signalling as evidenced by reduced p42/p44 phosphorylation after 24 h treatment although U0126 seemed to cause a greater inhibition (Fig. 35A). Concomitantly with this reduction in ERK activation the content of RBP4 in the tissue lysates was determined by ELISA and found to be decreased following the treatment with inhibitors (Fig. 35B). Again, U0126 was found to have greater effects compared to PD98059. At the mRNA level, treatment with both MEK1/2 inhibitors reduced RBP4 mRNA relative abundance after 3 h (Fig. 35C). RBP4 mRNA abundance recovered completely after 24 h following the treatment with PD98059 whereas a 50% decrease was still noted for U0126 at this time point (Fig. 35C).

We then sought to confirm these findings in the 3T3L1 Cbl KD cell system. Cbl KD 3T3L1 adipocytes were left untreated or treated with MEK1/2 inhibitors (10 µM of PD98059 and 20 µM of U0126) for 15 h. Cell lysates were obtained and analysed by western blot (Fig. 35D). Both inhibitors significantly reduced ERK phosphorylation in Cbl KD cells. Relative mRNA abundance of RBP4 analysed by real time PCR and found to be significantly decreased after treatment with inhibitors (Fig. 35E). The U0126 inhibitor caused greater effects compared to PD98059.

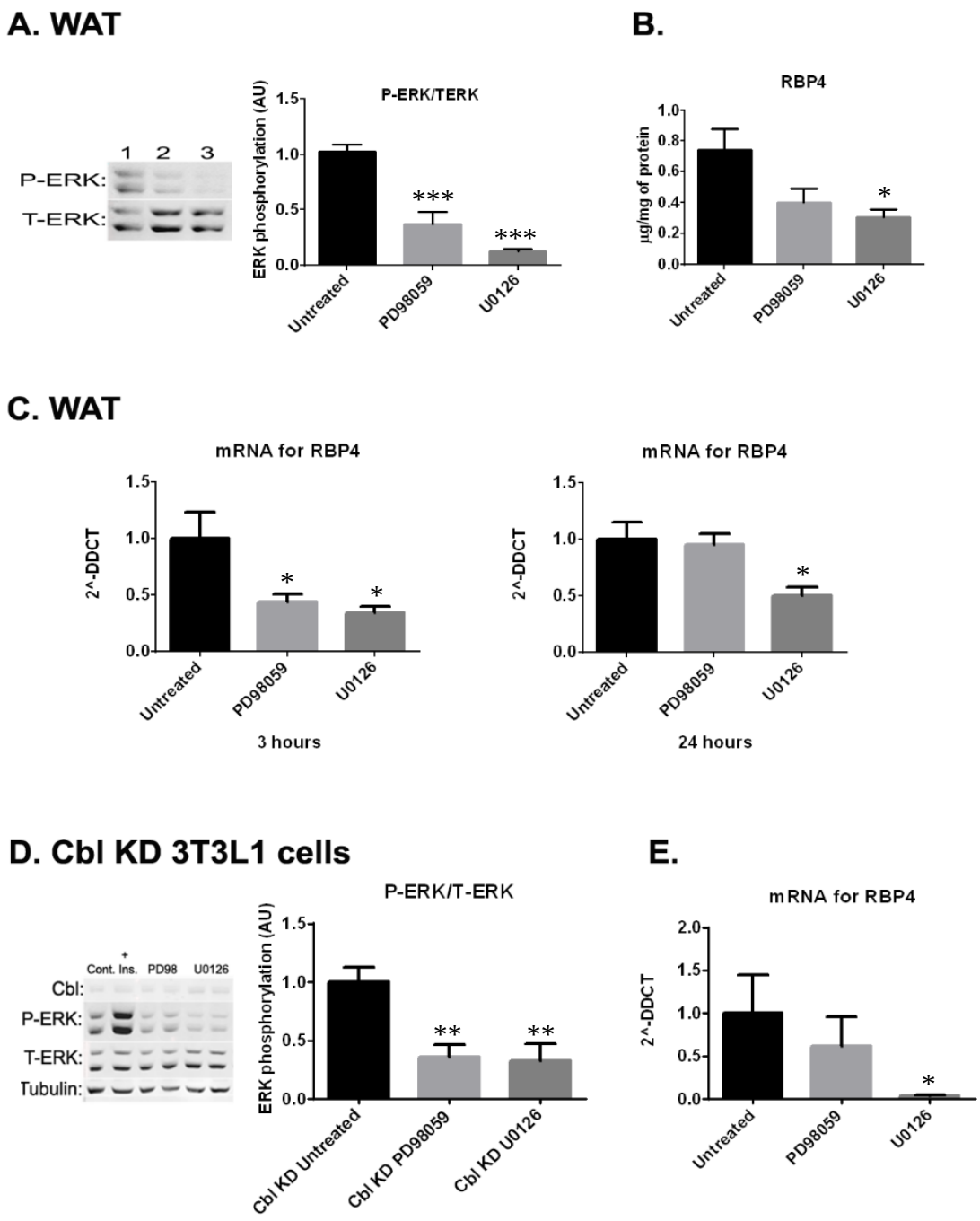

Fig. 35. Inhibition of ERK in adipose tissue explants of Cbl $^{-/-}$ mice and in c-Cbl depleted 3T3L1 adipocytes reduces RBP4 expression. **A)** Treatment of adipose tissue explants of Cbl $^{-/-}$ mice with ERK inhibitors (PD98059 and U0126) reduces phosphorylation of ERK. Adipose explants were treated with 10 µM of PD98059 and 20 µM of U0126 for 3 and 24 h. Tissue lysates were analysed by western blot with phospho-specific ERK antibodies as described in the methods section 2.12. Left shows a representative blot, right graph shows quantification of data obtained from n=3 animals with each inhibitor. **B)** RBP4 quantification by ELISA in tissue lysates of white adipose

tissue explants treated with ERK inhibitors for 24h. Data are the mean ± SEM for n=3 mice for each inhibitor. **C)** mRNA quantification of RBP4 in white adipose tissue explants left untreated or treated with ERK inhibitors for 3h (left panel) or 24h (right panel). Graphs are mean ± SEM of relative quantification to 18S as a housekeeping gene, data obtained from n=2 mice for each inhibitor, each sample quantified in triplicate. **D**) Cbl KD 3T3L1 adipocytes were either untreated or treated with ERK inhibitors for 15h. Cell lysates were obtained and analysed by western blot. Graph is quantitation of an experiment done in triplicate. Representative of two independent experiments each done in triplicate biological samples. **E**) mRNA abundance of RBP4 quantitated in c-Cbl depleted 3T3L1 adipocytes either untreated or incubated with inhibitors for 15h. Graph shows mean ± SEM. Representative experiment of n=2, with 3 biological replicates. Statistical analysis: One-Way ANOVA * indicates<0.05, ** p<0.01; ****p<0.0001.

4.4 Estrogen receptor regulates RBP4 expression in adipocytes

The previous findings indicate that RBP4 increased significantly in WAT of female Cbl $^{-/-}$ mice. Since WAT expresses abundant estrogen receptors (ER) we hypothesized that the increase in RBP4 in female Cbl $^{-/-}$ mice might be related to the effects of estrogen on adipocytes.

To test the hypothesis, we first examined whether 17β-estradiol regulates RBP4 expression in adipocytes. Differentiated 3T3L1 adipocytes were treated with 17β-estradiol (E2) at a range of concentrations (0, 10^{-7}, 10^{-8} and 10^{-9} M) for 15 h (Fig.36A). Total RNA was subsequently harvested and mRNA abundance of RBP4 determined by qPCR. We found that 17β-estradiol increased RBP4 mRNA in adipocytes (Fig. 36A) compared with untreated cells.

We next examined whether c-Cbl depletion in adipocytes would alter the expression or activation of estrogen receptors (ER). We determined the expression of ERα and ERβ by qPCR in control cells and in cells stably expressing shRNAs for c-Cbl KD. We observed that Cbl KD 3T3L1 did not change the expression of estrogen receptors as no change was found in mRNA of ER-α and mRNA of ER-β between control and Cbl KD cells (Fig. 36B).

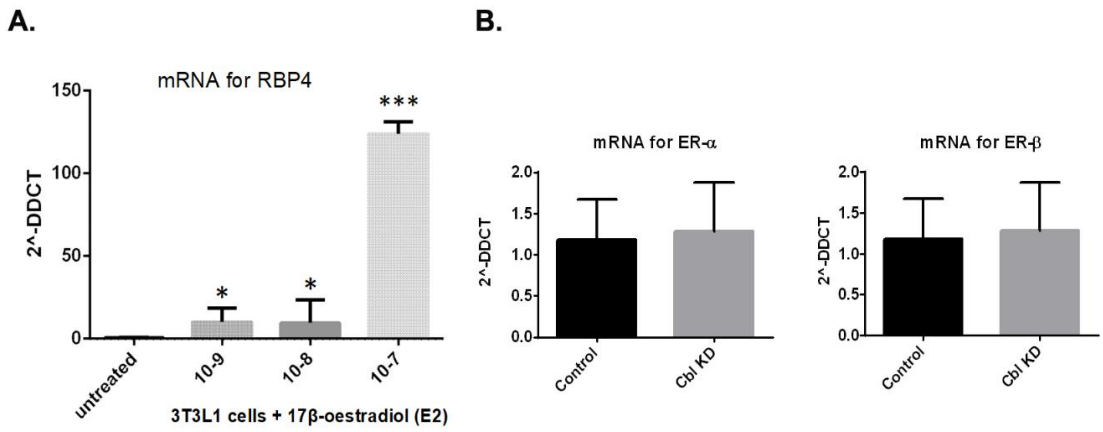

Fig. 36. Expression of RBP4 mRNA and ER-α and ER-β mRNA in 3T3L cells. **A)** 17β-estradiol increases RBP4 mRNA in 3T3l1 cells. Differentiated adipocytes were treated with E2 at a range of concentrations from 0 to 10^{-9}M as indicated for 15 h. **A)** Total RNA was isolated and RBP4 mRNA abundance relative to 18S was determined by qPCR as described in the methods. Graphs shows mean ± SEM of n=3 cell dishes. One-Way ANOVA *** indicates<0.001. **B)** Expression of ER receptors in Cbl KD 3T3L1 cells. Total RNA was isolated from control or c-Cbl depleted 3T3L1 adipocytes and the mRNA abundance of ERα and ERβ relative to 18S were determined by qPCR as described in the methods. Graphs shows mean ± SEM of n=3 cell biological replicates.

4.5 c-Cbl depletion increases the phosphorylation of estrogen receptor alpha (ER-α) at S118

Previous published studies [223-225] have established that ER-α can be activated by MAPK (P44/42) at phosphorylation site S118. Having determined that c-Cbl deficient adipocytes have increased ERK signalling, we next tested whether c-Cbl depletion would increase the phosphorylation of ER-α at this site. We evaluated the phosphorylation of ERα receptor at S118 by western blot analysis in WAT explants obtained from Cbl $^{-/-}$ and Cbl $^{+/+}$ mice and in 3T3L1 Cbl KD and control cells. Tissue and cellular lysates were separated by SDS-PAGE and immunoblotted with a phospho-ERα S118 antibody and a total ERα antibody as loading control.

We observed a two-fold increase in ER phosphorylation in female Cbl $^{-/-}$ compared to female Cbl $^{+/+}$ control, although this did not reach statistical significance (Fig. 37A); in Cbl KD cells the phosphorylation of ER-α at S118 was significantly increased (Fig. 37B).

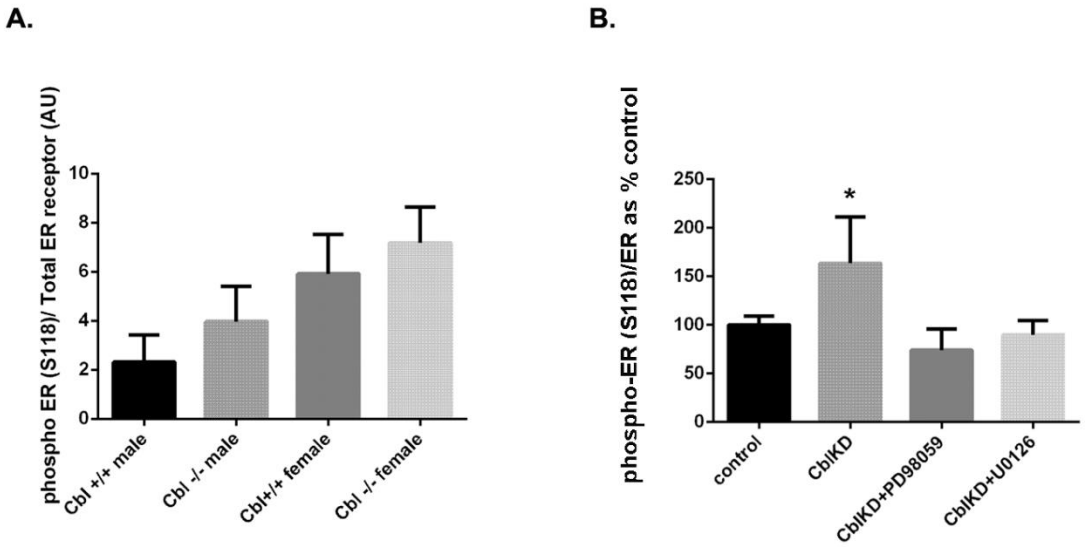

Fig. 37. ERα S118 phosphorylation in WAT of Cbl $^{-/-}$ and Cbl $^{+/+}$ and in Cbl KD 3T3L1 adipocytes. Increased ERα S118 phosphorylation in Cbl depleted adipocytes. **A)** White adipose tissue extracts obtained from Cbl $^{-/-}$ or Cbl $^{+/+}$ mice (n=3 male and n=3 female for each genotype) were immunoblotted with anti-phospho ERα (S118) antibody or ER antibody as loading control. The blot was quantified with Image J. Graph shows mean ± SEM of intensities in arbitrary units. **B)** Whole cell lysates obtained from either control 3T3L1 adipocytes or c-Cbl depleted cells were immunoblotted with anti-phospho ERα (S118) antibody or total ER as loading control. Graph shows the quantification in Image J of n=3-5 replicate samples per group and represents the mean ± SEM of phospho ER/ER ratio in arbitrary units as % of control cells which do not express shRNAs for Cbl. Statistical analysis: multiple t-test. * indicates $p<0.05$.

4.6 Discussion

WAT secretes numerous adipokines that affect body physiology. In the current study, I tested the hypothesis that Cbl $^{-/-}$ mice have altered expression of adipokines that might regulate whole body insulin sensitivity and/or glucose and lipid homeostasis. We determined the adipokine expression profile in WAT and plasma and confirmed the results in 3T3L1 cells.

Regarding gender, we observed a clear dimorphism in WAT content of some adipokines notably that of RBP4 in WAT of female Cbl $^{-/-}$ mice. 3T3L1 Cbl KD cells also displayed elevated RBP4 compared with control cells, but there was. no significant difference in RBP4 content in the liver or in the circulating plasma levels in Cbl $^{-/-}$ mice in the steady state. It is known that some adipokines are expressed differently depending on gender. For example, higher circulating concentrations of leptin and adiponectin are found in women [226, 227]. A possible direct role of gonadotropins on the expression of RBP4 has also been suggested, as circulating RBP4 concentrations are higher in postmenopausal compared with premenopausal women and in women older than 50 years when compared with those younger than 50 years [129, 228, 229].

In the present study, we examined other adipokines involved in insulin sensitivity including adiponectin and leptin, and cytokines IL-6 and TNF-α in Cbl $^{-/-}$, Cbl $^{+/+}$ and 3T3L1 cells. We found that adiponectin was significantly reduced in WAT of female Cbl $^{-/-}$ mice, whereas, no significant changes were observed in adiponectin levels in Cbl KD 3T3L1 cells. On the other hand, we found that leptin was markedly increased in WAT in female Cbl $^{-/-}$ mice accompanied with an increase in Cbl KD 3T3L1 cells. In contrast to our results, Shimizu *et al.* [230] observed higher circulating levels of leptin in women compared to men and Kennedy *et al.* [231] suggested that the gender

differences in leptin synthesis are due to the stimulating roles of estrogen s and/or an inhibition effect of circulating androgens, while other authors have been unable to find a correlation with gender or sex hormones [232]. In the case of IL-6 there was a reduction in WAT of male Cbl $^{-/-}$ mice, with no change observed in females. Also, no significant change was observed in TNF-α in Cbl $^{-/-}$ mice for either male or female.

In terms of fasting, it is known that adipose tissue shrinks during calorie restriction, anti-inflammatory adipokines rise and proinflammatory adipokines decline, resulting in increased insulin sensitivity, suppressed inflammation, protection against cardiovascular disease, improved glucose homeostasis in T2D and increased the life span in mice [222]. We determined the effects of overnight fasting on adipokine expression in Cbl $^{-/-}$ and control Cbl $^{+/+}$ mice. We found that RBP4 was increased in WAT of female Cbl $^{-/-}$ mice after an overnight fast, with no difference observed in the circulating RBP4 or in RBP4 content in the liver. The liver is the major site for the synthesis and secretion of RBP4 [233-235] which presumably explains why circulating RBP4 was not significantly altered in Cbl $^{-/-}$ mice. Consistent with our findings, Kos *et al*. [138] reported that circulating RBP4 concentrations were independent of AT-RBP4 secretion and that there was higher RBP4 mRNA expression in adipose tissue in women when compared with men. Several studies however, have found no correlation between adipose RBP4 mRNA expression and serum protein concentrations [137, 138, 236, 237]. Ost *et al.* [238] showed that RBP4 is likely released from the adipocytes and acts locally to inhibit phosphorylation of IRS1 at serine 307, thereby disrupting insulin-mediated nutrient sensing. However, Norseen *et al*. [133] found that RBP4 indirectly impairs insulin action in adipocytes by inducing proinflammatory cytokine production from macrophages. This effect of RBP4 is

mediated, in part, through the activation of JNK and toll-like receptor 4 (TLR4) pathways and is independent of retinol binding to RBP4 [133].

On the other hand, circulating adiponectin in Cbl $^{-/-}$ mice fasted overnight was significantly decreased in both genders. Our data contrasts with the findings of Molero *et al.* [22] who reported no change in fasting adiponectin levels in the circulation in Cbl $^{-/-}$ mice. Also, in human, Merl *et al.* [239] reported that serum adiponectin concentrations remain stable after 3 days of fasting and decline slightly during a prolonged fast. On the other hand, we observed that circulating leptin in male Cbl $^{-/-}$ was significantly decreased following an overnight fast, which is consistent with previous studies [240, 241], and it is consistent with the findings of Molero *et al*. [22] in Cbl $^{-/-}$ mice. A Previous study by Ahren *et al.* [242] reported that plasma leptin was reduced during fasting related to the changes of plasma insulin in mice [242].

We reported in previous chapters that ERK activation was increased in basal conditions in WAT of Cbl $^{-/-}$ mice and in Cbl KD 3T3L1 cells. In the current chapter, we found that there is an increase in RBP4 protein expression in WAT of female Cbl $^{-/-}$ and Cbl KD cells. We hypothesized that increased signalling through ERK may regulate RBP4 levels in WAT in Cbl $^{-/-}$ mice. To test this hypothesis and to investigate whether ERK signalling has a role in regulating RBP4 expression in Cbl $^{-/-}$ mice, we used chemical inhibitors (PD98059 and U0126) of MEK1/2 kinases to block ERK phosphorylation in adipose tissue explants of Cbl $^{-/-}$ and 3T3L1 Cbl KD cells. We found that inhibition of ERK1/2 phosphorylation in Cbl-depleted 3T3L1 adipocytes or in adipose tissue explants of Cbl $^{-/-}$ mice reduced RBP4 at the protein and mRNA levels. These findings suggest that c-Cbl may regulate RBP4 expression through ERK1/2 activation. Li *et al.* [243] reported that RBP4 enhanced ERK phosphorylation in vascular smooth muscle cells (RASMCs). A recent study observed that activation

of MAPK signaling increased in response to RBP4 treatment, and MAPK inhibitors significantly reduced RBP4-mediated expression of proinflammatory genes [244]. However, in contrast to our finding, Öst *et al.* [238] reported that RBP4 impaired insulin-stimulated ERK signaling in adipocytes [238].

Regarding the gender dimorphism, we observed elevated RBP4 only in female mice. Similar findings were found previously in humans [138]. It is known that both ER-α and ER-β estrogen receptors are expressed in WAT with ER-α being the most abundant. These receptors play an important role during adipose tissue differentiation, and act as ligand-dependent transcription factors to regulate the expression of specific genes [245-247]. The estrogen receptors are members of the nuclear hormone receptor superfamily of transcription factors that bind estrogen response elements (ERE) sequences as homo or heterodimers. ERs contain two transcription activation functions: AF1 located in the N-terminal A/B domain and the AF2 located in the C terminal domain. AF2 is activated through ligand (hormone) binding, whereas AF1 can modulate gene transcription in the absence of ligand [248], but this is weak. Binding of estradiol to the ER-α facilitates ligand-dependent activation and transactivation of ERE in target genes, which activate or repress gene expression [249, 250]. Estrogen actions are also mediated by ligand-independent ERα signalling that alter the phosphorylation of ERα [251, 252]. The human RBP4 promoter has ERE sequences in conserved regions, which suggests a role for ER in controlling expression. In support of this, we found that incubation of mouse adipose cells with 17β-estradiol increased RBP4 mRNA. Our data are consistent with previous findings by Jung and coworkers [253] who found that in 3T3L1 adipocytes, ER-α but not ER-β activation increased RBP4 mRNA abundance. Also, Tan *et al.* [254] showed in an earlier study that the RBP4 expression is influenced by effect of sex hormones and

suggested 17β-estradiol has a direct regulatory effect on RBP4 concentrations in women with polycystic ovary syndrome.

We did not determine the oestrous cycle in our female mice or indeed measured the circulating estradiol levels to correlate them with RBP4 expression levels. Further work along these lines is required. However, there is already evidence from human studies for a correlation of RBP4 serum concentrations with those of estradiol and estradiol/testosterone [255], which supports the role of ER in the *in vivo* regulation of RBP4 expression. The effects of other female hormones released during the oestrous cycle on the expression of RBP4, however, have not been extensively studied. A recent study in heifers showed RBP4 at the mRNA and protein levels to be raised in endometrium during the dioestrus phase with elevated progesterone [256]. This may be related to the role of retinoic acid signalling in the expression of proteins important for embryo implantation [257]. Unfortunately, the authors did not measure RBP4 in WAT of these animals.

AKT and ERK phosphorylation sites on ER-α map to S167 for AKT and S118 for ERK, both within the AF1 domain, and potentially leading to ligand-independent activation of ER-α [248, 252]. AF1 works to synergize with AF2 in the promotion of ligand-dependent transcription activation by the receptor [258]. Thus, we postulated that this mechanism may operate in the female Cbl $^{-/-}$ mice to enhance the expression of RBP4. We observed increased phosphorylation of ER-α at S118, in Cbl $^{-/-}$ and in Cbl KD 3T3L1 cells. Based on our findings, we suggest that along with the increased number of ER receptors and estrogen circulating concentrations present in females, c-Cbl depletion may activate ER through ERK-mediated phosphorylation of ER-α at S118 which results in higher RBP4 expression.

All our data suggest that inhibition of c-Cbl in adipose tissue will increase RBP4 expression locally. It was previously reported that Cbl signalling is impaired in animal models of insulin deficiency and in obesity [259]. This study reveals a potential new molecular mechanism that may contribute locally to the dysregulation of RBP4 that occurs in obesity and insulin resistance.

In conclusion, in the current chapter a marked gender dimorphism was found in WAT content of some adipokines, leptin and RBP4 were significantly increased in WAT of female Cbl $^{-/-}$, whereas adiponectin was reduced in female Cbl $^{-/-}$ mice. Fasting increased RBP4 protein expression in WAT of female Cbl $^{-/-}$ mice and decreased circulating adiponectin in both genders in Cbl $^{-/-}$ mice, while circulating leptin decreased only in male Cbl $^{-/-}$ mice compared to littermates control Cbl $^{+/+}$. In Cbl KD 3T3L1 adipocyte, RBP4 levels were increased compared to control cells. 17β-estradiol increases RBP4 mRNA in 3T3l1 cells, whereas c-Cbl depletion increases the phosphorylation of ER-α at S118 in WAT and Cbl KD cells.

Chapter 5

Adaptation of Cbl $^{-/-}$ mice to a high fat diet

5 Introduction

Obesity is considered a multi-factorial metabolic disturbance, prominent factors that determine the onset of obesity are the caloric content of the diet and the level of physical activity [260].

Obesity affects the release of adipokines which are thought to cause insulin resistance and diabetes [261]. For example: in both humans and animals obesity leads to an increase in the circulating concentrations of leptin [262] and increased production of inflammatory cytokines such as TNF-α and IL-6, and the activation of the inflammatory signaling network [263, 264]. Kahn and colleagues reported that the development of obesity leads to increased expression of RBP4 by adipocytes, influencing metabolic disease development [127, 265]. Furthermore, both experimental and clinical studies have demonstrated a role for RBP4 in the development of insulin resistance [266, 267]. Thus, targeting the adipokines associated with visceral obesity may be a useful strategy for preventing obesity-induced metabolic disorders [261].

In chapter 3 I established that Cbl $^{-/-}$ mice displayed increased insulin sensitivity compared to Cbl $^{+/+}$ mice. I also showed in chapter 4 that several adipokines including adiponectin, leptin and RBP4 were differentially expressed in WAT of female Cbl $^{-/-}$ mice. In this chapter we hypothesized that a high fat diet differentially affects the release of these adipokines in Cbl $^{-/-}$ mice. We hypothesize that the release of insulin-sensitizing adipokines (adiponectin, leptin) is greater in Cbl $^{-/-}$ mice whereas pro-inflammatory cytokines (RBP4, TNF-α and IL6) levels are lower in Cbl $^{-/-}$ mice exposed to HFD. We further hypothesized that Cbl $^{-/-}$ mice maintain insulin sensitivity *in vivo* when exposed to high fat diet in part due the release of insulin-sensitizing adipokines.

The specific aims for this chapter are: to determine insulin sensitivity *in vivo*, adiposity and adipokine profiles of WAT in Cbl $^{-/-}$ and wild type mice fed a high-fat diet (HFD) and compare them to mice fed regular chow (RC).

5.1 Effects high fat diet on body weight, food intake and adiposity

Dietary lifestyles that incorporate a high-fat diet are prone to cause obesity and T2D over time. Obesity is commonly seen with a variety of mice and rat strains, particularly in C57BL/6J (B6) mice when weaned onto these diets during juvenile stages, as it increases the risk for weight gain, hypertension and increases susceptibility to T2D symptoms, which include hyperglycaemia, as well as hyperinsulinemia [268, 269]. To study the physiological adaptation of Cbl $^{-/-}$ mice to a HFD, we selected a diet containing 45 % of fat [18, 270, 271]. We chose to feed the mice HFD for 8 weeks following the post-weaning period starting from week 4 [272].

Body weight (BW) was recorded twice per week (as detailed in section 2.2). While the animals did put on weight, significant differences were observed between genotype groups (Fig. 38A). BW in both male and female Cbl $^{-/-}$ mice fed a HFD were significantly increased compared to HFD-fed control mice Cbl $^{+/+}$.

Regarding food intake, male Cbl $^{-/-}$ mice on a RC diet displayed a significant increase in food intake compared to their littermate controls (Cbl $^{+/+}$) on the same diet (Fig. 38B). No significant difference was observed in food intake of either male or female Cbl $^{-/-}$ mice on a HFD compared to control Cbl $^{+/+}$ mice fed the same diet.

Adipocyte cell size and triglyceride content from perigonadal visceral fat were measured in animals fed a regular diet or HFD (Fig. 39). Adiposoft-ImageJ software was used for the analysis of WAT cell area and diameters as indicated in the methods section 2.14.1. Male Cbl $^{-/-}$ mice fed a HFD showed a significant increase in adipocyte

cell diameter compared to control mice fed a regular chow diet (Fig. 39B), while no significant differences were detected in adipocyte cell size of female Cbl $^{-/-}$ mice compared to control female Cbl $^{+/+}$ for either regular chow or HFD (Fig. 39D). On the other hand, triglyceride content was not significantly different in male or female Cbl $^{-/-}$ mice on HFD compared with control Cbl $^{+/+}$ mice on the same diet (Fig. 40A, B).

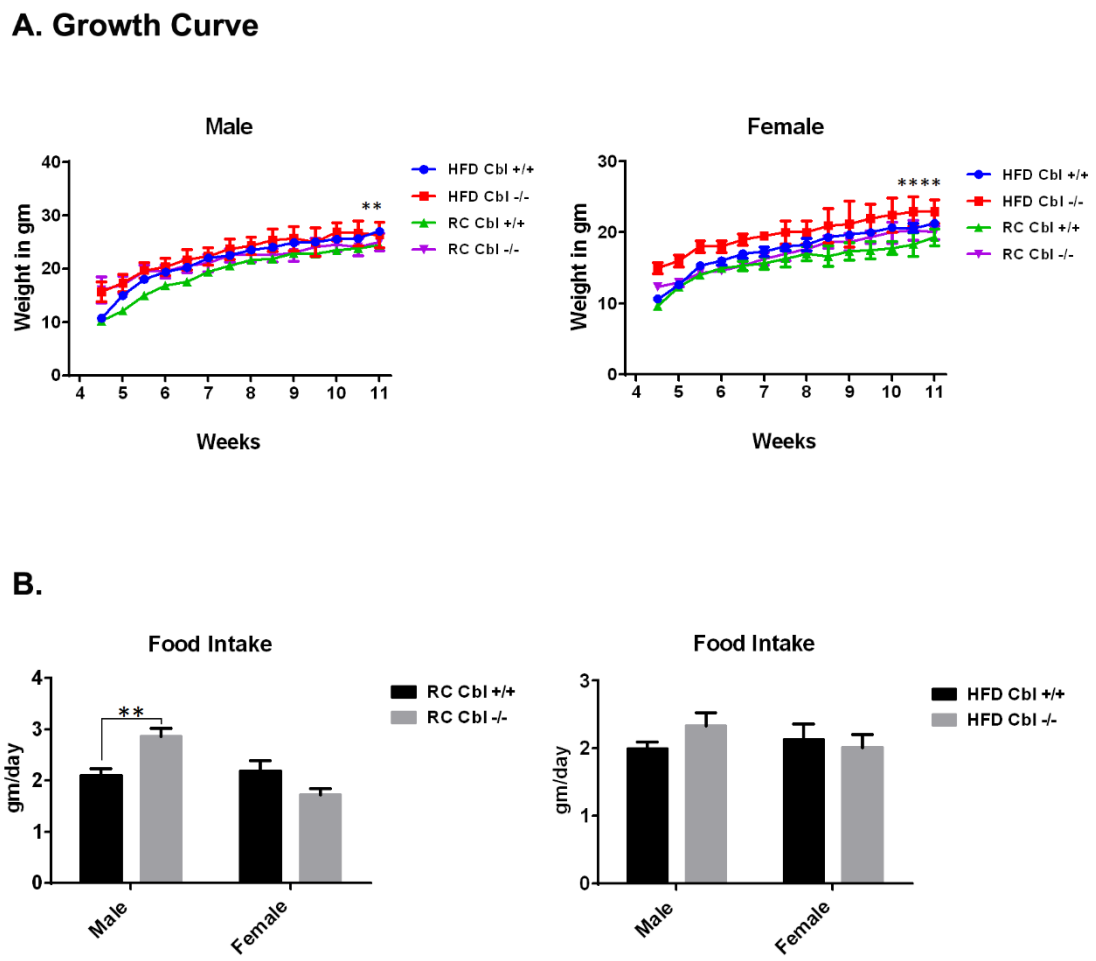

Fig. 38. Growth curve and food intake in Cbl $^{-/-}$ and Cbl $^{+/+}$ mice on HFD and RC diet. A) Growth curve of Cbl $^{-/-}$ and Cbl $^{+/+}$ mice on HFD and RC. Body weight in Cbl $^{-/-}$ on HFD was significantly increased in both genders. Data represent the mean ± SEM of weekly weight. Cbl $^{+/+}$ HFD, n=9 male and n=3 female, RC n=7 male and n=3 female; Cbl $^{-/-}$ HFD, n=4 male and n=3 female, RC n=3 male and n=3 female. Two-way ANOVA, Tukey's multiple comparisons test, ** indicates $p<0.01$, **** $p<0.0001$. **B**) Food intake in Cbl $^{+/+}$ and Cbl $^{-/-}$ mice. Daily food intake for both genotype which starting from week 4. RC and HFD (n=7-10 male per group and n=3 female per group). Food intake is significantly increased in RC male Cbl $^{-/-}$. Two-way ANOVA, Sidak's multiple comparisons test, ** indicates $p<0.01$.

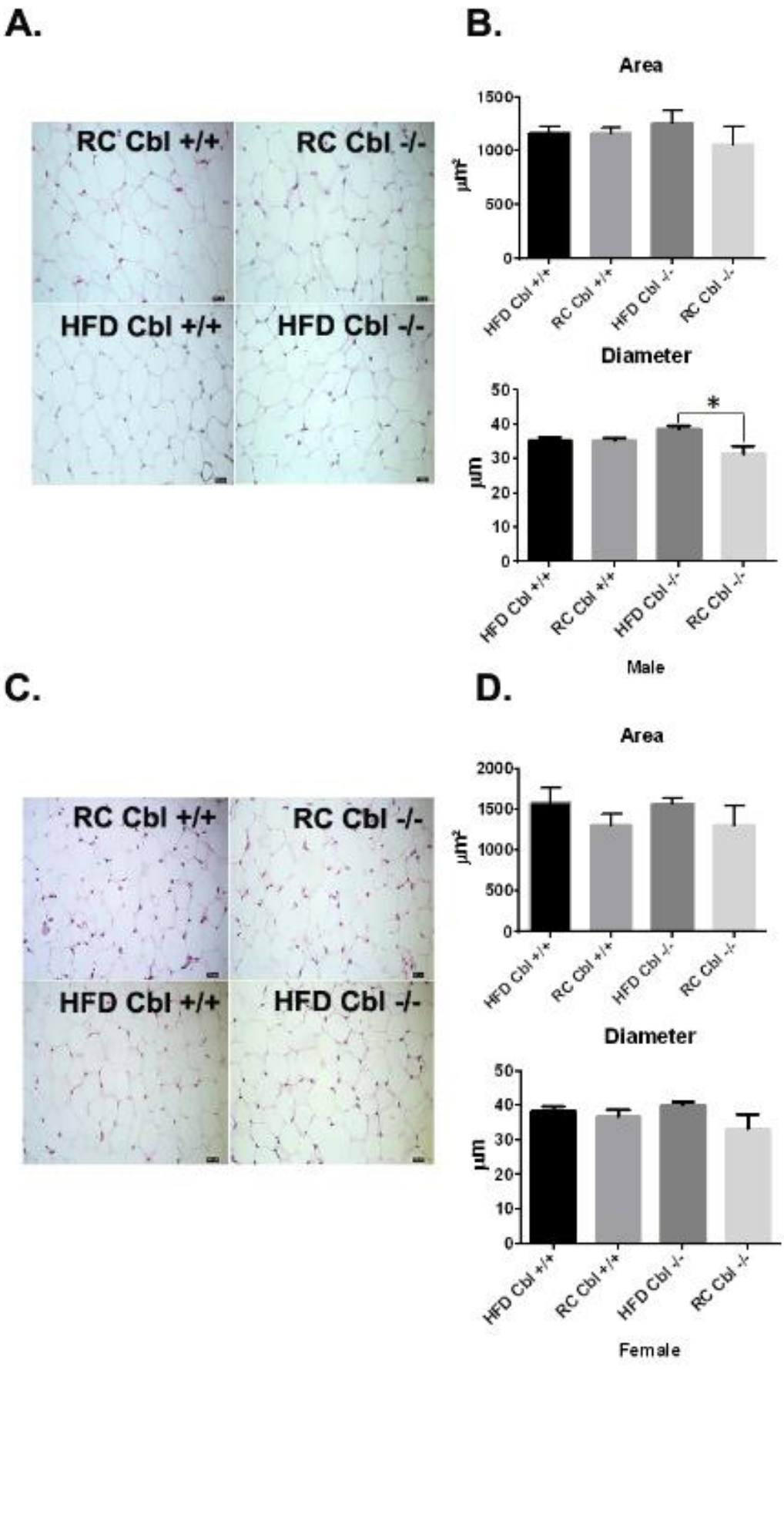
A.
RC Cbl +/+
RC Cbl -/-
HFD Cbl +/+
HFD Cbl -/-
B.
Area
µm²
1500
1000
500
0
HFD Cbl +/+
RC Cbl +/+
HFD Cbl -/-
RC Cbl -/-
Diameter
µm
50
40
30
20
10
0
*
Male
C.
RC Cbl +/+
RC Cbl -/-
HFD Cbl +/+
HFD Cbl -/-
D.
Area
µm²
2000
1500
1000
500
0
Diameter
µm
50
40
30
20
10
0
Female

Fig. 39. Morphology of WAT in Cbl $^{-/-}$ and Cbl $^{+/+}$ mice on HFD and RC diet. No changes in adiposity of HFD Cbl $^{-/-}$ mice. Haematoxylin-eosin staining of perigonadal WAT obtained from male **(A)** and female **(C)** Cbl $^{+/+}$ and Cbl $^{-/-}$ mice on RC and HFD. Representative images shown of pictures obtained at 40X magnification (RC: male Cbl $^{+/+}$ n=6, female Cbl $^{+/+}$ n=3 and male Cbl $^{-/-}$ n=4, female Cbl $^{-/-}$ n=3; HFD: male Cbl $^{+/+}$ n=7, female Cbl $^{+/+}$ n=3 and male Cbl $^{-/-}$ n=4, female n=3) mice. RC Cbl $^{-/-}$ (top right panel) and RC Cbl $^{+/+}$ (top left panel), HFD Cbl $^{-/-}$ (bottom right panel) and HFD Cbl $^{+/+}$ (bottom left panel). **B)** and **D)** Quantification: Adiposoft software was used to quantify cell diameter of n=100 cells and cell area n=50 cells per genotype and gender. Graphs show mean± SEM. Statistical Analysis: ANOVA-one way, Tukey's multiple comparisons test, * indicates $p<0.05$.

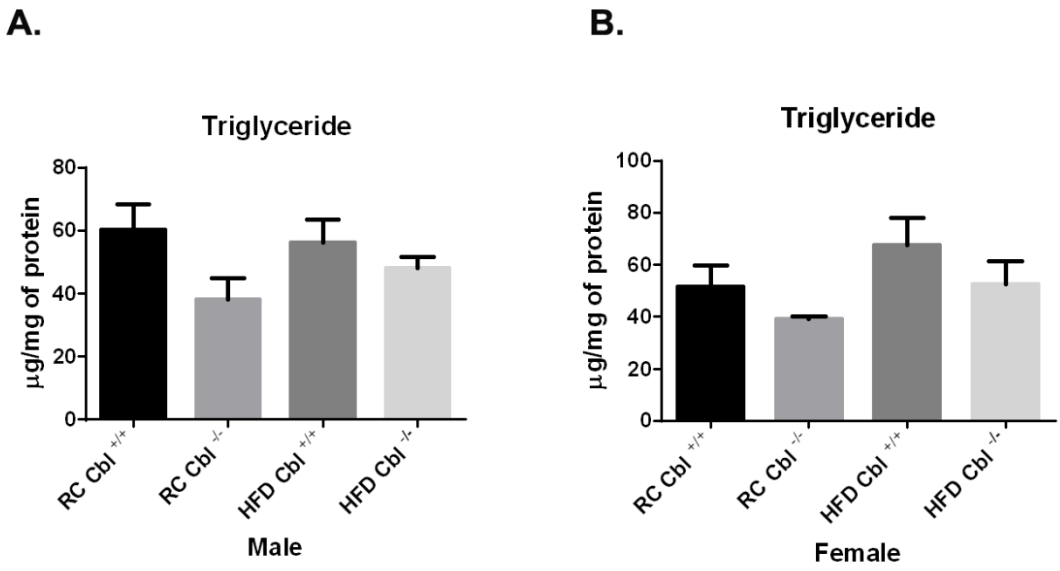

Fig. 40. Triglyceride content in adipose tissue obtained from Cbl $^{-/-}$ and Cbl $^{+/+}$ mice. Triglyceride content in perigonadal WAT obtained from male **(A)** and female **(B)** age matched Cbl $^{+/+}$ and Cbl $^{-/-}$ mice. (RC: male Cbl $^{+/+}$ n=6, female Cbl $^{+/+}$ n=3 and male Cbl $^{-/-}$ n=5, female Cbl $^{-/-}$ n=3, HFD: male Cbl $^{+/+}$ n=7, female Cbl $^{+/+}$ n=3 and male Cbl $^{-/-}$ n=5, female n=3) mice. Graphs show mean± SEM. Statistical Analysis: ANOVA-one way, Tukey's multiple comparisons test.

5.2 Insulin sensitivity studies in Cbl $^{-/-}$ mice fed a HFD

Glucose tolerance tests revealed that the Cbl $^{-/-}$ mice had an enhanced glucose clearance and significant improvement in insulin sensitivity when fed a HFD compared to Cbl $^{+/+}$ littermates (Fig. 41A, B). Insulin tolerance test were significantly lower in male Cbl $^{-/-}$ fed a HFD compared to control male Cbl $^{+/+}$ mice on a HFD (Fig. 41C, D), while no significant differences were observed in GTT or ITT in female Cbl $^{-/-}$ on a HFD compared to control female Cbl $^{+/+}$ mice on the same diet (Fig. 41A, B, C, D). Collectively these data indicate that Cbl $^{-/-}$ mice are protected from developing HFD-induced insulin resistance, similar to what have been determined previously by Molero *et al*. [22].

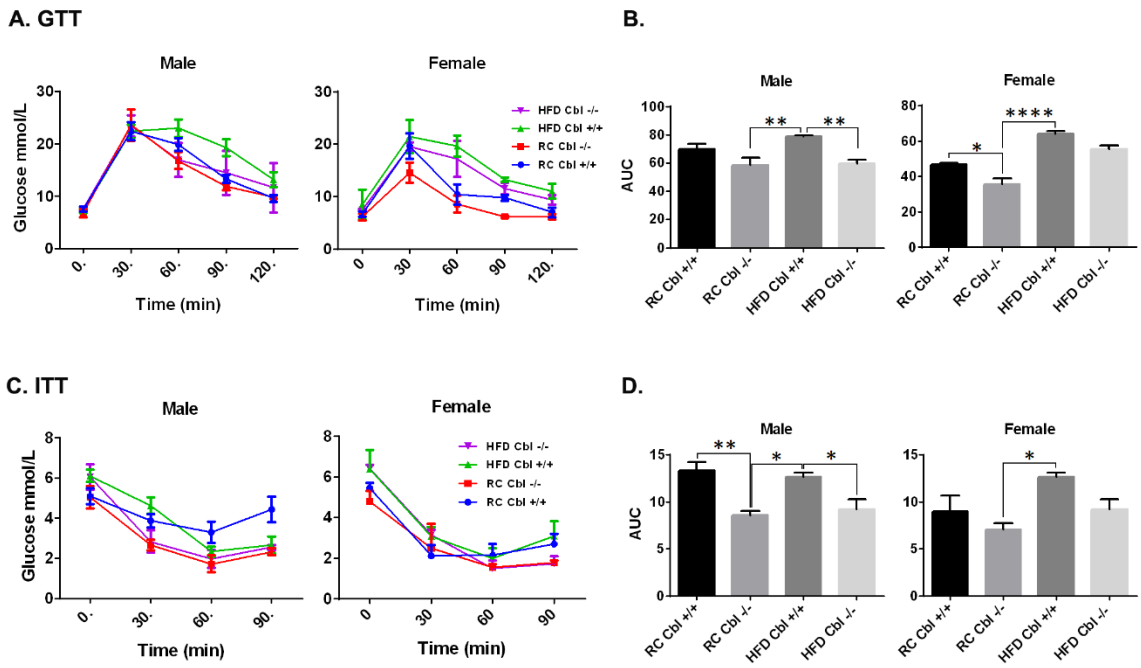

Fig. 41. Glucose and insulin tolerance tests in Cbl $^{-/-}$ and Cbl $^{+/+}$ mice on HFD. A) Glucose tolerance test (GTT) and **B)** Area under the curve (AUC) for GTT in male and female Cbl $^{-/-}$ and Cbl $^{+/+}$ mice. **C)** Insulin tolerance test (ITT) and **D)** AUC for ITT in male and female Cbl $^{-/-}$ and Cbl $^{+/+}$ mice. Tests were carried out at week 10-11 of age. Mice were injected with glucose 2 g/Kg of body weight (GTT) or insulin 0.75 U/Kg of body weight (ITT) and at the times indicated, blood tail samples were obtained, and glucose measured using a glucose meter as indicated in the methods section. Graph shows mean ± SEM of values. Male mice n=4, female mice n=3 per genotype. Statistical analysis: ANOVA-one way, Tukey's multiple comparisons test, * indicates $p<0.05$; ** $p<0.01$; **** $p<0.0001$

5.3 Respiratory quotient, energy expenditure and activity in Cbl $^{-/-}$ mice fed a HFD

We next examined substrate utilization and energy expenditure in mice after HFD feeding. Energy is generated by consuming substrates (carbohydrate, fat, and protein). Each substrate produces a different amount of energy (kcal) and a different cost in terms of CO_2 to be produced. The ratio of CO_2 produced to O_2 consumed is referred to as the respiratory quotient ($RQ = VCO_2/VO_2$) [188]. RQ measures energy expenditure, at rest it gives us the value of the basal metabolic rate. It gives an indication of the primary metabolic substrate that is used, and normally is a number between 0.7 and 1 [273]. The body mainly uses carbohydrates and lipids for oxidation to obtain ATP although amino acids can be used too [274]. In general, the reaction of oxidation for a metabolic substrate can be written as:

$C_xH_yO_z + (x + y/4 – z/2)\ O_2 \rightarrow x\ CO_2 + (y/2)\ H_2O$

So, knowing the volume of oxygen consumed and CO_2 produced an estimate can be made of the nutrient that has been used as a metabolic substrate.

Full oxidation reaction for a carbohydrate:

$C_nH_{2n}O_n + nO_2 \rightarrow nCO_2 + nH_2O$

gives us a RQ=1

So, if we consume carbohydrates RQ will be 1, whereas if we oxidize fatty acids, it will be approximately 0.7 [274].

In this study, following the diet intervention in which animals were fed a regular chow or high fat diet for 8 weeks, the mice were housed individually in a metabolic cage for 48 h to measure the respiratory quotient, energy expenditure and physical activity. This was accomplished using the OXYLET indirect calorimetry system, as described in the methods section 2.6.

We found that RQ significantly increased in male Cbl $^{-/-}$ mice on a RC diet during both dark and light phases compared to male control Cbl $^{+/+}$ mice on the same diet (Fig. 42A), with no change observed in RC female Cbl $^{-/-}$ mice (Fig. 42C). The mean ± SD of RQ in mice fed a RC was 1.067 ± 0.029 vs 1.038 ± 0.043 during the dark cycle and 0.985 ± 0.041 vs 0.947 ± 0.060 during the light cycle in male Cbl $^{-/-}$ and Cbl $^{+/+}$ mice respectively (Fig. 42A). While in female mice RQ was 1.029 ± 0.041 and 1.053 ± 0.052 during the dark cycle and 0.970 ± 0.044 and 0.960 ± 0.0515 in the light cycle in Cbl $^{-/-}$ and Cbl $^{+/+}$ mice respectively (Fig. 42C). Since these numbers are close to 1.0 the data indicate that carbohydrates are used as the main fuel source.

On the other hand, no change was found in the RQ in male Cbl $^{-/-}$ mice fed a HFD compared to control Cbl $^{+/+}$ mice. The RQ was decreased significantly in female Cbl $^{-/-}$ mice fed a HFD during dark and light cycle. The average RQ in mice fed a HFD was 0.956 ± 0.016 and 0.948 ± 0.015 during the dark cycle and 0.922 ± 0.022 and 0.911±0.018 during the light cycle in male Cbl $^{-/-}$ and Cbl $^{+/+}$ respectively (Fig. 42B). However, in female mice the average RQ on HFD was 0.874 ± 0.043 and 0.906 ± 0.021 in dark cycle and 0.852 ± 0.017 and 0.889 ± 0.021 in Cbl $^{-/-}$ and Cbl $^{+/+}$ mice respectively (Fig. 42D). The RQ between 0.85-0.90 is an indication that both protein and carbohydrate have been used as a primary source of energy. These findings suggest that the substrate utilization of mixed protein and carbohydrate was used specially in the female Cbl $^{-/-}$ mice which exhibited significantly lower RQ than the male mice.

Male Cbl $^{-/-}$ mice on RC diet exhibited a significant higher energy expenditure, during both dark and light cycle (Fig. 43A) whereas female Cbl $^{-/-}$ showed higher EE during the light cycle (Fig. 43C) only when compared to their control Cbl $^{+/+}$ littermates. The average of EE in mice on RC diet was 136.66 ± 5.52 vs 128.19 ± 6.37 during dark cycle and 120.35 ± 3.89 vs 113.33 ± 7.41 during light cycle in male Cbl $^{-}$

$^{-/-}$ and Cbl $^{+/+}$ mice respectively (Fig. 43A). While in female mice the average of EE was 136.61 ± 5.30 and 135.64 ± 7.60 in dark cycle and 124.58 ± 5.33 and 120.88 ± 5.20 in the light cycle for Cbl $^{-/-}$ and Cbl $^{+/+}$ mice respectively (Fig. 43C).

However, both genders of Cbl $^{-/-}$ mice fed a HFD showed a higher EE during the dark phase (Fig. 43B, D) compared to Cbl $^{+/+}$ control mice. The average EE in mice fed a HFD was 133.18 ± 4.66 and 127.92 ± 9.01 during dark cycle and 116.03 ± 6.16 and 116.69 ± 3.18 during light cycle in male Cbl $^{-/-}$ and Cbl $^{+/+}$ mice respectively (Fig. 43B). While in female mice the average EE in HFD was 134.63 ± 8.50 and 126.17 ± 6.89 in the dark cycle and 118.75 ± 9.94 and 119.72 ± 9.25 in the light cycle for Cbl $^{-/-}$ and Cbl $^{+/+}$ mice respectively (Fig. 43D). This increase in energy expenditure in Cbl $^{-/-}$ mice is due to either nutrient processing and utilization [275, 276] or to the thermic effect of food [276, 277].

We also measured physical activity of individual mice for a period of 48 hours. Analysis of these data revealed that the activity of male Cbl $^{-/-}$ RC mice was significantly higher than that of male Cbl $^{+/+}$ mice (Fig. 44A). However, this difference was reduced in male Cbl $^{-/-}$ mice fed a HFD during the light cycle (Fig. 44B). In contrast, female Cbl $^{-/-}$ mice had lower activity than Cbl $^{+/+}$ controls regardless of the diet used (Fig. 44C, D).

1. Respiratory Quotient (RQ)

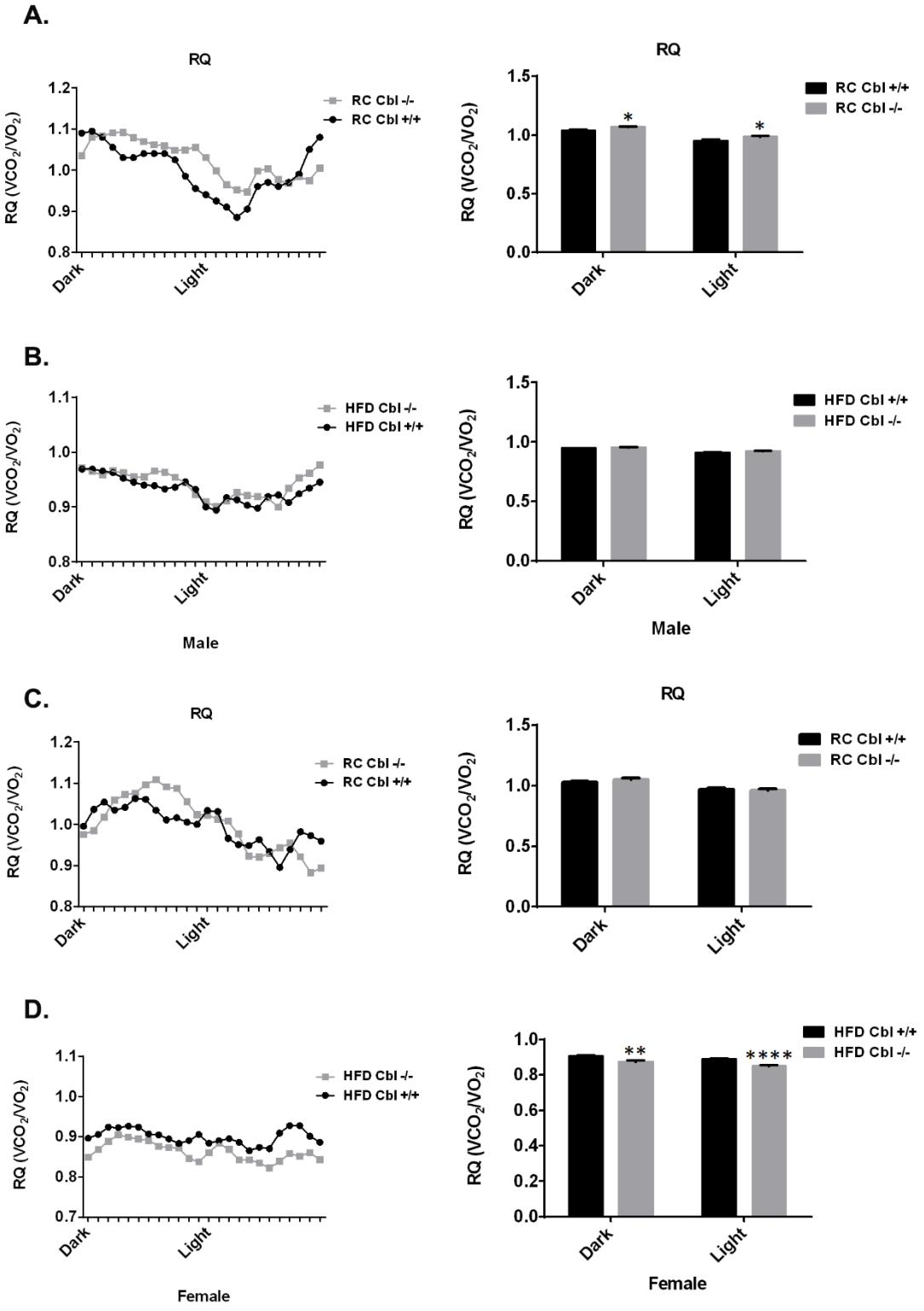

Fig. 42. Respiratory quotient in Cbl $^{-/-}$ and Cbl $^{+/+}$ mice (male and female) on RC and HFD diet. Values plotted at 1-hour intervals (the average was taken for every 2 hours from 6 PM to the 4 PM of the next day). **A)** male and **C)** female RC Cbl $^{-/-}$ mice and RC Cbl $^{+/+}$ mice. **B)** male and **D)** female HFD Cbl $^{-/-}$ and HFD Cbl $^{+/+}$ mice respectively, male mice n=4, female mice n=3. RQ was increased in male Cbl $^{-/-}$ on RC and decreased in female Cbl$^{-/-}$ mice on HFD. Data represent the means ± SEM, Statistical Analysis: Multiple t-test * indicates $p<0.05$; ** $p<0.01$; ****$p<0.0001$.

2. Energy Expenditure (EE)

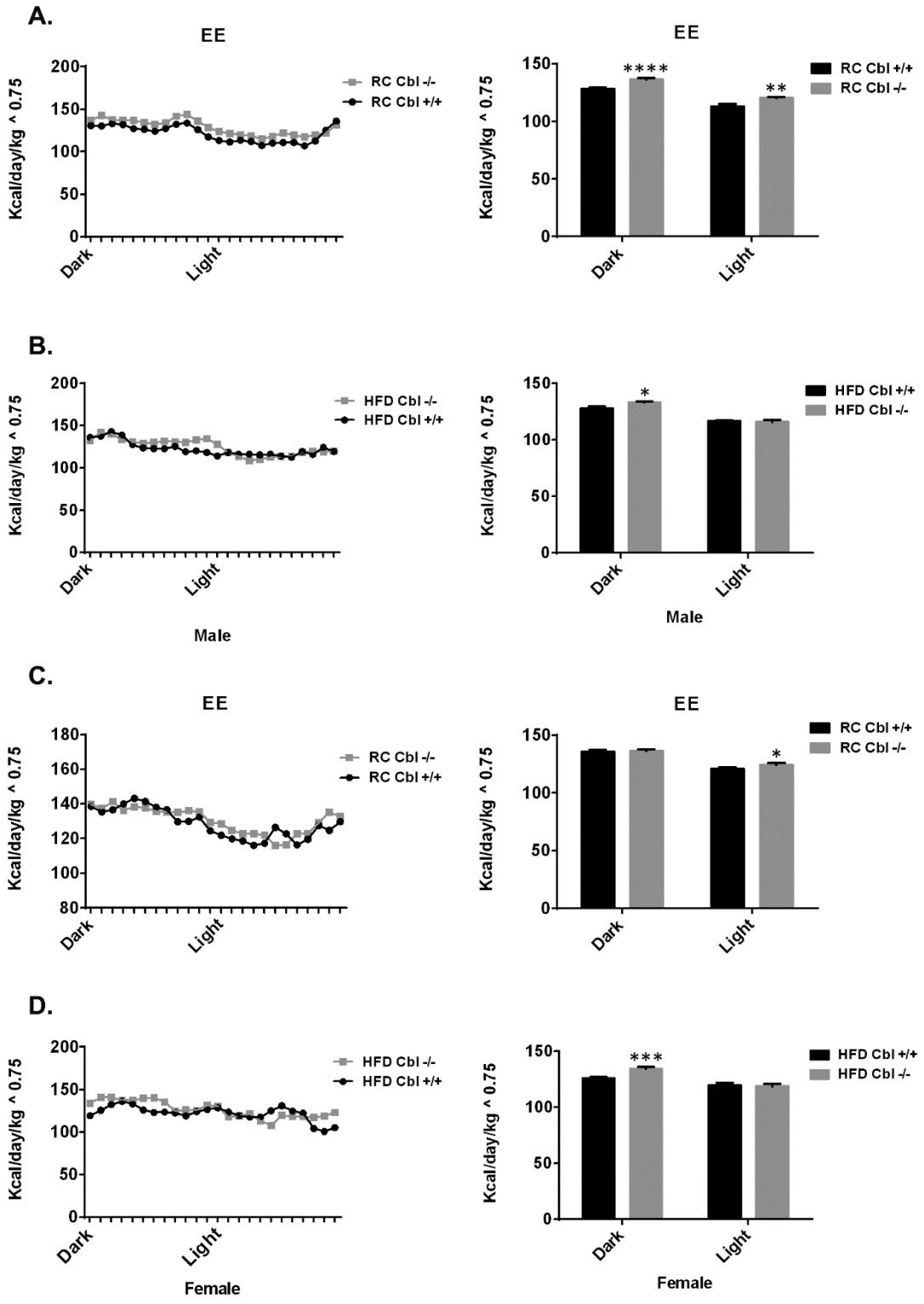

Fig. 43. Energy Expenditure in Cbl $^{-/-}$ and Cbl $^{+/+}$ mice (male and female) on RC and HFD diet. Values plotted at 1-hour intervals (the average was taken for every 2 hours from 6 PM to the 4 PM of the next day). **A)** male and **C)** female RC Cbl $^{-/-}$ mice and RC Cbl $^{+/+}$ mice. **B)** male and **D)** female HFD Cbl $^{-/-}$ and HFD Cbl $^{+/+}$ mice respectively, male mice n=4, female mice n=3. EE is increased significantly in Cbl $^{-/-}$. Data represent as means ± SEM. Statistical analysis: Multiple t test, * indicates $p<0.05$; ** $p<0.01$; *** $p < 0.001$; ****$p<0.0001$.

3. Activity

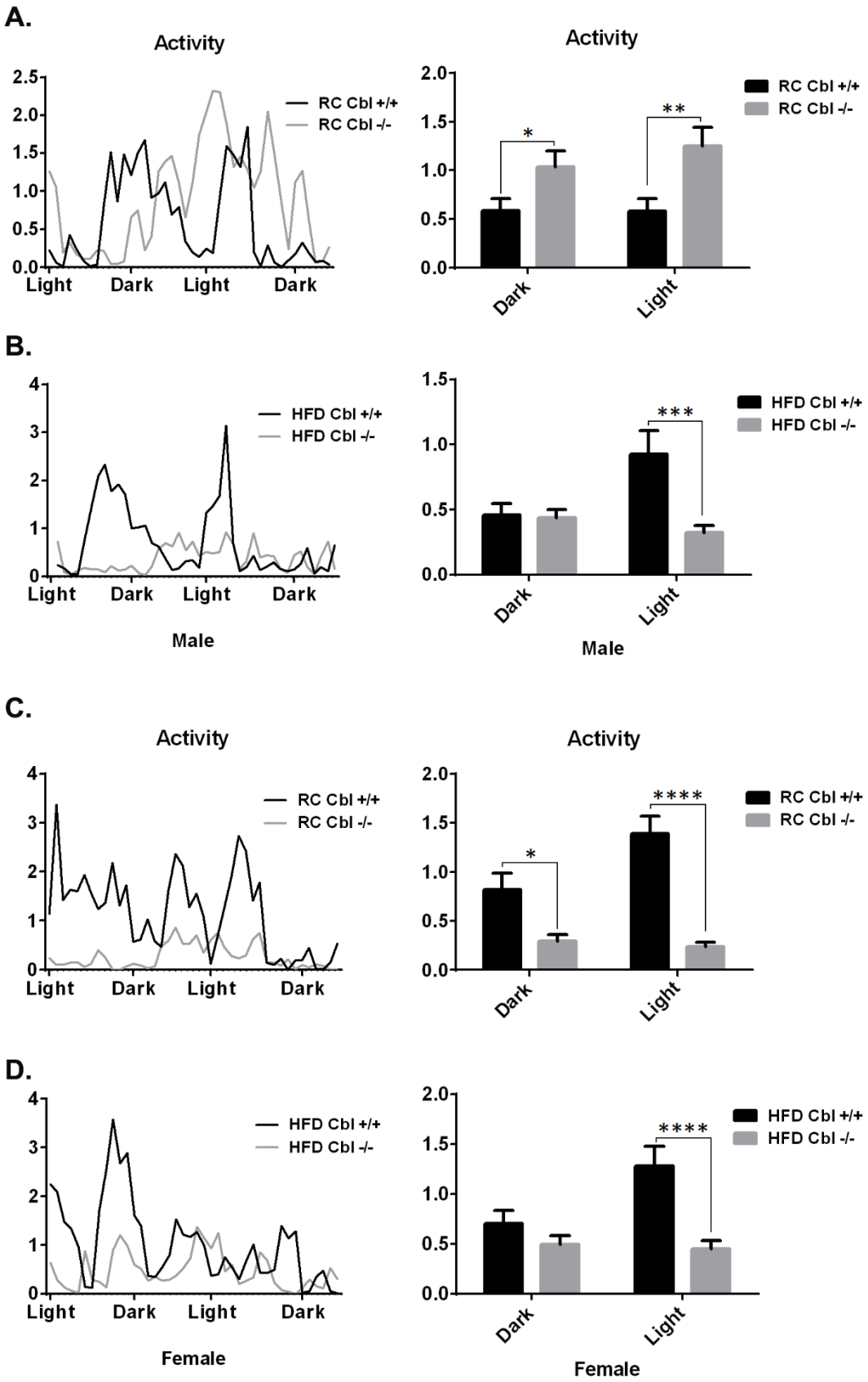
A.
Activity
RC Cbl +/+
RC Cbl -/-
Light
Dark
Light
Dark
Activity
RC Cbl +/+
RC Cbl -/-
*
**
Dark
Light
B.
HFD Cbl +/+
HFD Cbl -/-
Light
Dark
Light
Dark
Male
HFD Cbl +/+
HFD Cbl -/-
***
Dark
Light
Male
C.
Activity
RC Cbl +/+
RC Cbl -/-
Light
Dark
Light
Dark
Activity
RC Cbl +/+
RC Cbl -/-
****
*
Dark
Light
D.
HFD Cbl +/+
HFD Cbl -/-
Light
Dark
Light
Dark
Female
HFD Cbl +/+
HFD Cbl -/-
****
Dark
Light
Female

Fig. 44. Activity in Cbl $^{-/-}$ and Cbl $^{+/+}$ mice (male and female) on RC and HFD diet. **A)** male and **C)** female RC Cbl $^{-/-}$ mice and RC Cbl $^{+/+}$ mice. **B)** male and **D)** female HFD Cbl $^{-/-}$ and HFD Cbl $^{+/+}$ mice respectively, male mice n=4, female mice n=3. Data represent as means ± SEM. Statistical analysis: Two-way ANOVA, Sidak's multiple comparisons test,

* indicates $p<0.05$; ** $p<0.01$; ***$p<0.001$; ****$p<0.0001$.

5.4 Adipokine content in the Cbl $^{-/-}$ mice fed a HFD

Obesity is closely linked to chronic low-grade inflammation resulting from macrophage infiltration and activation within adipose tissue, resulting in increased released of proinflammatory cytokines. Since Cbl $^{-/-}$ mice maintain insulin responsiveness under a HFD, we hypothesized that the release of insulin sensitizing adipokines (adiponectin, leptin) is greater whereas pro-inflammatory adipocytokines (RBP4, TNF-α and IL6) levels are lower in Cbl $^{-/-}$ compared to Cbl $^{+/+}$ mice when fed a HFD.

To find out how HFD affects adipokine profile expression in Cbl $^{-/-}$ mice, we examined the adipokine profile in WAT, liver and plasma in mice fed a HFD and compared it to mice fed a regular chow diet.

As we previously found in chapter 4 adiponectin levels were slightly higher in the WT mice than in Cbl $^{-/-}$ mice. We found that a high fat diet had no impact on adiponectin content in WAT and plasma in Cbl $^{-/-}$ and Cbl $^{+/+}$ mice (Fig. 45A, B).

However, leptin content was reduced significantly in male Cbl $^{-/-}$ mice fed a HFD compared to Cbl $^{+/+}$ mice on a RC in WAT (Fig. 46A). Similar results were found in circulating leptin content in female Cbl $^{-/-}$ on HFD compared to Cbl $^{-/-}$ on a RC diet (Fig. 46B).

RBP4 content in WAT was not different in Cbl $^{-/-}$ mice fed a HFD compared to the control Cbl $^{+/+}$ mice for either gender (Fig. 47A). Also, no change was found in the

expression of RBP4 in plasma for either gender fed RC or HFD diets (Fig. 47C). However, RBP4 abundance in liver was decreased in female Cbl $^{-/-}$ mice fed a HFD compared to female Cbl $^{+/+}$ mice on the same diet (Fig. 47B).

We also examined the content of IL-6 and TNF-α in WAT and plasma. We found that IL-6 content was no different in WAT or plasma in Cbl $^{-/-}$ mice compared to control Cbl $^{+/+}$ littermates (Fig. 48A, C) and no change was observed in TNF-α protein content in WAT of Cbl $^{-/-}$ mice compared to Cbl $^{+/+}$ on either diet (Fig. 48B).

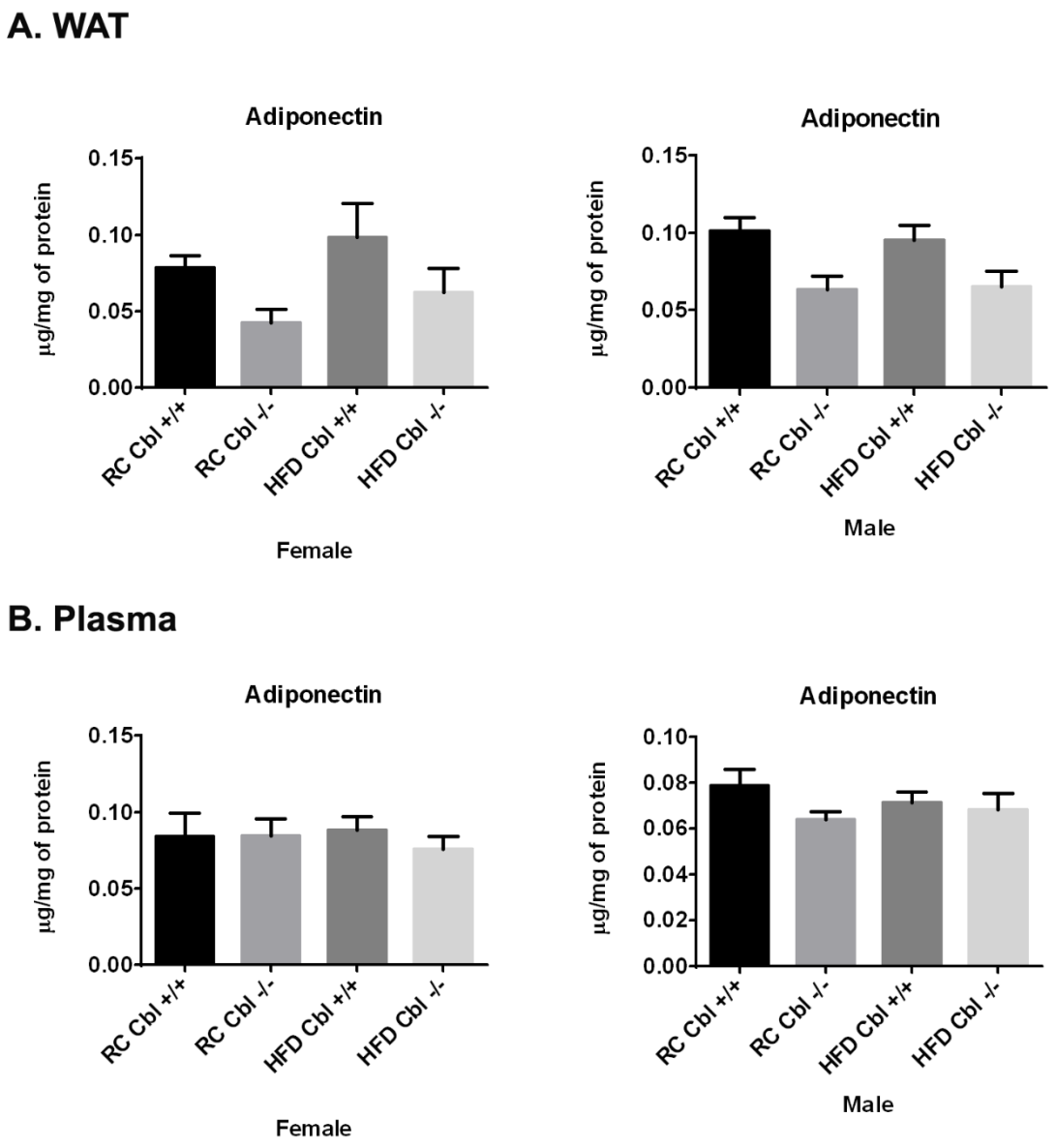

Fig. 45. Expression of adiponectin in WAT and plasma in Cbl $^{-/-}$ and Cbl $^{+/+}$ on HFD and RC diet. No change in the expression of adiponectin in WAT and plasma of mice fed either a HFD or RC diet **A)** Adiponectin levels in white adipose tissue. **B)** Adiponectin expression in plasma. (RC Cbl $^{-/-}$ male n= 3, HFD Cbl $^{-/-}$ male n=3, RC Cbl $^{-/-}$ female n= 3, HFD Cbl $^{-/-}$ female n=3, RC Cbl $^{+/+}$ male n=7, HFD Cbl $^{+/+}$male n= 9, RC Cbl $^{+/+}$ female n=3, HFD Cbl $^{+/+}$ female n=3). Data represent means ± SE. Statistical analysis: ANOVA-one way, Tukey's multiple comparisons test.

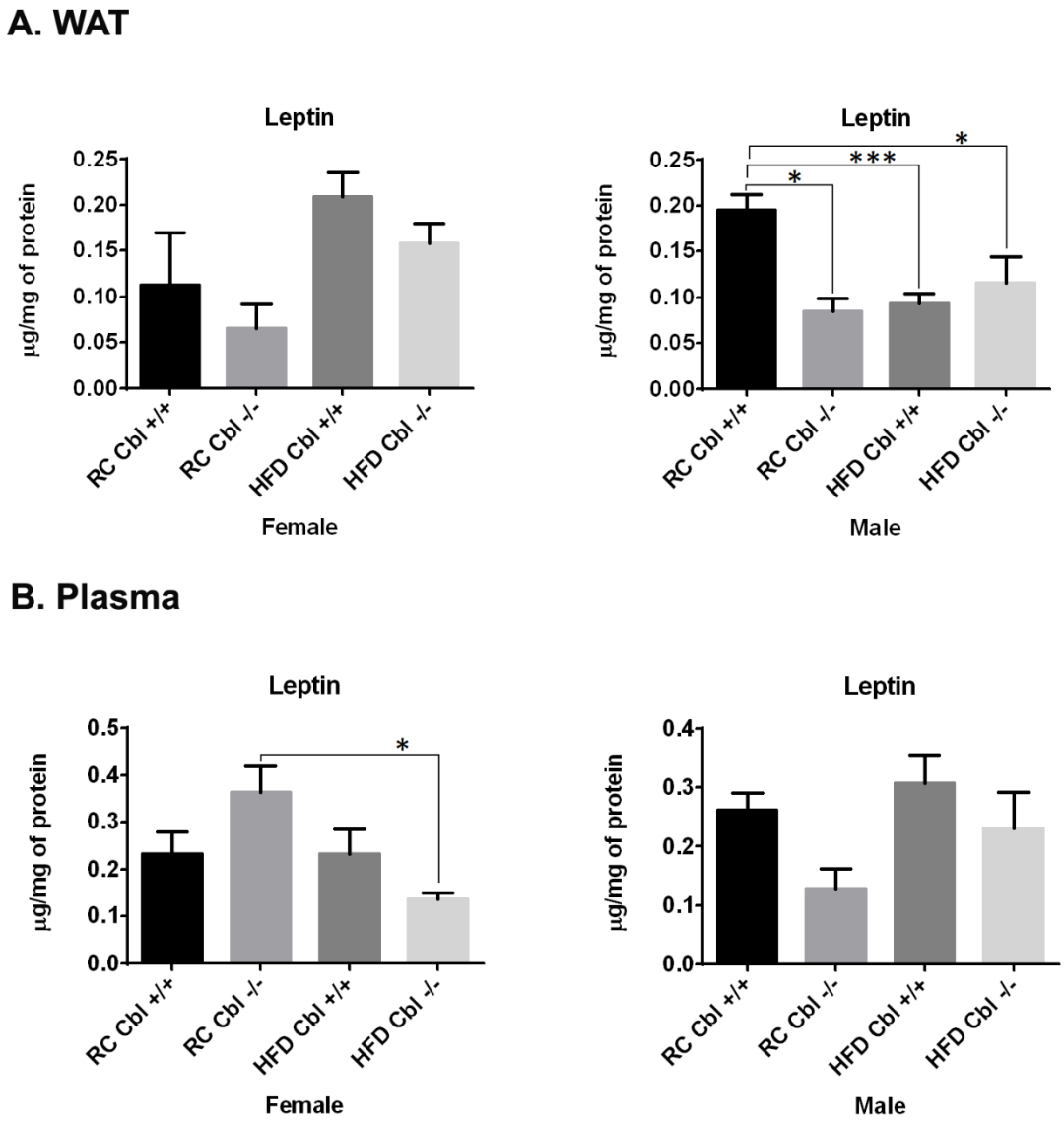

Fig. 46. Expression of leptin in WAT and plasma in Cbl $^{-/-}$ and Cbl $^{+/+}$ mice fed a HFD or RC diet. Leptin content in WAT in male and female circulating leptin of HFD Cbl $^{-/-}$ was significantly reduced. **A)** Leptin expressed in white adipose tissue. **B)** Leptin expression in in plasma. (RC Cbl $^{-/-}$ male n= 3, HFD Cbl $^{-/-}$ male n=3, RC Cbl $^{-/-}$ female n= 3, HFD Cbl $^{-/-}$ female n=3, RC Cbl $^{+/+}$ male n=7, HFD Cbl $^{+/+}$male n= 9, RC Cbl $^{+/+}$ female n=3, HFD Cbl $^{+/+}$ female n=3). Data represent means ± SE. Statistical analysis: ANOVA-one way, Tukey's multiple comparisons test, * indicates $p<0.05$; *** $p < 0.001$.

A. WAT

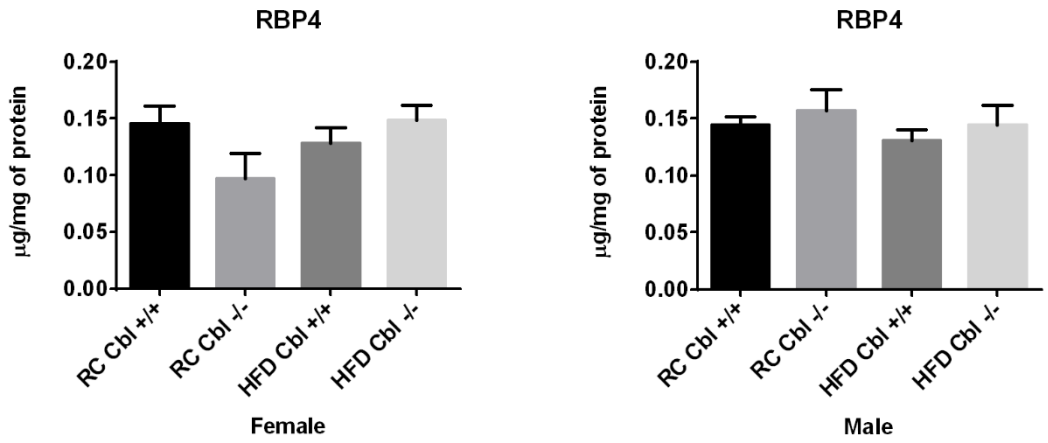

B. Liver

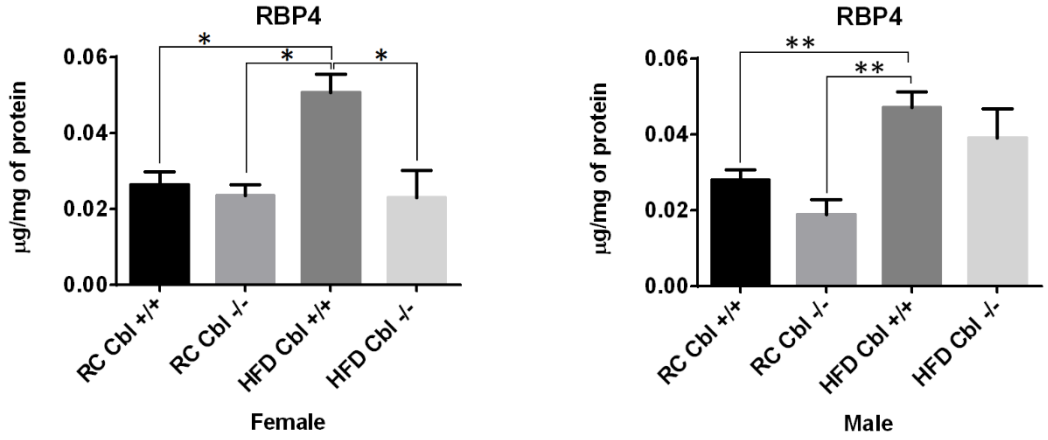

C. Plasma

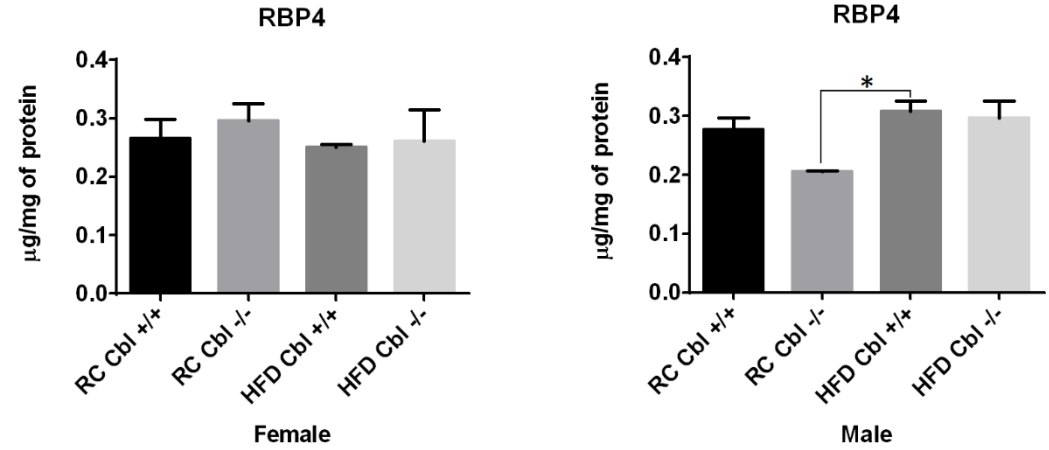

Fig. 47. Expression of RBP4 in WAT, liver and plasma in Cbl $^{-/-}$ and Cbl $^{+/+}$ on HFD and RC diet. RBP4 abundance in liver of female Cbl $^{-/-}$ fed a HFD was reduced. **A)** RBP4 levels in white adipose tissue. **B)** RBP4 expression in Liver. **C)** RBP4 expression in plasma. (RC Cbl $^{-/-}$ male n= 3, HFD Cbl $^{-/-}$ male n=3, RC Cbl $^{-/-}$ female n= 3, HFD Cbl $^{-/-}$ female n=3, RC Cbl $^{+/+}$ male n=7, HFD Cbl $^{+/+}$male n= 9, RC Cbl $^{+/+}$ female n=3, HFD Cbl $^{+/+}$ female n=3). Data represent means ± SEM. Statistical analysis: ANOVA-one way, Tukey's multiple comparisons test, * indicates $p<0.05$; ** $p<0.01$.

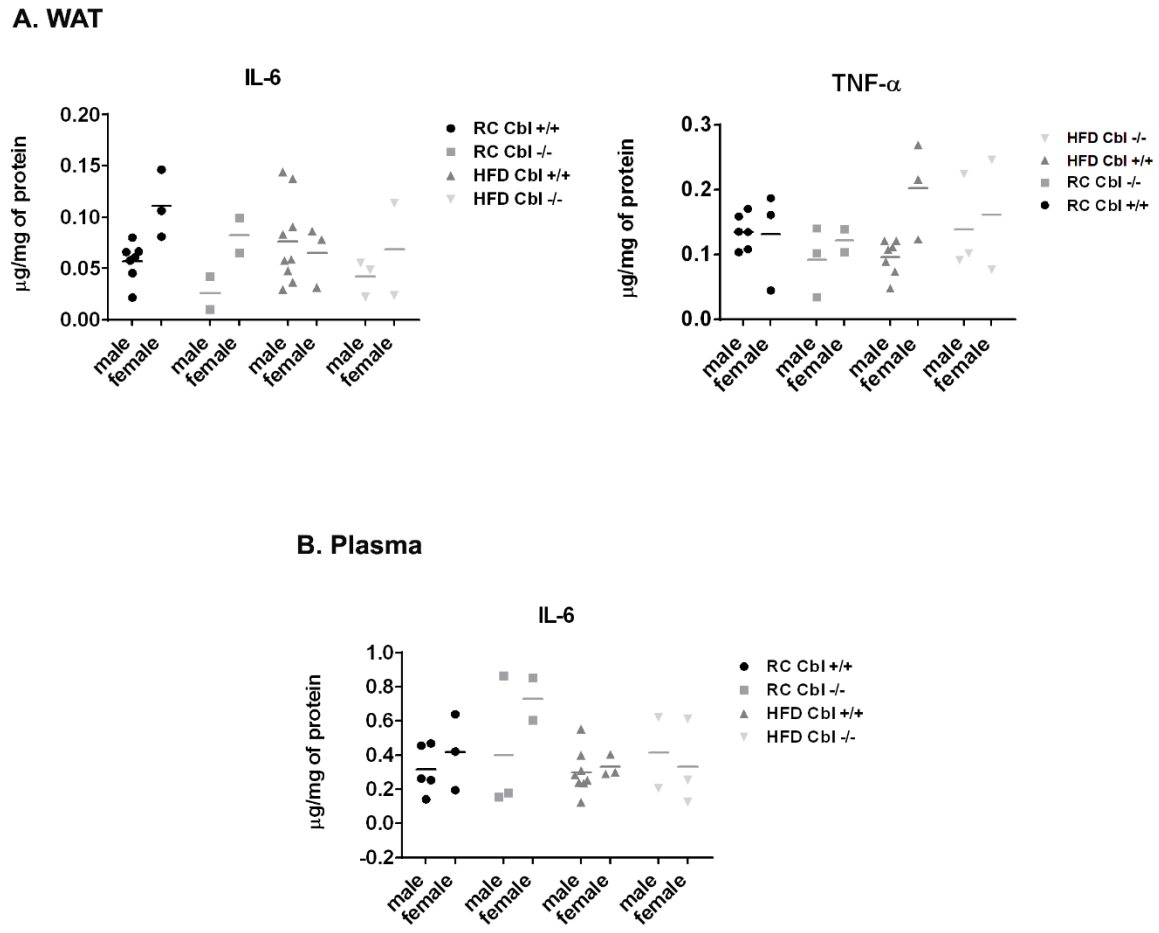

Fig. 48. Expression of IL-6 in WAT and plasma, and TNF-α in WAT in Cbl $^{-/-}$ and Cbl $^{+/+}$ on HFD and RC diet. No changes in the expression of IL-6 or TNF-α in white adipose tissue or plasma in Cbl $^{-/-}$ fed a HFD or RC diet **A)** IL-6 levels in white adipose tissue. **B)** IL-6 levels in plasma. **C)** TNF-α levels in white adipose tissue. (male and female RC Cbl $^{-/-}$ n=5, HFD Cbl $^{-/-}$ n=5, male and females RC Cbl $^{+/+}$ n=8 RC, HFD=11). Data represent means ± SEM. Statistical analysis: Two-way ANOVA, Tukey's multiple comparisons test.

5.5 Discussion

In this chapter, we hypothesized that Cbl $^{-/-}$ mice would adapt differently to the metabolic challenges imposed by a high fat feeding. Thus, we evaluated how a HFD diet affected insulin sensitivity, substrate utilization (RQ, and EE) and activity and WAT adipokine expression in Cbl $^{-/-}$ mice and compared to control Cbl $^{+/+}$ mice. We showed that exposure to a HFD resulted in persistent body weight gain in Cbl $^{-/-}$ mice which was inconsistent with previous findings by Molero *et al.* [18]. However, food intake was not significantly different in Cbl $^{-/-}$ mice fed a HFD compared to control wild type mice on the same diet and these data are in disagreement with those of Molero *et al.* [18, 22] who detected a significant increase in food intake in Cbl $^{-/-}$ mice.

In vivo insulin sensitivity and glucose clearance was increased in Cbl $^{-/-}$ mice fed a HFD compared with control Cbl $^{+/+}$ animals fed the same diet in agreement with the previous study [18] where Cbl $^{-/-}$ mice (Jvs 129 x C57BL6) fed a HFD displayed a significantly better glucose tolerance compared to wild type control.

Several factors may account for the differences observed (weight gain, food intake, adipocytes cells size and adipokine expression) in our results compared to Molero *et al.* studies [18, 22]. These include: 1) the different genetic background of the mice (C57BL6 vs JVS129); 2) we started our experiments at a younger age (at weeks 4 post-weaning) compared to 20 weeks of age; 3) the duration of the diet intervention for 8 weeks vs 16 weeks [22]; and 4) the severity of the fat content in the diet, we used 45% of HFD, as previous studies [270, 271] while Molero *et al.* used 60% HFD [18, 201]. These factors, likely contributed to these differences between our observations and those of Molero *et al.* [18, 22].

The increase in food intake observed in male Cbl $^{-/-}$ mice with approximately less body weight gain and decreased triglyceride content in RC Cbl $^{-/-}$ mice, suggested that these mice may have increased energy expenditure and activity.

In terms of ambulatory activity, we observed a significant increase in activity in Cbl $^{-/-}$ male but not female mice, while male and female HFD Cbl $^{-/-}$ mice displayed a reduction in the activity during the light cycle compared to their controls (Fig. 44). These findings disagree with those of Molero *et al.* [18], who observed that ambulatory activity was increased in HFD Cbl $^{-/-}$ mice compared to wild type during both day and night phases of the cycle.

Our RQ and EE analyses revealed that RQ was higher in male Cbl $^{-/-}$ mice compared to control Cbl $^{+/+}$ mice, pointing to increased carbohydrate oxidation relative to lipid oxidation in these animals, while the mice were fed a regular chow diet, and no further differences were observed when mice were fed a HFD. Moreover, energy expenditure was increased in RC male Cbl $^{-/-}$ mice during light and dark cycle compared to male RC Cbl $^{+/+}$ mice (Fig. 43A). In addition, EE during the dark cycle was higher in male Cbl $^{-/-}$ mice fed a HFD compared to control male Cbl $^{+/+}$ mice fed the same diet (Fig. 43B).

However, RQ was lower in female Cbl $^{-/-}$ mice fed a HFD during both dark and light cycle compared to female Cbl $^{+/+}$ control mice, indicating increased fat oxidation (Fig. 42B). RQ was closer to 1.0 on RC diet and it was reduced to approximately 0.85 in female Cbl $^{-/-}$ mice fed a HFD (Fig. 42D). This suggested that the metabolism switched from carbohydrates (CHO) to lipid utilization as a source of energy. While energy expenditure was only increased in RC female Cbl $^{-/-}$ during the light cycle compared to RC female Cbl $^{+/+}$ (Fig. 43C). On the other hand, EE in female Cbl $^{-/-}$ mice

fed a HFD during the dark cycle was higher compared to their control female Cbl $^{+/+}$ mice fed the same diet (Fig. 43D).

Our results were consistent with Molero *et al.* [18] results, who proposed that the increase in energy expenditure is the main cause of reducing fat stores in Cbl $^{-/-}$ mice. Molero and coworkers found a significant increase in the activity of fatty acid oxidation enzymes in skeletal muscle in Cbl $^{-/-}$ mice [18]. However, we did not determine these in our mouse model. We conclude that as a consequence of decreased fat stores, Cbl $^{-/-}$ mice are protected against the deleterious effects of excess fat on insulin signal transduction that has been detected previously in both humans and rodents [39, 278-280]. It is established that enhanced energy expenditure as a result of improved insulin action leads to reduced fat accumulation [281, 282]. Consistent with this, some mouse models, such as APS- or Grb14-deficient mice or mice expressing reduced levels of the regulatory subunits of phosphatidylinositol 3-kinase, exhibit improved insulin action and/or signal transduction without any related change in adipose mass [283-285]. It was reported by Molero *et al.* [18] that the increase in insulin action is unlikely to be upregulated by increased energy expenditure, because the HFD Cbl $^{-/-}$ mice in the previous study [18] had similar glucose tolerance, insulin action and fat content to that in the RC Cbl $^{+/+}$ mice [22] that consume much more calories to support their increased energy expenditure. Therefore, they concluded [18] that the reduction in lipid accumulation as a result of the increased energy expenditure is the main contributor to improved insulin action in Cbl $^{-/-}$ mice fed a HFD. That was consistent with our finding that male Cbl $^{-/-}$ increased glucose tolerance and EE in both RC and HFD, with reduction in triglyceride content in Cbl $^{-/-}$ fed a RC diet.

To help explain the role of adipose tissue in the enhanced insulin sensitivity of this model we sought to determine the adipokine profile in the mice fed a high fat diet. In

this study, leptin content was reduced significantly WAT of male Cbl $^{-/-}$ and also in plasma of the female Cbl $^{-/-}$ mice after exposure to HFD, while no significant changes in adiponectin or RBP4 abundance were detected in WAT or plasma in mice fed a HFD. Compatible with our findings, van der Heijden *et al*. [286] observed that leptin levels were significantly reduced with prolonged HFD-feeding (±30 weeks of HFD-feeding) although body weight remained high. Leptin levels also declined in mice fed the LFD, suggesting an age-related decline in circulating leptin [286]. It has previously been found in rodents [287] and humans [288] that circulating leptin levels decline with age. However, in contrast to our finding, Ahren *et al*. [242] reported that plasma leptin content in C57BL/6J mice was increased with HFD or as a result of aging as it correlated with fat content, body weight and plasma insulin levels. Indeed, as adipocytes expand due to enhanced triglyceride storage, leptin secretion increases proportionately [289]. Whereas, Kamohara *et al.* [290] reported that leptin has anti-diabetic effects independent of its regulation of body weight and energy intake [290]. The effects of leptin are mediated by activating the PI3K/AKT pathway that stimulates insulin sensitivity in peripheral tissues [291].

In contrast to our results, Barnea *et al*. [292] found that mice fed a HFD with higher body weight had lower adiponectin mRNA and protein content in AT than control mice without a reduction of adiponectin plasma levels. Also, another study [293], reported that adiponectin expression in WAT was reduced after HF dietary supplementation in mice. While, Ouchi *et al.* [51] reported that adiponectin gene expression in AT was decreased in obesity with a decrease in adiponectin plasma level in humans and rodents [51, 293]. On the other hand, in support of our findings, Peake *et al.* [294] showed that in normal and diabetic subjects, a fat meal challenge did not lead to significant changes in adiponectin levels in the circulation [294]. This

association between obesity and decreased adiponectin expression is suspected to be linked to the increased inflammatory status of AT [295].

We found no change in RBP4 protein content in WAT and plasma after a high fat diet in Cbl $^{-/-}$ mice compared to Cbl $^{+/+}$ controls. However, RBP4 abundance in liver was reduced significantly in female Cbl $^{-/-}$ compared to female Cbl $^{+/+}$ mice upon exposure to a HFD. RBP4 is an adipokine proposed to be a marker insulin resistance and type 2 diabetes in human [296]. However, many studies have not been able to show this association between human obesity and insulin resistance and have found no correlation between BMI and serum and/or adipose tissue mRNA RBP4 levels [137]. Kahn and colleagues reported that the development of obesity leads to increased expression of RBP4 by adipocytes, influencing metabolic disease development [127, 265]. Asha *et al.* [297] reported that high fat diet induced hyperglycaemia in mice, which could be partly explained by the RBP4 elevation in circulation, due to its over-expression, particularly in visceral adipose depots (both retroperitoneal and gonadal WAT) [297].

In the current study, we found no differences in TNFα or IL-6 in WAT of Cbl $^{-/-}$ compared to Cbl $^{+/+}$ mice for either gender, following an 8-week HFD. van der Heijden *et al.* [286] showed that AT inflammation is associated with the increased secretion of TNF-α and leptin to the circulation after 24 weeks of HFD. IL-6 and TNF-α have been shown to induce SOCS-3 [119, 298], a protein that was previously thought to interfere with cytokine signal transduction but it is also known to inhibit tyrosine phosphorylation of the insulin receptor and IRS-1 and causes ubiquitination and proteosomal degradation of IRS-1 [299]. This, in turn, diminishes AKT activation that normally causes GLUT4 translocation to the plasma membrane [300]. It has been found in rodents, that TNF-α is overexpressed in AT from obese animals. Another

study reported that the adipocytes of obese patients, including those with morbid obesity, overexpressed TNF-α in proportion to the degree of adiposity [301]. On the other hand, Matthews *et al.* [302] demonstrated that deletion of IL-6 (IL6 $^{-/-}$) in mice results in obesity, hepatosteatosis, liver inflammation and insulin resistance when animals are maintained on a standard chow diet. However, when IL6$^{-/-}$ mice are challenged with HF feeding, inflammation and insulin resistance remain, despite equivalent fat mass and ectopic lipid levels in liver relative to control animals [302], which indicated that IL-6 is required for protection against hepatic inflammation and insulin resistance when mice are challenged with a HFD.

In this study, no changes were observed in the pro-inflammatory cytokines (TNF-α and IL-6) in Cbl $^{-/-}$ mice fed a HFD. This might be because of some limitations in the HFD diet such as the diet duration was not long enough and/or the composition of the diet which contains 45% fat, that may have impacted on the detection of some proinflammatory cytokines or observe differences in their (TNF-α and IL-6) protein expression levels.

In conclusion, we determined that Cbl $^{-/-}$ mice on a HFD had a higher EE. Male Cbl $^{-/-}$ mice were more insulin sensitive than their control Cbl $^{+/+}$ mice. Adiponectin protein content did not change in Cbl $^{-/-}$ mice. However, leptin content in WAT was reduced in male Cbl $^{-/-}$ mice with a reduction in circulating leptin in female Cbl $^{-/-}$ mice. RBP4 was reduced in liver of female Cbl $^{-/-}$ compared to the control Cbl $^{+/+}$ mice. No differences were observed in TNFα or IL-6 content in WAT of Cbl $^{-/-}$ compared to Cbl $^{+/+}$ mice for either gender.

These finding suggests that Cbl $^{-/-}$ (C57BL6 background) mice fed a HFD for 8 weeks following the post-weaning period, are protected from high-fat-diet induced

insulin resistance, consistent with the findings of reported previously by Molero *et al*. [22] on Cbl $^{-/-}$ (Jvs 129 x C57BL6 background) mice.

Chapter 6

General discussion

6.1 Overview

The studies in this thesis highlight the potential effects of c-Cbl depletion in overall glucose homeostasis and WAT physiology. The results show that c-Cbl depletion is likely to have a role in the regulation of insulin action in adipose tissue mainly through the potentiation of insulin mediated ERK signaling and the modulation of adipokine expression. In addition, this study is the first to demonstrate a direct effect of the c-Cbl pathway in upregulating RBP4 expression in adipose tissue through a ER mediated mechanism (Fig. 49).

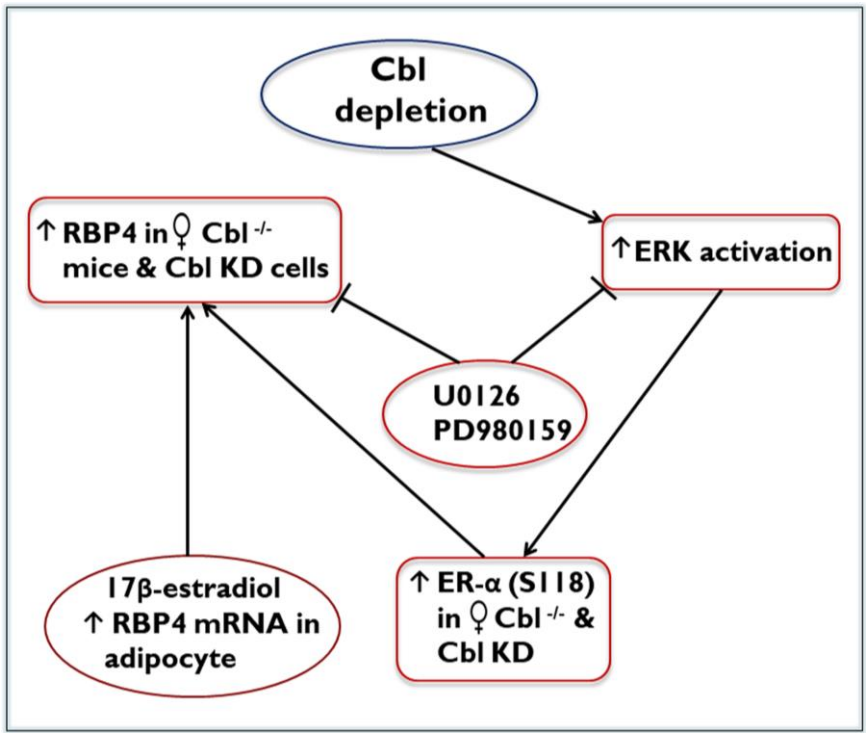

Fig. 49. Hypothetical mechanism of action of c-Cbl depletion in WAT and in 3T3L1 Cbl KD cells. c-Cbl depletion mediates activation of ERK1/2 by increased phosphorylation of ER-α at S118 that leads to upregulated RBP4 expression in WAT of female Cbl $^{-/-}$ mice and 3T3L1 Cbl KD cells. Where → = stimulation, ⊥ = inhibition ↑= increase, ♀= female.

Specifically, we have shown that c-Cbl depletion in C57BL6 mice improves insulin sensitivity and changes adipokine expression. We found that RBP4 expression in visceral WAT of female Cbl $^{-/-}$ mice was increased locally without affecting RBP4 protein levels in liver, which is the main site for RBP4 production. However, this was not true under a HFD where c-Cbl depletion did not protect against RBP4 production in the liver. This finding is supported by a study that reported RBP4 is predominantly expressed in the liver in rodents [303]. Thus, the effect of HFD on RBP4 protein expression was specific to liver and did not occur in visceral fat. As the liver is the major tissue to produce and secrete RBP4, it was predictable that a HFD should increase liver RBP4 expression. In addition, however, we suggest that the effect of HFD on adipose tissue RBP4 expression and serum RBP4 might be mediated through a reduction in adipose tissue inflammation or reduction in visceral fat. This assumption was supported by evidence that showed a close connection between RBP4 expression and its protein level, and inflammatory markers [137, 304]. Furthermore, our studies confirmed that a period of 8 weeks on HFD started at early age and using with 45% fat calories, was not a determinant factor for changing inflammatory marker expression such as TNF-α and IL-6, which might be induced by longer term HFD.

On the basis of the current study, we suggest that inhibition or depletion of c-Cbl genes in humans might provide a therapeutic approach for prevention/treatment of diabetes and insulin resistance.

6.2 Pleiotropic effects

c-Cbl mediated signaling has pleiotropic effects in various cell types and tissues, which reflects the c-Cbl protein interactome. Studies in other systems illustrate the potential for targeting c-Cbl, although inevitably caution should be applied in extrapolating to c-Cbl targets to improve glucose homeostasis.

The data from the earlier studies [18, 22, 201] suggested that c-Cbl ubiquitin ligase activity plays an essential role in the lean phenotype, and may be essential in regulating the expression of proteins involved in control of energy expenditure. These studies reported that it is c-Cbl ubiquitin ligase activity that plays an important role in the regulation of whole-body energy metabolism [201]. An *in vivo* study in mice by Wu *et al*. [305] showed that generating c-Cbl RING domain inhibitors through modified peptides 10, 34, 49 and 51 protected mice from HFD-induced obesity and insulin resistance. This research provided several c-Cbl RING domain inhibitors that specifically inhibit c-Cbl-UbcH7 binding and could be used to test the efficacy of Cbl inhibition in regulation of metabolism.

In this context it is interesting that Rathinam *et al*. [306] showed that the E3 ubiquitin ligase activity of c-Cbl is required to restrict myeloid leukaemia development, based on observations in mice with a mutation in the RING finger domain of c-Cbl. They noted that myeloproliferative disease (MPD) invariably leads to a lethal myeloid leukaemia in the c-Cbl RING finger mutant mouse. In contrast, the c-Cbl $^{-/-}$ mouse develops a mild MPD that does not lead to leukaemia. Whether or not mutation of c-Cbl is implicated in glucose homeostasis remains largely unexplored. Even so, characterization of the perturbations mentioned above provides a direction for therapeutics that may aid the treatment of patients with c-Cbl mutations [306].

However, Rush *et al*. [307] reported that attenuating c-Cbl activity, either through RNAi or pharmacological inhibitors ([4-amino-5-(4-methylphenyl)-7-(t-butyl)pyrazolo-d-3,4-pyrimidine] or PP1) in immortalized human corneal epithelial cells (hTCEpi), caused a decrease in receptor ubiquitylation, altered trafficking of the ligand-receptor complex, and increase EGFR phosphorylation. Ultimately, these biochemical changes culminated in enhanced corneal epithelial wound healing *in vitro* and *in vivo*. Based on these findings, c-Cbl is a new therapeutic target to increase EGFR-activity, which is directly correlates with an increased rate of corneal epithelial wound healing.

In keeping with the pleiotropic role of c-Cbl, Rafiq *et al*. [308] suggested that c-Cbl deletion protects the heart against ischemia reperfusion (IR) injury by decreasing/preventing ubiquitination and subsequent degradation of EGFR and focal adhesion kinase (FAK) and myocyte death. These findings provide evidence for an important role of c-Cbl in direct modulation of EGFR and focal adhesion protein turnover in the heart. Given that EGFR and FAK signaling downregulation also underlie cardiac hypertrophy and other form of heart disease, it is likely that c-Cbl plays a role in a variety of stress settings.

Furthermore, Sévère *et al*. [309, 310] reported that inhibition of c-Cbl activity influence intracellular signaling and promote osteoblast differentiation.

Taken together the work described on other systems indicates the scope for further investigation of the role of c-Cbl in diabetes.

6.3 Limitations and future work

A major perceived limitation of this study was the experimental design of the HFD study which was not sufficient to produce effects on AT expansion, TG content and inflammation (by increasing pro-inflammatory cytokines (IL-6 and TNF-α), and macrophage infiltration) causing insulin resistance and T2D. In support of the experimental design, it should be noted that others have used a similar protocol [272, 311]. Nevertheless, it may be the case that we started our study on animals at too early an age (post-weaning), that the duration of the HFD was insufficient and that the fat content of the diet was insufficient. All these factors may have significant effects on adipose tissue metabolism. In follow up studies, animals could be fed a HFD when mice are more developed, for example from weeks 8 -16. The duration of the diet intervention should be extended to, for example, 16 weeks of age, or it could be started later in adult mice. Moreover, the number of calories as fat could be increased to 60% instead of 45%.

Due to the lack of time, the studies here did not explore the impact of c-Cbl depletion in brown adipose tissue in detail. In recent years it has become apparent that BAT also plays a key role in regulating overall glucose and lipid homeostasis [312, 313]. Our data suggested that c-Cbl depletion in BAT has no effect in terms of cell size and lipid content as no differences were detected in cell size or triglyceride levels within BAT. However, to expand these findings we could explore BAT in terms of mitochondrial activation that might shed the light on how Cbl $^{-/-}$ mice increase energy expenditure and to see if there is a relation between BAT mitochondrial activation and UCP-1 expression or there are some [313] alternative mechanisms.

Other areas with the potential for future exploration include the determination of estrogen levels at different ages throughout the life time of female mice (both Cbl $^{-/-}$

and Cbl $^{+/+}$) and to relate these findings to adipokine expression in WAT and in the circulation. Potentially this would help explain the gender-differences between males and females.

In addition, further work to examine subcutaneous adipose would be useful, since this depot is associated with protection from obesity-related insulin resistance. For example, further study could be directed at how c-Cbl depletion influences subcutaneous adipose tissue properties, particularly insulin sensitivity and adipokine expression compared with visceral fat in Cbl $^{-/-}$ mice.

6.4 Conclusions

The work in this thesis suggests new ways of understanding the pathogenesis of T2D and specifically role of c-Cbl. It is now clear that there are opportunities to investigate possible strategies to examine genetic influences of c-Cbl deficiency for the prevention or progression of obesity related insulin resistance and T2D in human. Augmenting this approach may have therapeutic potential in the management of T2D disease in the context of insulin resistance

This work will be worthwhile not least because it holds promise for new treatments by increasing whole-body insulin sensitivity and energy expenditure. In particular, there emerges the possibility that c-Cbl depletion could act as a drug target for the prevention and development of T2D.

7 Appendix

7.1 Chemical reagents All common chemicals were purchased from Sigma Chemical Co., Bio-Rad Laboratories and Life Technologies, unless specified below or in the text.

Bio-Rad Laboratories	β-mercaptoethanol
	TEMED (#1610801)
	Precision plus protein dual color-standards (# 161-0374)
Sigma	Dulbecco's Modified Eagle Medium (DMEM)
	DAP solution (# 868272-85-9)
	Free Glycerol Reagent (# F6428)
	Insulin solution, human recombinant (#I9278)
	TRI reagent (#T9424)
	Chloroform (#C2432)
	2-propanol (#I9516)
Trajan Scientific and Medical	DPX mounting medium (# 1.00579.0500)
Thermo Fisher Scientific	TMB (# 34028)
	HRP-Conjugated Streptavidin (#N100)
	Agarose (BP1356)
	TrackIt 100 bp DNA Ladder (# 10488-058)

7.2 Enzymes and commercially prepared kits

Roche.com	Proteinase K (REF 03115887001)
Promega.com	GoTaq DNA polymerase (# 9PIM317)
	GoTaq Hot Start Polymerase (# 9PIM500)
Bio-Rad Laboratories	Bradford Protein Quantification (# 500-0006)
	iScript cDNA synthesis kit (#170-8891)
Life Technologies	iTAQ Universal probes supermix (#172-5130)
Sigma	Lipase enzyme (L1754)
Vector Laboratories	ImmPRESS HRP Anti-Goat IgG Reagent (# MP-7405)
R&D Systems	Mouse adipokine array kit (# 607680).

7.3 Solutions and buffers

Solutions used in this thesis are listed below, alphabetically within each section. Final concentrations of reagents are given for all solutions.

Buffer

Tissue lysis buffer for genotype PCR (pH 8.5)
100 mM Tris
20 mM acetic acid
200 mM NaCl
0.2 % SDS (Sodium Dodecyl Sulfate)
100 µg/ml proteinase K

Tris-acetate-EDTA (TAE) buffer
40 mM Tris (pH 7.6)
5 mM EDTA
1 mM EDTA

3T3L1 lysis buffer
50 mM Hepes
150 mM NaCl
10 mM EDTA
10 mM sodium pyrophosphate ($Na_4P_2O_7$)
10% Glycerol
2mM sodium vanadate (Na_3VO_4)
100mM NaF
2µg/ml Pepstatin
2µg/ml Leupeptin
2µg/ml Aprotinin
2mM of Phenylmethylsulfonyl fluoride (PMSF)
1% Triton x-100 or 1% NP-40.

Adipose tissue lysis buffer
100mM NaCl
1mM EDTA
1% Triton X-100
50mM NaF
2mM sodium pyrophosphate
1mM sodium vanadate
1mM PMSF
2µg/ml Pepstatin
2µg/ml Leupeptin
2µg/ml Aprotinin

1x PBS buffer (Phosphate-buffered saline, pH 7.4)
10 mM Potassium phosphate monobasic (KH_2PO_4)
10 mM Sodium hydrogen phosphate (Na_2HPO_4)
2.7 mM Potassium chloride (KCl)
0.137 mM Sodium chloride (NaCl)

1x TBS buffer (pH 7.6)

(Tris-buffered saline)

20 mM Tris base

150 mM NaCl

distilled water

1x TBST buffer (pH 7.6)

(Tris-buffered saline, 0.1% Tween 20)

1X TBS buffer

0.1% Tween 20

Tris-EDTA buffer (pH 9.0)

10mM Tris-HCl

1mM disodium EDTA

distilled water

7.4 Electrophoresis Solutions and Western Blotting Solution

Blocking Solution (10 ml)

5% non-fat milk powder
1x TBST
5g milk in 100 ml TBST

3x Laemmli Sample Buffer (LSB)

1 M Tris pH 6.8 (2.4 ml)
20% SDS (3ml)
100% Glycerol (3ml)
0.03% Bromophenol Blue (6 mg)
15% β-mercaptoethanol (0.5 ml)

1x Running Buffer pH 8.6

25 mM Tris base

192 mM Glycine
0.1% SDS

1x Transfer Buffer pH 8.3

25 mM Tris

192 mM Glycine
20% Methanol
0.1 % SDS

10 ml of 8% running Gel

4.69 ml sterile water (dd H_2O)

2.66 ml acrylamide (30%)

2.5 ml Tris (1.5 M pH 8.8)

100 µl SDS (10%)

100 µl APS (10%)

6 µl TEMED

10 ml of 10% running Gel

3.96 ml dd H_2O

3.33 ml acrylamide (30%)

2.5 ml Tris (1.5 M pH 8.8)

100 µl SDS (10%)

100 µl APS (10%)

6 µl TEMED.

10 ml of 12% running Gel

3.3 ml dd H_2O

4 ml acrylamide (30%)

2.5 ml Tris (1.5 M pH 8.8)

100 µl SDS (10%)

100 µl APS (10%)

6 µl TEMED.

5 ml stacking Gel

2.98 ml dd H2O

0.66 ml acrylamide (30%)

1.25 ml Tris (1.5 M pH 6.8)

50 µl SDS (10%)

50 µl APS (10%)

7 µl TEMED

DNA Agarose Gel (100 ml)

2 gm agarose

100 ml TAE

2 µl ethidium bromide

7.5 Antibodies and primer used in this study are listed in the following tables:

Table 1. Primary antibodies used for western blot. Indicated are the primary antibodies used in this study, dilution, species, Cat. No. and source

Primary Antibody	Dilution	Species	Cat. No.	Company
Phospho-p44/42 MAPK (Erk1/2) (Thr202/Tyr204)	1:1000	rabbit	#9101	Cell Signaling
Total- p44/42 MAPK (Erk1/2)	1:2000	mouse	#9107	Cell Signaling
Phospho-Akt (Ser473)	1:2000	rabbit	#4060	Cell Signaling
Total- Akt Antibody	1:1000	mouse	#2966	Cell Signaling
UCP1 (C-17): sc-6528	1:1000	goat	sc-6528	Santa Cruz
Phospho-AMPKα (Thr172)	1:1000	rabbit	#2531	Cell Signaling
Cbl (A-9): sc-1651	1:100-1:1000	mouse	sc-1651	Santa Cruz
Phospho-IRS-1 (Ser307)	1:1000	rabbit	#2381	Cell Signaling
Anti-β-Tubulin, Clone AA2	1:1000	mouse	#T8328	Sigma
Anti-Actin	1:100	rabbit	# A2066	Sigma
GLUT4	1:2000	rabbit	-------	From J Pessin (Albert Einstein, NY)
Anti-Estrogen Receptor alpha (phospho S118)	1:1000	rabbit	ab31477	Abcam

Table 2. Secondary antibodies used for western blot. Indicated are the secondary antibodies used in this study, dilution, species, Cat. No. and source.

Secondary Antibody	Dilution	Species	Cat. No.	Company
Anti-mouse IgG (H+L) (DyLight™ 680 Conjugate)	1:15000	Donkey	#4570	Cell Signaling
Anti-rabbit IgG (H+L) (DyLight™ 800 4X PEG Conjugate)	1:30000	Rabbit	#5151	Cell Signaling

Table 3. Antibodies used for ELISA. Indicated are the antibodies used in this study for ELISA, species, Cat. No. and source.

Antibodies	Species	Cat. No.	Company
Mouse Adiponectin/Acrp30	mouse	DY1119	R&D SYSTEMS
Mouse Leptin	mouse	DY498	R&D SYSTEMS
Mouse RBP4	mouse	DY3476	R&D SYSTEMS
TNF-α	mouse	555268	BD biosciences (pharmingen)
IL-6	mouse	555240	BD biosciences (pharmingen)

Table .4 Primer sequences used for RT-PCR

Primer	Sequence	Amplicon	Reference
ERα	F: 5'TGATTGGTCTCGTCTGGCG3'	101	Henderson *et al.* [314].
	R: 5'CATGCCCTCTACACATTTTCCC3'		
ERβ	F: 5'CCTGGCTAACCTCCTGATGCT3'	92	Henderson *et al.* [314].
	R: 5'CCACATTTTTGCACTTCATGTTG3'		

References

8 References

1. Myneni V, Melino G, Kaartinen M: **Transglutaminase 2—a novel inhibitor of adipogenesis**. *Cell death & disease* 2015, **6**(8):e1868.
2. Pettersson A: **Novel aspects of metabolic regulation and inflammation in human adipocytes**: Inst för medicin, Huddinge/Dept of Medicine, Huddinge; 2015.
3. Dalmas E: **Adipose tissue inflammation in obesity and during surgery induced-weight loss: emerging paracrine dialogue between macrophages and lymphocytes**. Université Pierre et Marie Curie-Paris VI; 2012.
4. Danielsson A: **Insulin signalling in human adipocytes: mechanisms of insulin resistance in type 2 diabetes**. 2007.
5. Kusminski CM: **Adipose tissue derived factors in obesity, inflammation & energy homeostasis**. University of Warwick; 2006.
6. Matthä S: **Adipocytes and their metabolic function on hepatocytes**. Technische Universität München; 2014.
7. Landgraf K, Rockstroh D, Wagner IV, Weise S, Tauscher R, Schwartze JT, Löffler D, Bühligen U, Wojan M, Till H: **Evidence of early alterations in adipose tissue biology and function and its association with obesity-related inflammation and insulin resistance in children**. *Diabetes* 2015, **64**(4):1249-1261.
8. Jung UJ, Choi M-S: **Obesity and its metabolic complications: the role of adipokines and the relationship between obesity, inflammation, insulin resistance, dyslipidemia and nonalcoholic fatty liver disease**. *International journal of molecular sciences* 2014, **15**(4):6184-6223.
9. Dahl RC: **The present master thesis (60 etcs),"Establishment of an adipocyte cell-based model to investigate the effect of short-chain fatty acids, especially butyrate, on insulin sensitivity and glucose homeostasis in fat tissue", was carried out at Aarhus University, Faculty of Science and Technology, at the Department of An-imal science, in the period November 2012 to November 2013. The project was made with supervision from Lotte Bach Larsen, Stig Purup, Tina Skau Nielsen, and Peter Kappel Theil**.
10. Lindstad T: **Molecular Mechanisms of Adipogenesis and Adipocyte Biology: Possible role of MKPs and STAMPs**. 2010.
11. Maury E, Brichard S: **Adipokine dysregulation, adipose tissue inflammation and metabolic syndrome**. *Molecular and cellular endocrinology* 2010, **314**(1):1-16.
12. Joe AW, Yi L, Even Y, Vogl AW, Rossi F: **Depot-specific differences in adipogenic progenitor abundance and proliferative response to high-fat diet**. *Stem cells* 2009, **27**(10):2563-2570.
13. Meissburger B: **Molecular mechanisms of adipogenesis in obesity and the metabolic syndrome**. Diss., Eidgenössische Technische Hochschule ETH Zürich, Nr. 19107, 2010; 2010.
14. Ahmadian M, E Duncan R, Jaworski K, Sarkadi-Nagy E, Sul HS: **Triacylglycerol metabolism in adipose tissue**. 2007.
15. Landrier J-F, Marcotorchino J, Tourniaire F: **Lipophilic micronutrients and adipose tissue biology**. *Nutrients* 2012, **4**(11):1622-1649.

16. Pessin JE, Kwon H: **Adipokines mediate inflammation and insulin resistance**. *Frontiers in endocrinology* 2013, **4**:71.
17. Gilliam LA, Neufer PD: **Transgenic mouse models resistant to diet-induced metabolic disease: is energy balance the key?** *Journal of Pharmacology and Experimental Therapeutics* 2012, **342**(3):631-636.
18. Molero JC, Waring SG, Cooper A, Turner N, Laybutt R, Cooney GJ, James DE: **Casitas b-lineage lymphoma–deficient mice are protected against high-fat diet–induced obesity and insulin resistance**. *Diabetes* 2006, **55**(3):708-715.
19. Reitman ML: **Metabolic lessons from genetically lean mice**. *Annual review of nutrition* 2002, **22**(1):459-482.
20. Schrauwen P, Hardie D, Roorda B, Clapham J, Abuin A, Thomason-Hughes M, Green K, Frederik P, Hesselink M: **Improved glucose homeostasis in mice overexpressing human UCP3: a role for AMP-kinase?** *International Journal of Obesity* 2004, **28**(6):824.
21. Schrauwen P, Hesselink MK: **Oxidative capacity, lipotoxicity, and mitochondrial damage in type 2 diabetes**. *Diabetes* 2004, **53**(6):1412-1417.
22. Molero JC, Jensen TE, Withers PC, Couzens M, Herzog H, Thien CB, Langdon WY, Walder K, Murphy MA, Bowtell DD: **c-Cbl–deficient mice have reduced adiposity, higher energy expenditure, and improved peripheral insulin action**. *The Journal of clinical investigation* 2004, **114**(9):1326-1333.
23. Liu J, DeYoung SM, Hwang JB, O'Leary EE, Saltiel AR: **The roles of Cbl-b and c-Cbl in insulin-stimulated glucose transport**. *Journal of Biological Chemistry* 2003, **278**(38):36754-36762.
24. Saltiel AR, Pessin JE: **Insulin signaling in microdomains of the plasma membrane**. *Traffic* 2003, **4**(11):711-716.
25. White P: **Obesity-linked insulin resistance, inflammation, and omega-3 fatty acids: exploring the anti-diabetic potential of novel omega-3 derived pro-resolution mediators**. Citeseer; 2012.
26. Fauci AS: **Harrison's principles of internal medicine**, vol. 2: McGraw-Hill, Medical Publishing Division; 2008.
27. Abel ED, O'Shea KM, Ramasamy R: **Insulin resistance: metabolic mechanisms and consequences in the heart**. *Arteriosclerosis, thrombosis, and vascular biology* 2012, **32**(9):2068-2076.
28. Blair M: **Diabetes Mellitus Review**. *Urologic nursing* 2016, **36**(1).
29. Fernandez Mejia C: **Molecular Basis of Type 2 Diabetes**. *Mol Endo* 2006, **87**:87.
30. Yan L-J: **Pathogenesis of chronic hyperglycemia: from reductive stress to oxidative stress**. *Journal of diabetes research* 2014, **2014**.
31. Zaccardi F, Webb DR, Yates T, Davies MJ: **Pathophysiology of type 1 and type 2 diabetes mellitus: a 90-year perspective**. *Postgraduate medical journal* 2015:postgradmedj-2015-133281.
32. Kahn SE, Hull RL, Utzschneider KM: **Mechanisms linking obesity to insulin resistance and type 2 diabetes**. *Nature* 2006, **444**(7121):840-846.
33. Patel TP, Rawal K, Bagchi AK, Akolkar G, Bernardes N, da Silva Dias D, Gupta S, Singal PK: **Insulin resistance: an additional risk factor in the pathogenesis of cardiovascular disease in type 2 diabetes**. *Heart failure reviews* 2016, **21**(1):11-23.

34. Morino K, Petersen KF, Shulman GI: **Molecular mechanisms of insulin resistance in humans and their potential links with mitochondrial dysfunction**. In.: Am Diabetes Assoc; 2006.
35. DeFronzo RA, Tripathy D: **Skeletal muscle insulin resistance is the primary defect in type 2 diabetes**. *Diabetes care* 2009, **32**(suppl 2):S157-S163.
36. Mason RR, Mokhtar R, Matzaris M, Selathurai A, Kowalski GM, Mokbel N, Meikle PJ, Bruce CR, Watt MJ: **PLIN5 deletion remodels intracellular lipid composition and causes insulin resistance in muscle**. *Molecular metabolism* 2014, **3**(6):652-663.
37. Morales PE, Bucarey JL, Espinosa A: **Muscle Lipid Metabolism: Role of Lipid Droplets and Perilipins**. *Journal of diabetes research* 2017, **2017**.
38. Holland WL, Brozinick JT, Wang L-P, Hawkins ED, Sargent KM, Liu Y, Narra K, Hoehn KL, Knotts TA, Siesky A: **Inhibition of ceramide synthesis ameliorates glucocorticoid-, saturated-fat-, and obesity-induced insulin resistance**. *Cell metabolism* 2007, **5**(3):167-179.
39. Yu C, Chen Y, Cline GW, Zhang D, Zong H, Wang Y, Bergeron R, Kim JK, Cushman SW, Cooney GJ: **Mechanism by which fatty acids inhibit insulin activation of insulin receptor substrate-1 (IRS-1)-associated phosphatidylinositol 3-kinase activity in muscle**. *Journal of Biological Chemistry* 2002, **277**(52):50230-50236.
40. Itani SI, Ruderman NB, Schmieder F, Boden G: **Lipid-induced insulin resistance in human muscle is associated with changes in diacylglycerol, protein kinase C, and IκB-α**. *Diabetes* 2002, **51**(7):2005-2011.
41. Hulver MW, Berggren JR, Cortright RN, Dudek RW, Thompson RP, Pories WJ, MacDonald KG, Cline GW, Shulman GI, Dohm GL: **Skeletal muscle lipid metabolism with obesity**. *American Journal of Physiology-Endocrinology and Metabolism* 2003, **284**(4):E741-E747.
42. Kasuga M: **Insulin resistance and pancreatic β cell failure**. *Journal of Clinical Investigation* 2006, **116**(7):1756.
43. Waldén TB: **Regulatory Factors that Reveal Three Distinct Adipocytes: The Brown, the White and the Brite**. 2010.
44. Andersson DP: **Significance of adipose tissue characteristics for development of metabolic complications in obesity**: Inst för medicin, Huddinge/Dept of Medicine, Huddinge; 2014.
45. Qian S, Huang H, Tang Q: **Brown and beige fat: the metabolic function, induction, and therapeutic potential**. *Frontiers of medicine* 2015, **9**(2):162-172.
46. Keipert S, Jastroch M: **Brite/beige fat and UCP1—is it thermogenesis?** *Biochimica et Biophysica Acta (BBA)-Bioenergetics* 2014, **1837**(7):1075-1082.
47. Park A, Kim WK, Bae K-H: **Distinction of white, beige and brown adipocytes derived from mesenchymal stem cells**. *World journal of stem cells* 2014, **6**(1):33.
48. Tang T: **Regulation of Adipose Tissue Metabolism by NFkB P65 in Transgenic Mice**. Sun Yat-sen University; 2009.
49. Cao H: **Adipocytokines in obesity and metabolic disease**. *Journal of Endocrinology* 2014, **220**(2):T47-T59.
50. Lau DC, Dhillon B, Yan H, Szmitko PE, Verma S: **Adipokines: molecular links between obesity and atheroslcerosis**. *American Journal of Physiology-Heart and Circulatory Physiology* 2005, **288**(5):H2031-H2041.

51. Ouchi N, Parker JL, Lugus JJ, Walsh K: **Adipokines in inflammation and metabolic disease**. *Nature Reviews Immunology* 2011, **11**(2):85-97.
52. Zhou H, Wan B, Grubisic I, Kaplan T, Tjian R: **TAF7L modulates brown adipose tissue formation**. *Elife* 2014, **3**:e02811.
53. Kissig M, Shapira SN, Seale P: **SnapShot: Brown and Beige Adipose Thermogenesis**. *Cell*, **166**(1):258-258.e251.
54. Orava J: **Characterisation of Functional Brown Adipose Tissue In Adult Humans**. 2014.
55. Tam CS, Lecoultre V, Ravussin E: **Brown adipose tissue mechanisms and potential therapeutic targets**. *Circulation* 2012, **125**(22):2782-2791.
56. Saely CH, Geiger K, Drexel H: **Brown versus white adipose tissue: a mini-review**. *Gerontology* 2010, **58**(1):15-23.
57. Brondani LdA, Assmann TS, Duarte GCK, Gross JL, Canani LHS, Crispim D: **The role of the uncoupling protein 1 (UCP1) on the development of obesity and type 2 diabetes mellitus**. *Arquivos brasileiros de endocrinologia & metabologia= Brazilian archives of endocrinology and metabolism Vol 56, n 4 (2012), p 215-225* 2012.
58. Ray RB: **Manipulating Lipolysis to Reduce Fatness and Improve Carcass Composition in Commercial Broilers**. 2013.
59. Goldberg IJ, Eckel RH, Abumrad NA: **Regulation of fatty acid uptake into tissues: lipoprotein lipase-and CD36-mediated pathways**. *Journal of lipid research* 2009, **50**(Supplement):S86-S90.
60. Ward CLaliMDrnAfhdod: **Lipolysis and lipogenesis [internet].** *Diapedia 51040851148 rev no 17* 2015 May 15.
61. Saponaro C, Gaggini M, Carli F, Gastaldelli A: **The subtle balance between lipolysis and lipogenesis: a critical point in metabolic homeostasis**. *Nutrients* 2015, **7**(11):9453-9474.
62. Coelho M, Oliveira T, Fernandes R: **Biochemistry of adipose tissue: an endocrine organ**. *Archives of medical science: AMS* 2013, **9**(2):191.
63. Kersten S: **Mechanisms of nutritional and hormonal regulation of lipogenesis**. *EMBO reports* 2001, **2**(4):282-286.
64. Grahn THM, Kaur R, Yin J, Schweiger M, Sharma V, Lee M-J, Yasuo I, Smas C, Zechner R, Lass A: **FSP27 interacts with ATGL to regulate lipolysis and insulin sensitivity in human adipocytes (LB60)**. *The FASEB Journal* 2014, **28**(1 Supplement):LB60.
65. Serr J, Li X, Lee K: **The Regulation of Lipolysis in Adipose Tissue**. *Journal of Animal Science and Technology* 2013, **55**(4):303-314.
66. Villena JA, Roy S, Sarkadi-Nagy E, Kim K-H, Sul HS: **Desnutrin, an adipocyte gene encoding a novel patatin domain-containing protein, is induced by fasting and glucocorticoids ectopic expression of desnutrin increases triglyceride hydrolysis**. *Journal of Biological Chemistry* 2004, **279**(45):47066-47075.
67. Ahmadian M, Wang Y, Sul HS: **Lipolysis in adipocytes**. *The international journal of biochemistry & cell biology* 2010, **42**(5):555-559.
68. Zimmermann R, Lass A, Haemmerle G, Zechner R: **Fate of fat: the role of adipose triglyceride lipase in lipolysis**. *Biochimica et Biophysica Acta (BBA)-Molecular and Cell Biology of Lipids* 2009, **1791**(6):494-500.
69. Zimmermann R, Strauss JG, Haemmerle G, Schoiswohl G, Birner-Gruenberger R, Riederer M, Lass A, Neuberger G, Eisenhaber F, Hermetter A:

Fat mobilization in adipose tissue is promoted by adipose triglyceride lipase. *Science* 2004, **306**(5700):1383-1386.
70. Choi SM, Tucker DF, Gross DN, Easton RM, DiPilato LM, Dean AS, Monks BR, Birnbaum MJ: **Insulin regulates adipocyte lipolysis via an Akt-independent signaling pathway**. *Molecular and cellular biology* 2010, **30**(21):5009-5020.
71. Brasaemle DL: **Thematic review series: adipocyte biology. The perilipin family of structural lipid droplet proteins: stabilization of lipid droplets and control of lipolysis**. *Journal of lipid research* 2007, **48**(12):2547-2559.
72. Arner P, Langin D: **Lipolysis in lipid turnover, cancer cachexia, and obesity-induced insulin resistance**. *Trends in Endocrinology & Metabolism* 2014, **25**(5):255-262.
73. Choi YH, Park S, Hockman S, Zmuda-Trzebiatowska E, Svennelid F, Haluzik M, Gavrilova O, Ahmad F, Pepin L, Napolitano M: **Alterations in regulation of energy homeostasis in cyclic nucleotide phosphodiesterase 3B–null mice**. *Journal of Clinical Investigation* 2006, **116**(12):3240.
74. Duncan RE, Sarkadi-Nagy E, Jaworski K, Ahmadian M, Sul HS: **Identification and functional characterization of adipose-specific phospholipase A2 (AdPLA)**. *Journal of Biological Chemistry* 2008, **283**(37):25428-25436.
75. Jaworski K, Ahmadian M, Duncan RE, Sarkadi-Nagy E, Varady KA, Hellerstein MK, Lee H-Y, Samuel VT, Shulman GI, Kim K-H: **AdPLA ablation increases lipolysis and prevents obesity induced by high-fat feeding or leptin deficiency**. *Nature medicine* 2009, **15**(2):159.
76. Arner P: **Human fat cell lipolysis: biochemistry, regulation and clinical role**. *Best practice & research Clinical endocrinology & metabolism* 2005, **19**(4):471-482.
77. Lago F, Dieguez C, Conde J, Scotece M, Gualillo O, Gómez R: **Functions of adipose tissue and adipokines in health and disease**: INTECH Open Access Publisher; 2011.
78. Abella V, Scotece M, Conde J, López V, Lazzaro V, Pino J, Gómez-Reino JJ, Gualillo O: **Adipokines, metabolic syndrome and rheumatic diseases**. *Journal of immunology research* 2014, **2014**.
79. Sá RD, Crisma AR, Cruz MM, Martins AR, Masi LN, do Amaral CL, Curi R, Alonso-Vale MI: **Fish oil prevents changes induced by a high-fat diet on metabolism and adipokine secretion in mice subcutaneous and visceral adipocytes**. *The Journal of Physiology* 2016, **594**(21):6301-6317.
80. Farb MG, Gokce N: **Visceral adiposopathy: a vascular perspective**. *Hormone molecular biology and clinical investigation* 2015, **21**(2):125-136.
81. Dalamaga M, Diakopoulos KN, Mantzoros CS: **The role of adiponectin in cancer: a review of current evidence**. *Endocrine reviews* 2012, **33**(4):547-594.
82. Scotece M, Conde J, Gomez R, López V, Pino J, González A, Lago F, Gómez-Reino JJ, Gualillo O: **Role of adipokines in atherosclerosis: interferences with cardiovascular complications in rheumatic diseases**. *Mediators of inflammation* 2012, **2012**.
83. Yadav A, Kataria MA, Saini V, Yadav A: **Role of leptin and adiponectin in insulin resistance**. *Clinica Chimica Acta* 2013, **417**:80-84.

84. Pilch PF, Bergenhem N: **Pharmacological targeting of adipocytes/fat metabolism for treatment of obesity and diabetes**. *Molecular pharmacology* 2006, **70**(3):779-785.
85. Guerre-Millo M: **Adiponectin: an update**. *Diabetes & metabolism* 2008, **34**(1):12-18.
86. Civitarese A, Jenkinson C, Richardson D, Bajaj M, Cusi K, Kashyap S, Berria R, Belfort R, DeFronzo R, Mandarino L: **Adiponectin receptors gene expression and insulin sensitivity in non-diabetic Mexican Americans with or without a family history of Type 2 diabetes**. *Diabetologia* 2004, **47**(5):816-820.
87. Park HS, Lim JH, Kim MY, Kim Y, Hong YA, Choi SR, Chung S, Kim HW, Choi BS, Kim YS: **Resveratrol increases AdipoR1 and AdipoR2 expression in type 2 diabetic nephropathy**. *Journal of Translational Medicine* 2016, **14**(1):1.
88. Fujimoto N, Matsuo N, Sumiyoshi H, Yamaguchi K, Saikawa T, Yoshimatsu H, Yoshioka H: **Adiponectin is expressed in the brown adipose tissue and surrounding immature tissues in mouse embryos**. *Biochimica et Biophysica Acta (BBA)-Gene Structure and Expression* 2005, **1731**(1):1-12.
89. Antuna-Puente B, Feve B, Fellahi S, Bastard J-P: **Adipokines: the missing link between insulin resistance and obesity**. *Diabetes & metabolism* 2008, **34**(1):2-11.
90. Combs TP, Marliss EB: **Adiponectin signaling in the liver**. *Reviews in Endocrine and Metabolic Disorders* 2014, **15**(2):137-147.
91. Esteve E, Ricart W, Fernández-Real JM: **Adipocytokines and insulin resistance**. *Diabetes care* 2009, **32**(suppl 2):S362-S367.
92. Maeda N, Shimomura I, Kishida K, Nishizawa H, Matsuda M, Nagaretani H, Furuyama N, Kondo H, Takahashi M, Arita Y: **Diet-induced insulin resistance in mice lacking adiponectin/ACRP30**. *Nature medicine* 2002, **8**(7):731-738.
93. Yamauchi T, Nio Y, Maki T, Kobayashi M, Takazawa T, Iwabu M, Okada-Iwabu M, Kawamoto S, Kubota N, Kubota T: **Targeted disruption of AdipoR1 and AdipoR2 causes abrogation of adiponectin binding and metabolic actions**. *Nature medicine* 2007, **13**(3):332-339.
94. Park H-K, Ahima RS: **Physiology of leptin: energy homeostasis, neuroendocrine function and metabolism**. *Metabolism* 2015, **64**(1):24-34.
95. Rabe K, Lehrke M, Parhofer KG, Broedl UC: **Adipokines and insulin resistance**. *Molecular medicine* 2008, **14**(11-12):741.
96. Kelesidis T, Kelesidis I, Chou S, Mantzoros CS: **Narrative review: the role of leptin in human physiology: emerging clinical applications**. *Annals of internal medicine* 2010, **152**(2):93-100.
97. Bjørbæk C, Elmquist JK, Michl P, Ahima RS, van Bueren A, McCall AL, Flier JS: **Expression of leptin receptor isoforms in rat brain microvessels**. *Endocrinology* 1998, **139**(8):3485-3491.
98. Ahima RS, Kelly J, Elmquist JK, Flier JS: **Distinct physiologic and neuronal responses to decreased leptin and mild hyperleptinemia**. *Endocrinology* 1999, **140**(11):4923-4931.
99. Cowley MA, Smart JL, Rubinstein M, Cerdán MG, Diano S, Horvath TL, Cone RD, Low MJ: **Leptin activates anorexigenic POMC neurons through a neural network in the arcuate nucleus**. *Nature* 2001, **411**(6836):480-484.

100. Clément K, Sorensen TI: **Obesity: genomics and postgenomics**: CRC Press; 2007.
101. Yau SW, Henry BA, Russo VC, McConell GK, Clarke IJ, Werther GA, Sabin MA: **Leptin enhances insulin sensitivity by direct and sympathetic nervous system regulation of muscle IGFBP-2 expression: evidence from nonrodent models**. *Endocrinology* 2014, **155**(6):2133-2143.
102. Kievit P, Howard JK, Badman MK, Balthasar N, Coppari R, Mori H, Lee CE, Elmquist JK, Yoshimura A, Flier JS: **Enhanced leptin sensitivity and improved glucose homeostasis in mice lacking suppressor of cytokine signaling-3 in POMC-expressing cells**. *Cell metabolism* 2006, **4**(2):123-132.
103. Slevin SM, Egan LJ: **New Insights into the Mechanisms of Action of Anti–Tumor Necrosis Factor-α Monoclonal Antibodies in Inflammatory Bowel Disease**. *Inflammatory bowel diseases* 2015, **21**(12):2909-2920.
104. Carswell E, Old LJ, Kassel R, Green S, Fiore N, Williamson B: **An endotoxin-induced serum factor that causes necrosis of tumors**. *Proceedings of the National Academy of Sciences* 1975, **72**(9):3666-3670.
105. Aggarwal BB, Moffat B, Harkins RN: **Human lymphotoxin. Production by a lymphoblastoid cell line, purification, and initial characterization**. *Journal of Biological Chemistry* 1984, **259**(1):686-691.
106. Zhou X, Li Z, Zhou J: **Tumor necrosis factor α in the onset and progression of leukemia**. *Experimental Hematology* 2016.
107. Horiuchi T, Mitoma H, Harashima S-i, Tsukamoto H, Shimoda T: **Transmembrane TNF-α: structure, function and interaction with anti-TNF agents**. *Rheumatology* 2010, **49**(7):1215-1228.
108. Popa C, Netea MG, Van Riel PL, van der Meer JW, Stalenhoef AF: **The role of TNF-α in chronic inflammatory conditions, intermediary metabolism, and cardiovascular risk**. *Journal of lipid research* 2007, **48**(4):751-762.
109. Silva F, Cisternas M, Specks U: **TNF-α blocker therapy and solid malignancy risk in ANCA-associated vasculitis**. *Current rheumatology reports* 2012, **14**(6):501-508.
110. Li ZY, Wang P, Miao CY: **Adipokines in inflammation, insulin resistance and cardiovascular disease**. *Clinical and Experimental Pharmacology and Physiology* 2011, **38**(12):888-896.
111. Nielsen ST, Lehrskov-Schmidt L, Krogh-Madsen R, Solomon TP, Lehrskov-Schmidt L, Holst JJ, Møller K: **Tumour necrosis factor-alpha infusion produced insulin resistance but no change in the incretin effect in healthy volunteers**. *Diabetes/metabolism research and reviews* 2013, **29**(8):655-663.
112. Wolf J, Rose-John S, Garbers C: **Interleukin-6 and its receptors: a highly regulated and dynamic system**. *Cytokine* 2014, **70**(1):11-20.
113. Hirano T, Yasukawa K, Harada H, Taga T, Watanabe Y, Matsuda T, Kashiwamura S-i, Nakajima K, Koyama K, Iwamatsu A: **Complementary DNA for a novel human interleukin (BSF-2) that induces B lymphocytes to produce immunoglobulin**. 1986.
114. Rothaug M, Becker-Pauly C, Rose-John S: **The role of interleukin-6 signaling in nervous tissue**. *Biochimica et Biophysica Acta (BBA)-Molecular Cell Research* 2016, **1863**(6):1218-1227.
115. Schaper F, Rose-John S: **Interleukin-6: biology, signaling and strategies of blockade**. *Cytokine & growth factor reviews* 2015, **26**(5):475-487.
116. Riethmueller S, Somasundaram P, Ehlers JC, Hung C-W, Flynn CM, Lokau J, Agthe M, Düsterhöft S, Zhu Y, Grötzinger J: **Proteolytic Origin of the**

Soluble Human IL-6R In Vivo and a Decisive Role of N-Glycosylation. *PLoS biology* 2017, **15**(1):e2000080.

117. Kim H-J, Higashimori T, Park S-Y, Choi H, Dong J, Kim Y-J, Noh H-L, Cho Y-R, Cline G, Kim Y-B: **Differential effects of interleukin-6 and-10 on skeletal muscle and liver insulin action in vivo**. *Diabetes* 2004, **53**(4):1060-1067.
118. Inoue H, Ogawa W, Asakawa A, Okamoto Y, Nishizawa A, Matsumoto M, Teshigawara K, Matsuki Y, Watanabe E, Hiramatsu R: **Role of hepatic STAT3 in brain-insulin action on hepatic glucose production**. *Cell metabolism* 2006, **3**(4):267-275.
119. Senn JJ, Klover PJ, Nowak IA, Zimmers TA, Koniaris LG, Furlanetto RW, Mooney RA: **Suppressor of cytokine signaling-3 (SOCS-3), a potential mediator of interleukin-6-dependent insulin resistance in hepatocytes**. *Journal of Biological Chemistry* 2003, **278**(16):13740-13746.
120. Sabio G, Das M, Mora A, Zhang Z, Jun JY, Ko HJ, Barrett T, Kim JK, Davis RJ: **A stress signaling pathway in adipose tissue regulates hepatic insulin resistance**. *Science* 2008, **322**(5907):1539-1543.
121. Fedders R, Muenzner M, Schupp M: **Retinol binding protein 4 and its membrane receptors: a metabolic perspective**. *Hormone molecular biology and clinical investigation* 2015, **22**(1):27-37.
122. Alapatt P, Guo F, Komanetsky SM, Wang S, Cai J, Sargsyan A, Díaz ER, Bacon BT, Aryal P, Graham TE: **Liver retinol transporter and receptor for serum retinol-binding protein (RBP4)**. *Journal of Biological Chemistry* 2013, **288**(2):1250-1265.
123. Muenzner M, Tuvia N, Deutschmann C, Witte N, Tolkachov A, Valai A, Henze A, Sander LE, Raila J, Schupp M: **Retinol-binding protein 4 and its membrane receptor STRA6 control adipogenesis by regulating cellular retinoid homeostasis and retinoic acid receptor α activity**. *Molecular and cellular biology* 2013, **33**(20):4068-4082.
124. Ma X, Zhou Z, Chen Y, Wu Y, Liu Y: **RBP4 functions as a hepatokine in the regulation of glucose metabolism by the circadian clock in mice**. *Diabetologia* 2016, **59**(2):354-362.
125. Abel ED, Peroni O, Kim JK, Kim Y-B, Boss O, Hadro E, Minnemann T, Shulman GI, Kahn BB: **Adipose-selective targeting of the GLUT4 gene impairs insulin action in muscle and liver**. *Nature* 2001, **409**(6821):729-733.
126. Kotnik P, Fischer-Posovszky P, Wabitsch M: **RBP4: a controversial adipokine**. *European Journal of Endocrinology* 2011, **165**(5):703-711.
127. Yang Q, Graham TE, Mody N, Preitner F, Peroni OD, Zabolotny JM, Kotani K, Quadro L, Kahn BB: **Serum retinol binding protein 4 contributes to insulin resistance in obesity and type 2 diabetes**. *Nature* 2005, **436**(7049):356-362.
128. Cheng J, Song Z-Y, Pu L, Yang H, Zheng J-M, Zhang Z-Y, Shi X-E, Yang G-S: **Retinol binding protein 4 affects the adipogenesis of porcine preadipocytes through insulin signaling pathways**. *Biochemistry and Cell Biology* 2013, **91**(4):236-243.
129. Cho YM, Youn B-S, Lee H, Lee N, Min S-S, Kwak SH, Lee HK, Park KS: **Plasma retinol-binding protein-4 concentrations are elevated in human subjects with impaired glucose tolerance and type 2 diabetes**. *Diabetes care* 2006, **29**(11):2457-2461.

130. Gavi S, Stuart LM, Kelly P, Melendez MM, Mynarcik DC, Gelato MC, McNurlan MA: **Retinol-binding protein 4 is associated with insulin resistance and body fat distribution in nonobese subjects without type 2 diabetes**. *The Journal of Clinical Endocrinology & Metabolism* 2007, **92**(5):1886-1890.
131. Jia W, Wu H, Bao Y, Wang C, Lu J, Zhu J, Xiang K: **Association of serum retinol-binding protein 4 and visceral adiposity in Chinese subjects with and without type 2 diabetes**. *The Journal of Clinical Endocrinology & Metabolism* 2007, **92**(8):3224-3229.
132. Lee D-C, Lee J-W, Im J-A: **Association of serum retinol binding protein 4 and insulin resistance in apparently healthy adolescents**. *Metabolism* 2007, **56**(3):327-331.
133. Norseen J, Hosooka T, Hammarstedt A, Yore MM, Kant S, Aryal P, Kiernan UA, Phillips DA, Maruyama H, Kraus BJ: **Retinol-binding protein 4 inhibits insulin signaling in adipocytes by inducing proinflammatory cytokines in macrophages through a c-Jun N-terminal kinase-and toll-like receptor 4-dependent and retinol-independent mechanism**. *Molecular and cellular biology* 2012, **32**(10):2010-2019.
134. Chavez AO, Coletta DK, Kamath S, Cromack DT, Monroy A, Folli F, DeFronzo RA, Tripathy D: **Retinol-binding protein 4 is associated with impaired glucose tolerance but not with whole body or hepatic insulin resistance in Mexican Americans**. *American Journal of Physiology-Endocrinology and Metabolism* 2009, **296**(4):E758-E764.
135. Gómez-Ambrosi J, Rodriguez A, Catalan V, Ramírez B, Silva C, Rotellar F, Gil M, Salvador J, Frühbeck G: **Serum retinol-binding protein 4 is not increased in obesity or obesity-associated type 2 diabetes mellitus, but is reduced after relevant reductions in body fat following gastric bypass**. *Clinical endocrinology* 2008, **69**(2):208-215.
136. Promintzer M, Krebs M, Todoric J, Luger A, Bischof MG, Nowotny P, Wagner O, Esterbauer H, Anderwald C: **Insulin resistance is unrelated to circulating retinol binding protein and protein C inhibitor**. *The Journal of Clinical Endocrinology & Metabolism* 2007, **92**(11):4306-4312.
137. Yao-Borengasser A, Varma V, Bodles AM, Rasouli N, Phanavanh B, Lee M-J, Starks T, Kern LM, Spencer III HJ, Rashidi AA: **Retinol binding protein 4 expression in humans: relationship to insulin resistance, inflammation, and response to pioglitazone**. *The Journal of Clinical Endocrinology & Metabolism* 2007, **92**(7):2590-2597.
138. Kos K, Wong S, Tan BK, Kerrigan D, Randeva HS, Pinkney JH, Wilding JP: **Human RBP4 adipose tissue expression is gender specific and influenced by leptin**. *Clinical endocrinology* 2011, **74**(2):197-205.
139. Liu Y, Chen H, Wang J, Zhou W, Sun R, Xia M: **Elevated retinol binding protein 4 induces apolipoprotein B production and associates with hypertriglyceridemia**. *The Journal of Clinical Endocrinology & Metabolism* 2015, **100**(5):E720-E728.
140. Borkowski K: **The interplay between cyclic AMP and insulin during obesity development**. University of Copenhagen, Faculty of Science, Department of Biology; 2013.
141. Bryant NJ, Govers R, James DE: **Regulated transport of the glucose transporter GLUT4**. *Nature reviews Molecular cell biology* 2002, **3**(4):267-277.

142. Saltiel AR, Kahn CR: **Insulin signalling and the regulation of glucose and lipid metabolism**. *Nature* 2001, **414**(6865):799-806.
143. De Meyts P, Whittaker J: **Structural biology of insulin and IGF1 receptors: implications for drug design**. *Nature Reviews Drug Discovery* 2002, **1**(10):769-783.
144. Leto D, Saltiel AR: **Regulation of glucose transport by insulin: traffic control of GLUT4**. *Nature reviews Molecular cell biology* 2012, **13**(6):383-396.
145. Huang S, Czech MP: **The GLUT4 glucose transporter**. *Cell metabolism* 2007, **5**(4):237-252.
146. Bryant NJ, Gould GW: **SNARE Proteins Underpin Insulin-Regulated GLUT4 Traffic**. *Traffic* 2011, **12**(6):657-664.
147. McCarthy AM, Elmendorf JS: **GLUT4's itinerary in health & disease**. *Indian Journal of Medical Research* 2007, **125**(3):373.
148. Abe T, Hirasaka K, Kagawa S, Kohno S, Ochi A, Utsunomiya K, Sakai A, Ohno A, Teshima-Kondo S, Okumura Y: **Cbl-b is a critical regulator of macrophage activation associated with obesity-induced insulin resistance in mice**. *Diabetes* 2013, **62**(6):1957-1969.
149. Carlon A: **Modeling and simulation of insulin signaling**. 2013.
150. Beneit N, Fernández-García C, Martín-Ventura J, Perdomo L, Escribano Ó, Michel J, García-Gómez G, Fernández S, Díaz-Castroverde S, Egido J: **Expression of insulin receptor (IR) A and B isoforms, IGF-IR, and IR/IGF-IR hybrid receptors in vascular smooth muscle cells and their role in cell migration in atherosclerosis**. *Cardiovascular Diabetology* 2016, **15**(1):161.
151. Perks CM, Zielinska H, Wang J, Jarrett C, Frankow A, Ladomery MR, Bahl A, Rhodes A, Oxley J, Holly JM: **Insulin receptor isoform variations in prostate cancer cells**. *Frontiers in endocrinology* 2016, **7**.
152. Morcavallo A, Genua M, Palummo A, Kletvikova E, Jiracek J, Brzozowski AM, Iozzo RV, Belfiore A, Morrione A: **Insulin and insulin-like growth factor II differentially regulate endocytic sorting and stability of insulin receptor isoform A**. *Journal of Biological Chemistry* 2012, **287**(14):11422-11436.
153. Belfiore A, Malaguarnera R: **The insulin receptor: a new target for cancer therapy**. *Frontiers in endocrinology* 2011, **2**:93.
154. Taniguchi CM, Emanuelli B, Kahn CR: **Critical nodes in signalling pathways: insights into insulin action**. *Nature reviews Molecular cell biology* 2006, **7**(2):85-96.
155. Avruch J, Khokhlatchev A, Kyriakis JM, Luo Z, Tzivion G, Vavvas D, Zhang XF: **Ras activation of the Raf kinase: tyrosine kinase recruitment of the MAP kinase cascade**. *Recent progress in hormone research* 2000, **56**:127-155.
156. Nissan MH, Rosen N, Solit DB: **ERK pathway inhibitors: how low should we go?** *Cancer discovery* 2013, **3**(7):719-721.
157. Soares-Silva M, Diniz FF, Gomes GN, Bahia D: **The Mitogen-Activated Protein Kinase (MAPK) Pathway: Role in Immune Evasion by Trypanosomatids**. *Frontiers in microbiology* 2016, **7**.
158. Pearson G, Robinson F, Beers Gibson T, Xu B-e, Karandikar M, Berman K, Cobb MH: **Mitogen-activated protein (MAP) kinase pathways: regulation and physiological functions 1**. *Endocrine reviews* 2001, **22**(2):153-183.

159. Mazza S: **Role of Class II Phosphoinositide 3-Kinase PI3K-C2α in pancreatic β cell function**. Queen Mary University of London; 2014.
160. Jesus DLFd: **ß-cell reserve in insulin resistant pregnant mice**. 2013.
161. Castellano E, Downward J: **RAS interaction with PI3K: more than just another effector pathway**. *Genes & cancer* 2011, **2**(3):261-274.
162. Cross DA, Alessi DR, Cohen P, Andjelkovich M, Hemmings BA: **Inhibition of glycogen synthase kinase-3 by insulin mediated by protein kinase B**. *Nature* 1995, **378**(6559):785-789.
163. Mîinea CP, Sano H, Kane S, Sano E, Fukuda M, Peränen J, Lane WS, Lienhard GE: **AS160, the Akt substrate regulating GLUT4 translocation, has a functional Rab GTPase-activating protein domain**. *Biochemical Journal* 2005, **391**(1):87-93.
164. Tunduguru R, Thurmond DC: **Promoting Glucose Transporter-4 Vesicle Trafficking along Cytoskeletal Tracks: PAK-Ing Them Out**. *Frontiers in endocrinology* 2017, **8**:329.
165. Saltiel AR, Pessin JE: **Insulin signaling pathways in time and space**. *Trends in cell biology* 2002, **12**(2):65-71.
166. Thien CB, Langdon WY: **Cbl: many adaptations to regulate protein tyrosine kinases**. *Nature reviews Molecular cell biology* 2001, **2**(4):294-307.
167. Dou H, Buetow L, Hock A, Sibbet GJ, Vousden KH, Huang DT: **Structural basis for autoinhibition and phosphorylation-dependent activation of c-Cbl**. *Nature Structural and Molecular Biology* 2012, **19**(2):184.
168. Baumann CA, Ribon V, Kanzaki M, Thurmond DC, Mora S, Shigematsu S, Bickel PE, Pessin JE, Saltiel AR: **CAP defines a second signalling pathway required for insulin-stimulated glucose transport**. *Nature* 2000, **407**(6801):202-207.
169. Liu J, Kimura A, Baumann CA, Saltiel AR: **APS facilitates c-Cbl tyrosine phosphorylation and GLUT4 translocation in response to insulin in 3T3-L1 adipocytes**. *Molecular and cellular biology* 2002, **22**(11):3599-3609.
170. Langdon WY, Hartley JW, Klinken SP, Ruscetti SK, Morse HC: **v-cbl, an oncogene from a dual-recombinant murine retrovirus that induces early B-lineage lymphomas**. *Proceedings of the National Academy of Sciences* 1989, **86**(4):1168-1172.
171. Langdon W, Hyland C, Grumont R, Morse H: **The c-cbl proto-oncogene is preferentially expressed in thymus and testis tissue and encodes a nuclear protein**. *Journal of virology* 1989, **63**(12):5420-5424.
172. Swaminathan G, Tsygankov AY: **The Cbl family proteins: ring leaders in regulation of cell signaling**. *Journal of cellular physiology* 2006, **209**(1):21-43.
173. Thien CB, Langdon WY: **c-Cbl and Cbl-b ubiquitin ligases: substrate diversity and the negative regulation of signalling responses**. *Biochemical Journal* 2005, **391**(2):153-166.
174. Severe N, Dieudonne F, Marie P: **E3 ubiquitin ligase-mediated regulation of bone formation and tumorigenesis**. *Cell death & disease* 2013, **4**(1):e463.
175. Ogawa S, Shih L-Y, Suzuki T, Otsu M, Nakauchi H, Koeffler HP, Sanada M: **Deregulated intracellular signaling by mutated c-CBL in myeloid neoplasms**. *Clinical cancer research* 2010, **16**(15):3825-3831.
176. Meng W, Sawasdikosol S, Burakoff SJ, Eck MJ: **Structure of the amino-terminal domain of Cbl complexed to its binding site on ZAP-70 kinase**. *Nature* 1999, **402**:29-34.

177. Mohapatra B, Ahmad G, Nadeau S, Zutshi N, An W, Scheffe S, Dong L, Feng D, Goetz B, Arya P: **Protein tyrosine kinase regulation by ubiquitination: critical roles of Cbl-family ubiquitin ligases**. *Biochimica et Biophysica Acta (BBA)-Molecular Cell Research* 2013, **1833**(1):122-139.
178. Naramura M, Nadeau S, Bhopal Mohapatra GA, Mukhopadhyay C, Sattler M, Raja SM, Natarajan A, Band V, Band H: **Mutant Cbl proteins as oncogenic drivers in myeloproliferative disorders**. *Oncotarget* 2011, **2**(3):245.
179. Peschard P, Ishiyama N, Lin T, Lipkowitz S, Park M: **A conserved DpYR motif in the juxtamembrane domain of the Met receptor family forms an atypical c-Cbl/Cbl-b tyrosine kinase binding domain binding site required for suppression of oncogenic activation**. *Journal of Biological Chemistry* 2004, **279**(28):29565-29571.
180. Lipkowitz S, Weissman AM: **RINGs of good and evil: RING finger ubiquitin ligases at the crossroads of tumour suppression and oncogenesis**. *Nature reviews Cancer* 2011, **11**(9):629.
181. Kanzaki M: **Insulin receptor signals regulating GLUT4 translocation and actin dynamics**. *Endocrine journal* 2006, **53**(3):267-293.
182. Naramura M, Kole HK, Hu R-J, Gu H: **Altered thymic positive selection and intracellular signals in Cbl-deficient mice**. *Proceedings of the National Academy of Sciences* 1998, **95**(26):15547-15552.
183. Ross AW, Russell L, Helfer G, Thomson LM, Dalby MJ, Morgan PJ: **Photoperiod regulates lean mass accretion, but not adiposity, in growing F344 rats fed a high fat diet**. *PloS one* 2015, **10**(3):e0119763.
184. Balls M: **Animals (Scientific Procedures) Act 1986: the animal procedures committee**. 1986.
185. Laird PW, Zijderveld A, Linders K, Rudnicki MA, Jaenisch R, Berns A: **Simplified mammalian DNA isolation procedure**. *Nucleic acids research* 1991, **19**(15):4293.
186. Yang C, Coker KJ, Kim JK, Mora S, Thurmond DC, Davis AC, Yang B, Williamson RA, Shulman GI, Pessin JE: **Syntaxin 4 heterozygous knockout mice develop muscle insulin resistance**. *The Journal of clinical investigation* 2001, **107**(10):1311-1318.
187. Yang C, Mora S, Ryder JW, Coker KJ, Hansen P, Allen L-A, Pessin JE: **VAMP3 null mice display normal constitutive, insulin-and exercise-regulated vesicle trafficking**. *Molecular and cellular biology* 2001, **21**(5):1573-1580.
188. Tschöp MH, Speakman JR, Arch JR, Auwerx J, Brüning JC, Chan L, Eckel RH, Farese Jr RV, Galgani JE, Hambly C: **A guide to analysis of mouse energy metabolism**. *Nature methods* 2012, **9**(1):57-63.
189. Penicaud L, Benani A, Datiche F, Fioramonti X, Leloup C, Lienard F: **Animal Models and Methods to Study the Relationships Between Brain and Tissues in Metabolic Regulation**. In: *Animal Models for the Study of Human Disease*. Elsevier; 2013: 569-593.
190. Gupta RD, Ramachandran R, Padmanaban Venkatesan SA, Joseph M, Thomas N: **Indirect calorimetry: From bench to bedside**. *Indian journal of endocrinology and metabolism* 2017, **21**(4):594.
191. Levine JA: **Measurement of energy expenditure**. *Public health nutrition* 2005, **8**(7a):1123-1132.

192. Xie L, Boyle D, Sanford D, Scherer PE, Pessin JE, Mora S: **Intracellular trafficking and secretion of adiponectin is dependent on GGA-coated vesicles**. *Journal of Biological Chemistry* 2006, **281**(11):7253-7259.
193. Carson BP, Del Bas JM, Moreno-Navarrete JM, Fernandez-Real JM, Mora S: **The rab11 effector protein FIP1 regulates adiponectin trafficking and secretion**. *PloS one* 2013, **8**(9):e74687.
194. Fried SK, Moustaid-Moussa N: **Culture of adipose tissue and isolated adipocytes**. *Adipose tissue protocols* 2001:197-212.
195. Trinder P: **Determination of glucose in blood using glucose oxidase with an alternative oxygen acceptor**. *Annals of clinical Biochemistry* 1969, **6**(1):24-27.
196. Barham D, Trinder P: **An improved colour reagent for the determination of blood glucose by the oxidase system**. *Analyst* 1972, **97**(1151):142-145.
197. Galarraga M, Campión J, Muñoz-Barrutia A, Boqué N, Moreno H, Martínez JA, Milagro F, Ortiz-de-Solórzano C: **Adiposoft: automated software for the analysis of white adipose tissue cellularity in histological sections**. *Journal of lipid research* 2012, **53**(12):2791-2796.
198. Yang C, Aye CC, Li X, Ramos AD, Zorzano A, Mora S: **Mitochondrial dysfunction in insulin resistance: differential contributions of chronic insulin and saturated fatty acid exposure in muscle cells**. *Bioscience reports* 2012, **32**(5):465-478.
199. Livak KJ, Schmittgen TD: **Analysis of relative gene expression data using real-time quantitative PCR and the 2− ΔΔCT method**. *methods* 2001, **25**(4):402-408.
200. Blake T, Shapiro M, Morse 3rd H, Langdon W: **The sequences of the human and mouse c-cbl proto-oncogenes show v-cbl was generated by a large truncation encompassing a proline-rich domain and a leucine zipper-like motif**. *Oncogene* 1991, **6**(4):653-657.
201. Molero JC, Turner N, Thien CB, Langdon WY, James DE, Cooney GJ: **Genetic ablation of the c-Cbl ubiquitin ligase domain results in increased energy expenditure and improved insulin action**. *Diabetes* 2006, **55**(12):3411-3417.
202. Kurth-Kraczek EJ, Hirshman MF, Goodyear LJ, Winder WW: **5'AMP-activated protein kinase activation causes GLUT4 translocation in skeletal muscle**. *Diabetes* 1999, **48**(8):1667-1671.
203. Merrill G, Kurth E, Hardie D, Winder W: **AICA riboside increases AMP-activated protein kinase, fatty acid oxidation, and glucose uptake in rat muscle**. *American Journal of Physiology-Endocrinology and Metabolism* 1997, **273**(6):E1107-E1112.
204. Daval M, Foufelle F, Ferré P: **Functions of AMP-activated protein kinase in adipose tissue**. *The Journal of Physiology* 2006, **574**(1):55-62.
205. Daval M, Diot-Dupuy F, Bazin R, Hainault I, Viollet B, Vaulont S, Hajduch E, Ferré P, Foufelle F: **Anti-lipolytic action of AMP-activated protein kinase in rodent adipocytes**. *Journal of Biological Chemistry* 2005, **280**(26):25250-25257.
206. Mitra P, Zheng X, Czech MP: **RNAi-based analysis of CAP, Cbl, and CrkII function in the regulation of GLUT4 by insulin**. *Journal of Biological Chemistry* 2004, **279**(36):37431-37435.

207. Zhang J, Chiang YJ, Hodes RJ, Siraganian RP: **Inactivation of c-Cbl or Cbl-b differentially affects signaling from the high affinity IgE receptor**. *The Journal of Immunology* 2004, **173(**3):1811-1818.
208. Zhang T, Sawada K, Yamamoto N, Ashida H: **4-Hydroxyderricin and xanthoangelol from Ashitaba (Angelica keiskei) suppress differentiation of preadiopocytes to adipocytes via AMPK and MAPK pathways**. *Molecular nutrition & food research* 2013, **57**(10):1729-1740.
209. Hu E, Kim JB, Sarraf P, Spiegelman BM: **Inhibition of adipogenesis through MAP kinase-mediated phosphorylation of PPAR gamma**. *Science* 1996, **274**(5295):2100.
210. Bost F, Aouadi M, Caron L, Binétruy B: **The role of MAPKs in adipocyte differentiation and obesity**. *Biochimie* 2005, **87**(1):51-56.
211. Tang Q-Q, Otto TC, Lane MD: **Mitotic clonal expansion: a synchronous process required for adipogenesis**. *Proceedings of the National Academy of Sciences* 2003, **100**(1):44-49.
212. Dikic I, Giordano S: **Negative receptor signalling**. *Current opinion in cell biology* 2003, **15**(2):128-135.
213. Watson RT, Pessin JE: **Transmembrane domain length determines intracellular membrane compartment localization of syntaxins 3, 4, and 5**. *American Journal of Physiology-Cell Physiology* 2001, **281**(1):C215-C223.
214. Sullivan JE, Brocklehurst KJ, Marley AE, Carey F, Carling D, Beri RK: **Inhibition of lipolysis and lipogenesis in isolated rat adipocytes with AICAR, a cell-permeable activator of AMP-activated protein kinase**. *FEBS letters* 1994, **353**(1):33-36.
215. Anthony NM, Gaidhu MP, Ceddia RB: **Regulation of visceral and subcutaneous adipocyte lipolysis by acute AICAR-induced AMPK activation**. *Obesity* 2009, **17**(7):1312-1317.
216. Yin W, Mu J, Birnbaum MJ: **Role of AMP-activated protein kinase in cyclic AMP-dependent lipolysis in 3T3-L1 adipocytes**. *Journal of Biological Chemistry* 2003, **278**(44):43074-43080.
217. Koh H-J, Hirshman MF, He H, Li Y, Manabe Y, Balschi JA, Goodyear LJ: **Adrenaline is a critical mediator of acute exercise-induced AMP-activated protein kinase activation in adipocytes**. *Biochemical Journal* 2007, **403**(3):473-481.
218. Park H, Kaushik VK, Constant S, Prentki M, Przybytkowski E, Ruderman NB, Saha AK: **Coordinate regulation of malonyl-CoA decarboxylase, sn-glycerol-3-phosphate acyltransferase, and acetyl-CoA carboxylase by AMP-activated protein kinase in rat tissues in response to exercise**. *Journal of Biological Chemistry* 2002, **277**(36):32571-32577.
219. Sponarova J, Mustard KJ, Horakova O, Flachs P, Rossmeisl M, Brauner P, Bardova K, Thomason-Hughes M, Braunerova R, Janovska P: **Involvement of AMP-activated protein kinase in fat depot-specific metabolic changes during starvation**. *FEBS letters* 2005, **579**(27):6105-6110.
220. Ouchi N, Ohashi K, Shibata R, Murohara T: **Adipocytokines and obesity-linked disorders**. *Nagoya journal of medical science* 2012, **74**(1-2):19.
221. Whitehead J, Richards A, Hickman I, Macdonald G, Prins J: **Adiponectin–a key adipokine in the metabolic syndrome**. *Diabetes, Obesity and Metabolism* 2006, **8**(3):264-280.
222. Mancuso P: **The role of adipokines in chronic inflammation**. *ImmunoTargets and therapy* 2016, **5**:47.

223. Kato S, Endoh H, Masuhiro Y, Kitamoto T, Uchiyama S, Sasaki H, Masushige S, Gotoh Y, Nishida E, Kawashima H: **Activation of the estrogen receptor through phosphorylation by mitogen-activated protein kinase**. *Science* 1995, **270**(5241):1491-1494.
224. Bunone G, Briand P, Miksicek R, Picard D: **Activation of the unliganded estrogen receptor by EGF involves the MAP kinase pathway and direct phosphorylation**. *The EMBO journal* 1996, **15**(9):2174.
225. Driggers PH, Segars JH: **Estrogen action and cytoplasmic signaling pathways. Part II: the role of growth factors and phosphorylation in estrogen signaling**. *Trends in Endocrinology & Metabolism* 2002, **13**(10):422-427.
226. Nishizawa H, Shimomura I, Kishida K, Maeda N, Kuriyama H, Nagaretani H, Matsuda M, Kondo H, Furuyama N, Kihara S: **Androgens decrease plasma adiponectin, an insulin-sensitizing adipocyte-derived protein**. *Diabetes* 2002, **51**(9):2734-2741.
227. Wabitsch M, Blum WF, Muche R, Braun M, Hube F, Rascher W, Heinze E, Teller W, Hauner H: **Contribution of androgens to the gender difference in leptin production in obese children and adolescents**. *Journal of Clinical Investigation* 1997, **100**(4):808.
228. Suh J-B, Kim S-M, Cho G-J, Choi K-M, Han J-H, Geun HT: **Elevated serum retinol-binding protein 4 is associated with insulin resistance in older women**. *Metabolism* 2010, **59**(1):118-122.
229. Chiying A, Han W, Xiaomin L, Yanbo L, Ying S, Xinyuan G, Jiang W: **Serum retinol-binding protein 4 is elevated and positively associated with insulin resistance in postmenopausal women**. *Endocrine journal* 2009, **56**(8):987-996.
230. Shimizu H, Shimomura Y, Nakanishi Y, Futawatari a, Ohtani K, Sato N, Mori M: **Estrogen increases in vivo leptin production in rats and human subjects**. *Journal of Endocrinology* 1997, **154**(2):285-292.
231. Kennedy A, Gettys TW, Watson P, Wallace P, Ganaway E, Pan Q, Garvey WT: **The metabolic significance of leptin in humans: gender-based differences in relationship to adiposity, insulin sensitivity, and energy expenditure 1**. *The Journal of Clinical Endocrinology & Metabolism* 1997, **82**(4):1293-1300.
232. Saad MF, Damani S, Gingerich RL, Riad-Gabriel MG, Khan A, Boyadjian R, Jinagouda SD, El-Tawil K, Rude RK, Kamdar V: **Sexual Dimorphism in Plasma Leptin Concentration 1**. *The Journal of Clinical Endocrinology & Metabolism* 1997, **82**(2):579-584.
233. Quadro L, Blaner WS, Salchow DJ, Vogel S, Piantedosi R, Gouras P, Freeman S, Cosma MP, Colantuoni V, Gottesman ME: **Impaired retinal function and vitamin A availability in mice lacking retinol-binding protein**. *The EMBO journal* 1999, **18**(17):4633-4644.
234. Tsutsumi C, Okuno M, Tannous L, Piantedosi R, Allan M, Goodman D, Blaner W: **Retinoids and retinoid-binding protein expression in rat adipocytes**. *Journal of Biological Chemistry* 1992, **267**(3):1805-1810.
235. Klöting N, Graham TE, Berndt J, Kralisch S, Kovacs P, Wason CJ, Fasshauer M, Schön MR, Stumvoll M, Blüher M: **Serum retinol-binding protein is more highly expressed in visceral than in subcutaneous adipose tissue and is a marker of intra-abdominal fat mass**. *Cell metabolism* 2007, **6**(1):79-87.

236. Janke J, Engeli S, Boschmann M, Adams F, Böhnke J, Luft FC, Sharma AM, Jordan J: **Retinol-binding protein 4 in human obesity**. *Diabetes* 2006, **55**(10):2805-2810.
237. Vitkova M, Klimcakova E, Kovacikova M, Valle C, Moro C, Polak J, Hanacek J, Capel F, Viguerie N, Richterova B: **Plasma levels and adipose tissue messenger ribonucleic acid expression of retinol-binding protein 4 are reduced during calorie restriction in obese subjects but are not related to diet-induced changes in insulin sensitivity**. *The Journal of Clinical Endocrinology & Metabolism* 2007, **92**(6):2330-2335.
238. Öst A, Danielsson A, Lidén M, Eriksson U, Nystrom FH, Strålfors P: **Retinol-binding protein-4 attenuates insulin-induced phosphorylation of IRS1 and ERK1/2 in primary human adipocytes**. *The FASEB Journal* 2007, **21**(13):3696-3704.
239. Merl V, Peters A, Oltmanns K, Kern W, Born J, Fehm H, Schultes B: **Serum adiponectin concentrations during a 72-hour fast in over-and normal-weight humans**. *International Journal of Obesity* 2005, **29**(8):998-1001.
240. Howard JK, Lord GM, Matarese G, Vendetti S, Ghatei MA, Ritter MA, Lechler RI, Bloom SR: **Leptin protects mice from starvation-induced lymphoid atrophy and increases thymic cellularity in ob/ob mice**. *The Journal of clinical investigation* 1999, **104**(8):1051-1059.
241. Fujita Y, Yanagida H, Mimori T, Jin Z-X, Sakai T, Kawanami T, Sawaki T, Masaki Y, Fukushima T, Okazaki T: **Prevention of fasting-mediated bone marrow atrophy by leptin administration**. *Cellular immunology* 2012, **273**(1):52-58.
242. Ahren B, Mansson S, Gingerich RL, Havel PJ: **Regulation of plasma leptin in mice: influence of age, high-fat diet, and fasting**. *American Journal of Physiology-Regulatory, Integrative and Comparative Physiology* 1997, **273**(1):R113-R120.
243. Li F, Xia K, Sheikh MSA, Cheng J, Li C, Yang T: **Retinol binding protein 4 promotes hyperinsulinism-induced proliferation of rat aortic smooth muscle cells**. *Molecular medicine reports* 2014, **9**(5):1634-1640.
244. Du M, Martin A, Hays F, Johnson J, Farjo RA, Farjo KM: **Serum retinol-binding protein-induced endothelial inflammation is mediated through the activation of toll-like receptor 4**. *Molecular vision* 2017, **23**:185.
245. Nilsson S, Gustafsson J-Å: **Estrogen receptor transcription and transactivation Basic aspects of estrogen action**. *Breast Cancer Research* 2000, **2**(5):360.
246. Pallottini V, Bulzomi P, Galluzzo P, Martini C, Marino M: **Estrogen regulation of adipose tissue functions: involvement of estrogen receptor isoforms**. *Infectious Disorders-Drug Targets (Formerly Current Drug Targets-Infectious Disorders)* 2008, **8**(1):52-60.
247. Velickovic K, Cvoro A, Srdic B, Stokic E, Markelic M, Golic I, Otasevic V, Stancic A, Jankovic A, Vucetic M: **Expression and subcellular localization of estrogen receptors α and β in human fetal brown adipose tissue**. *The Journal of Clinical Endocrinology & Metabolism* 2014, **99**(1):151-159.
248. Murphy LC, Seekallu SV, Watson PH: **Clinical significance of estrogen receptor phosphorylation**. *Endocrine-related cancer* 2011, **18**(1):R1-R14.
249. Klinge CM: **Estrogen receptor interaction with estrogen response elements**. *Nucleic acids research* 2001, **29**(14):2905-2919.

250. Klinge CM, Jernigan S, Mattingly K, Risinger K, Zhang J: **Estrogen response element-dependent regulation of transcriptional activation of estrogen receptors α and β by coactivators and corepressors**. *Journal of molecular endocrinology* 2004, **33**(2):387-410.
251. Weigel NL, Zhang Y: **Ligand-independent activation of steroid hormone receptors**. *Journal of molecular medicine* 1998, **76**(7):469-479.
252. Barone I, Brusco L, Fuqua SA: **Estrogen receptor mutations and changes in downstream gene expression and signaling**. *Clinical cancer research* 2010, **16**(10):2702-2708.
253. Jung US, Jeong KJ, Kang JK, Yi K, Shin J-H, Seo HS, Kim T, Kim S-H, Hur J-Y: **Effects of estrogen receptor α and β on the expression of visfatin and retinol-binding protein 4 in 3T3-L1 adipocytes**. *International journal of molecular medicine* 2013, **32**(3):723-728.
254. Tan BK, Chen J, Lehnert H, Kennedy R, Randeva HS: **Raised serum, adipocyte, and adipose tissue retinol-binding protein 4 in overweight women with polycystic ovary syndrome: effects of gonadal and adrenal steroids**. *The Journal of Clinical Endocrinology & Metabolism* 2007, **92**(7):2764-2772.
255. Mohasseb M, Khalil GI: **Estradiol Testosterone Ratio, Serum Retinol Binding Protein 4 and Insulin Resistance in Overweight and Obese Egyptian Men**. 2014.
256. Mullen MP, Forde N, Parr MH, Diskin MG, Morris DG, Nally JE, Evans AC, Crowe MA: **Alterations in systemic concentrations of progesterone during the early luteal phase affect RBP4 expression in the bovine uterus**. *Reproduction, Fertility and Development* 2012, **24**(5):715-722.
257. Ma J-j, Han B-c, Yang Y, Peng J-p: **Retinoic acid synthesis and metabolism are concurrent in the mouse uterus during peri-implantation**. *Cell and tissue research* 2012, **350**(3):525-537.
258. Tsai M, O'Malley BW: **Molecular mechanisms of action of steroid/thyroid receptor superfamily members**. *Annual review of biochemistry* 1994, **63**(1):451-486.
259. Gupte A, Mora S: **Activation of the Cbl insulin signaling pathway in cardiac muscle; dysregulation in obesity and diabetes**. *Biochemical and biophysical research communications* 2006, **342**(3):751-757.
260. Crescenzo R, Bianco F, Mazzoli A, Giacco A, Cancelliere R, di Fabio G, Zarrelli A, Liverini G, Iossa S: **Fat quality influences the obesogenic effect of high fat diets**. *Nutrients* 2015, **7**(11):9475-9491.
261. Lee GR, Shin MK, Yoon DJ, Kim AR, Yu R, Park NH, Han IS: **Topical application of capsaicin reduces visceral adipose fat by affecting adipokine levels in high-fat diet-induced obese mice**. *Obesity* 2013, **21**(1):115-122.
262. Handjieva-Darlenska T, Boyadjieva N: **The effect of high-fat diet on plasma ghrelin and leptin levels in rats**. *Journal of physiology and biochemistry* 2009, **65**(2):157-164.
263. Hotamisligil GS: **Inflammation and metabolic disorders**. *Nature* 2006, **444**(7121):860-867.
264. MacPherson RE, Huber JS, Frendo-Cumbo S, Simpson JA, Wright DC: **Adipose tissue insulin action and IL-6 signaling after exercise in obese mice**. *Medicine & Science in Sports & Exercise* 2015, **47**(10):2034-2042.
265. Graham TE, Yang Q, Blüher M, Hammarstedt A, Ciaraldi TP, Henry RR, Wason CJ, Oberbach A, Jansson P-A, Smith U: **Retinol-binding protein 4**

and insulin resistance in lean, obese, and diabetic subjects. *New England Journal of Medicine* 2006, **354**(24):2552-2563.
266. Berry DC, Noy N: **Signaling by vitamin A and retinol-binding protein in regulation of insulin responses and lipid homeostasis**. *Biochimica et Biophysica Acta (BBA)-Molecular and Cell Biology of Lipids* 2012, **1821**(1):168-176.
267. Christou G, Tselepis A, Kiortsis D: **The metabolic role of retinol binding protein 4: an update**. *Hormone and Metabolic Research* 2012, **44**(01):6-14.
268. Hatzidis A: **Physiological and Behavioral Effects of High Fat Diet Removal and Wheel Running in C57BL/6J Mice**. 2016.
269. Wang C-Y, Liao JK: **A mouse model of diet-induced obesity and insulin resistance**. In: *mTOR*. Springer; 2012: 421-433.
270. Matsakas A, Prosdocimo DA, Mitchell R, Collins-Hooper H, Giallourou N, Swann JR, Potter P, Epting T, Jain MK, Patel K: **Investigating mechanisms underpinning the detrimental impact of a high-fat diet in the developing and adult hypermuscular myostatin null mouse**. *Skeletal muscle* 2015, **5**(1):38.
271. Verbeek J, Spincemaille P, Vanhorebeek I, Van den Berghe G, Vander Elst I, Windmolders P, van Pelt J, Van der Merwe S, Bedossa P, Nevens F: **Dietary intervention, but not losartan, completely reverses non-alcoholic steatohepatitis in obese and insulin resistant mice**. *Lipids in health and disease* 2017, **16**(1):46.
272. May S: **Influence of adipogenesis and high fat diet on the development of cell stress markers in adipose tissue**. *Doctoral dissertation.* Technische Universität München; 2013.
273. Patricia A Deuster PhD M, Yuval Heled PhD, : **Chapter 41 – Testing for Maximal Aerobic Power**; 2008.
274. Beals M, Gross, L. y Harrell, S. : **Metabolism for energy and the respiratory quotient.** 1999.
275. Armitage G, Hervey G, Tobin G: **Energy expenditure of rats tube-fed at different energy levels [proceedings]**. *The Journal of Physiology* 1979, **290**(2):17P-18P.
276. Harris RB, Kelso EW, Flatt WP, Bartness TJ, Grill HJ: **Energy expenditure and body composition of chronically maintained decerebrate rats in the fed and fasted condition**. *Endocrinology* 2006, **147**(3):1365-1376.
277. Brooks SL, Rothwell NJ, Stock MJ, Goodbody AE, Trayhurn P: **Increased proton conductance pathway in brown adipose tissue mitochondria of rats exhibiting diet-induced thermogenesis**. *Nature* 1980, **286**(5770):274.
278. Belfort R, Mandarino L, Kashyap S, Wirfel K, Pratipanawatr T, Berria R, DeFronzo RA, Cusi K: **Dose-response effect of elevated plasma free fatty acid on insulin signaling**. *Diabetes* 2005, **54**(6):1640-1648.
279. Kraegen E, James D, Storlien L, Burleigh K, Chisholm D: **In vivo insulin resistance in individual peripheral tissues of the high fat fed rat: assessment by euglycaemic clamp plus deoxyglucose administration**. *Diabetologia* 1986, **29**(3):192-198.
280. Storlien L, James D, Burleigh K, Chisholm D, Kraegen E: **Fat feeding causes widespread in vivo insulin resistance, decreased energy expenditure, and obesity in rats**. *American Journal of Physiology-Endocrinology and Metabolism* 1986, **251**(5):E576-E583.

281. Goodpaster BH, Kelley DE, Wing RR, Meier A, Thaete FL: **Effects of weight loss on regional fat distribution and insulin sensitivity in obesity**. *Diabetes* 1999, **48**(4):839-847.
282. Berggren JR, Hulver MW, Dohm GL, Houmard JA: **Weight loss and exercise: implications for muscle lipid metabolism and insulin action**. *Medicine and science in sports and exercise* 2004, **36**(7):1191-1195.
283. Minami A, Iseki M, Kishi K, Wang M, Ogura M, Furukawa N, Hayashi S, Yamada M, Obata T, Takeshita Y: **Increased insulin sensitivity and hypoinsulinemia in APS knockout mice**. *Diabetes* 2003, **52**(11):2657-2665.
284. Mauvais-Jarvis F, Ueki K, Fruman DA, Hirshman MF, Sakamoto K, Goodyear LJ, Iannacone M, Accili D, Cantley LC, Kahn CR: **Reduced expression of the murine p85α subunit of phosphoinositide 3-kinase improves insulin signaling and ameliorates diabetes**. *The Journal of clinical investigation* 2002, **109**(1):141-149.
285. Cooney GJ, Lyons RJ, Crew AJ, Jensen TE, Molero JC, Mitchell CJ, Biden TJ, Ormandy CJ, James DE, Daly RJ: **Improved glucose homeostasis and enhanced insulin signalling in Grb14-deficient mice**. *The EMBO journal* 2004, **23**(3):582-593.
286. van der Heijden RA, Sheedfar F, Morrison MC, Hommelberg PP, Kor D, Kloosterhuis NJ, Gruben N, Youssef SA, de Bruin A, Hofker MH: **High-fat diet induced obesity primes inflammation in adipose tissue prior to liver in C57BL/6j mice**. *Aging (Albany NY)* 2015, **7**(4):256-268.
287. Hamrick MW, Ding K-H, Pennington C, Chao YJ, Wu Y-D, Howard B, Immel D, Borlongan C, McNeil PL, Bollag WB: **Age-related loss of muscle mass and bone strength in mice is associated with a decline in physical activity and serum leptin**. *Bone* 2006, **39**(4):845-853.
288. Moller N, O'Brien P, Nair KS: **Disruption of the Relationship between Fat Content and Leptin Levels with Aging in Humans 1**. *The Journal of Clinical Endocrinology & Metabolism* 1998, **83**(3):931-934.
289. Unger RH, Scherer PE: **Gluttony, sloth and the metabolic syndrome: a roadmap to lipotoxicity**. *Trends in Endocrinology & Metabolism* 2010, **21**(6):345-352.
290. Kamohara S, Burcelin R, Halaas JL, Friedman JM, Charron MJ: **Acute stimulation of glucose metabolism in mice by leptin treatment**. *Nature* 1997, **389**(6649):374-377.
291. Morton GJ, Gelling RW, Niswender KD, Morrison CD, Rhodes CJ, Schwartz MW: **Leptin regulates insulin sensitivity via phosphatidylinositol-3-OH kinase signaling in mediobasal hypothalamic neurons**. *Cell metabolism* 2005, **2**(6):411-420.
292. Barnea M, Shamay A, Stark AH, Madar Z: **A high-fat diet has a tissue-specific effect on adiponectin and related enzyme expression**. *Obesity* 2006, **14**(12):2145-2153.
293. Landrier J-F, Kasiri E, Karkeni E, Mihály J, Béke G, Weiss K, Lucas R, Aydemir G, Salles J, Walrand S: **Reduced adiponectin expression after high-fat diet is associated with selective up-regulation of ALDH1A1 and further retinoic acid receptor signaling in adipose tissue**. *The FASEB Journal* 2017, **31**(1):203-211.
294. Peake P, Kriketos A, Denyer G, Campbell L, Charlesworth J: **The postprandial response of adiponectin to a high-fat meal in normal and**

insulin-resistant subjects. *International Journal of Obesity* 2003, **27**(6):657-662.
295. Gregor MF, Hotamisligil GS: **Inflammatory mechanisms in obesity**. *Annual review of immunology* 2011, **29**:415-445.
296. Hoggard N, Agouni A, Mody N, Delibegovic M: **Serum Levels of Retinol Binding Protein 4 (RBP4) and Adipose Tissue Expression Levels of Protein Tyrosine Phosphatase 1B (PTP1B) are Increased in Obese Men Resident in North East of Scotland Without Any Changes in Endoplasmic Reticulum (ER) Stress Response Marker Genes**. *International Journal of General Medicine* 2012, **2012**(5):403-411.
297. Asha G, Mahesh M, Vajreswari A, Jeyakumar S: **Male mice are susceptible to high fat diet-induced hyperglycaemia and display increased circulatory retinol binding protein 4 (RBP4) levels and its expression in visceral adipose depots**. *Archives of physiology and biochemistry*.
298. Emanuelli B, Peraldi P, Filloux C, Chavey C, Freidinger K, Hilton DJ, Hotamisligil GS, Van Obberghen E: **SOCS-3 inhibits insulin signaling and is up-regulated in response to tumor necrosis factor-α in the adipose tissue of obese mice**. *Journal of Biological Chemistry* 2001, **276**(51):47944-47949.
299. Rui L, Yuan M, Frantz D, Shoelson S, White MF: **SOCS-1 and SOCS-3 block insulin signaling by ubiquitin-mediated degradation of IRS1 and IRS2**. *Journal of Biological Chemistry* 2002, **277**(44):42394-42398.
300. Dimmeler S, Fleming I, Fisslthaler B, Hermann C, Busse R, Zeiher AM: **Activation of nitric oxide synthase in endothelial cells by Akt-dependent phosphorylation**. *Nature* 1999, **399**(6736):601-605.
301. Bullo M, Garcia-Lorda P, Peinado-Onsurbe J, Hernandez M, Del Castillo D, Argiles J, Salas-Salvado J: **TNF [alpha] expression of subcutaneous adipose tissue in obese and morbid obese females: relationship to adipocyte LPL activity and leptin synthesis**. *International Journal of Obesity* 2002, **26**(5):652.
302. Matthews V, Allen T, Risis S, Chan M, Henstridge D, Watson N, Zaffino L, Babb J, Boon J, Meikle P: **Interleukin-6-deficient mice develop hepatic inflammation and systemic insulin resistance**. *Diabetologia* 2010, **53**(11):2431-2441.
303. Blaner WS: **Retinol-binding protein: the serum transport protein for vitamin A**. *Endocrine reviews* 1989, **10**(3):308-316.
304. Park HS, Park JY, Yu R: **Relationship of obesity and visceral adiposity with serum concentrations of CRP, TNF-α and IL-6**. *Diabetes research and clinical practice* 2005, **69**(1):29-35.
305. Wu M, Sun L, Pessetto ZY, Zang Z, Xie X, Zhong L, Su Q, Zan W, Gao X, Zhao Y: **Casitas B-Lineage Lymphoma RING Domain Inhibitors Protect Mice against High-Fat Diet-Induced Obesity and Insulin Resistance**. *PloS one* 2015, **10**(8):e0135916.
306. Rathinam C, Thien CB, Flavell RA, Langdon WY: **Myeloid leukemia development in c-Cbl RING finger mutant mice is dependent on FLT3 signaling**. *Cancer cell* 2010, **18**(4):341-352.
307. Rush JS, Boeving MA, Berry WL, Ceresa BP: **Antagonizing c-Cbl enhances EGFR-dependent corneal epithelial homeostasis**. *Investigative ophthalmology & visual science* 2014, **55**(8):4691-4699.
308. Rafiq K, Kolpakov MA, Seqqat R, Guo J, Guo X, Qi Z, Yu D, Mohapatra B, Zutshi N, An W: **c-Cbl inhibition improves cardiac function and survival**

in response to myocardial ischemia. *Circulation* 2014:CIRCULATIONAHA. 113.007004.

309. Sévère N, Miraoui H, Marie PJ: **The Casitas B Lineage Lymphoma (Cbl) Mutant G306E Enhances Osteogenic Differentiation in Human Mesenchymal Stromal Cells in Part by Decreased Cbl-mediated Platelet-derived Growth Factor Receptor α and Fibroblast Growth Factor Receptor 2 Ubiquitination**. *Journal of Biological Chemistry* 2011, **286**(27):24443-24450.
310. Severe N, Dieudonne F, Marie P: **E3 ubiquitin ligase-mediated regulation of bone formation and tumorigenesis**. *Cell death & disease* 2014, **4**(1):e463.
311. de Fante T, Simino LA, Reginato A, Payolla TB, Vitoréli DCG, de Souza M, Torsoni MA, Milanski M, Torsoni AS: **Diet-induced maternal obesity alters insulin signalling in male mice offspring rechallenged with a high-fat diet in adulthood**. *PloS one* 2016, **11**(8):e0160184.
312. Festuccia WT, Blanchard P-G, Deshaies Y: **Control of brown adipose tissue glucose and lipid metabolism by PPARγ**. *Frontiers in endocrinology* 2011, **2**:84.
313. Kahn BB, Flier JS: **Obesity and insulin resistance**. *The Journal of clinical investigation* 2000, **106**(4):473-481.
314. Henderson TA, Saunders PT, Moffett-King A, Groome NP, Critchley HO: **Steroid receptor expression in uterine natural killer cells**. *The Journal of Clinical Endocrinology & Metabolism* 2003, **88**(1):440-449.